UNIVERSITY OF CALIFORNIA, SAN DIEGO

The Effect of Joint Scheduling and Diversity on a Multi-user Wireless Communication System

A dissertation submitted in partial satisfaction of the
requirements for the degree
Doctor of Philosophy

in

Electrical Engineering
(Communication Theory and Systems)

by

Seong-Ho Hur

Committee in charge:

Professor Bhaskar D. Rao, Chair
Professor William Hodgkiss
Professor Ryan Kastner
Professor Laurence B. Milstein
Dr. James R. Zeidler

2011

The dissertation of Seong-Ho Hur is approved, and it is acceptable in quality and form for publication on microfilm and electronically:

_____

_____

_____

_____

_____

Chair

University of California, San Diego

2011

DEDICATION

To almighty God and my family whom He has sent to me.

EPIGRAPH

Don't use your words to talk about your situation;
Use your words to change your situation.
— Joel Osteen

TABLE OF CONTENTS

LIST OF FIGURES

LIST OF TABLES

ACKNOWLEDGEMENTS

First, I thank my Lord, God, for guiding me to achieve what He has stored for me and sending people to support me whenever I have been facing challenges.

Just saying thanks to my advisor Professor Bhaskar D. Rao seems too hollow. I will be never able to forget his guidance, thoughtfulness, and deep insights for all my life. I have been always happy with discussing my researches with him. I truly wish a blessing in his future.

I would like to express my sincere gratitude to my committee members Professor William Hodgkiss, Professor Ryan Kastner, Professor Laurence Milstein and Dr. James Zeidler for their valuable comments and suggestions on this work. It was my great honor to have these tremendous researchers in my committee. I would also like to thank Professor Robert Lugannani for his thoughtfulness when I have been facing challenges.

I am thankful to my lab-mate Matt, Nandan, Yichao, Eddy, Oleg, Liwen, Sagnik, PhuongBang, Xiaofei, Furkan and Sheu-Sheu for the constructive discussion and informative seminar in our group meeting. I learned a lot about what to do and how to do it to be a good researcher. I am also thankful to Alireza Masnadi-Shirazi and Zhilin Zhang for their help. During my study in this land, I have come to know many people, who would be a great asset to me in my future. They helped and encouraged me whenever it was needed to me, especially Dr. Seok-Ho Chang and Dr. Ho-Bin Kim. I also thank people in Korean Catholic Church Choir for their cheering for me.

I would like to express my thanks to long-time friends, Dr. Hyuk-Joon Chung, Professor Wan Choi, Professor Young-Han Kim and Professor Soon-Ryeol Nam for their sincere concern and encouragement to help an old student stand and go straight. To a great young researcher Professor Bang-Chul Jung, I want to give special thanks for great help. To my high-school friends, Young-Dae You, Joo-Young Lee, and Jin-Hyuk Lee, I am thankful for their support. To Sang-Hyun and No-Hyun, I would like to be thankful for your help.

Finally, to my mother, parents-in-law, and grandmother-in-law, I am also thankful for their praying for me. I thank my brothers, sisters, and sister-in-law for showing me a great love. To my father, I hope that this dissertation will be a consolation to his un-filled desire for the study. To my wife, Sun-Young, I am thankful beyond words for her support to help me focus on my research. You and Ye-Won are the greatest gift that God has given me. I love you.

Chapter 2, in full, is a reprint of "*Sum rate analysis of a reduced feedback OFDMA system employing joint scheduling and diversity*," which is in revision for publication in IEEE Transactions on Signal Processing. Sections of Chapter 2 also appear in Vehicular Technology Conference 2011 Spring under the title "*Performance of a reduced feedback OFDMA system employing joint scheduling and diversity*". Both of these works are co-authored with Professor Bhaskar D. Rao. The material in Chapter 3 is work which is in preparation for submission to the IEEE Transactions on Signal Processing under the title "*On the optimal frequency selectivity to maximize multiuser diversity in an OFDMA scheduling system*". Sections of Chapter 3 appear in Asilomar Conference on Signals, Systems, and Computers 2010 under the title "*Determination of cyclic delay for CDD utilizing RMS delay spread in OFDMA multiuser scheduling systems*". Both of these works are co-authored with Professor Bhaskar D. Rao, Dr. James R. Zeidler, and Professor Min-Joong Rim. The material in Chapter 4 is work which is in preparation for submission to the IEEE Transactions on Signal Processing under the title "*Joint User Scheduling and Beamforming in an Uplink Interference-Limited Multi-Cell System*". Sections of Chapter 4 are submitted to Asilomar Conference on Signals, Systems, and Computers 2011 under the title "*Sum rate enhancement by maximizing DSINR in an opportunistic interference alignment scheme*". Both of these works are co-authored with Professor Bang-Chul Jung and Professor Bhaskar D. Rao.

VITA

1996	B. S. in Electrical Engineering *cum laude*, Seoul National University, Seoul, South Korea
1998	M. S. in Electrical Engineering, Seoul National University, Seoul, South Korea
1998-2006	Engineer and senior engineer in Samsung Electronics, Suwon, South Korea
2011	Ph. D. in Electrical and Computer Engineering, University of California, San Diego

PUBLICATIONS

S. H. Hur and B. D. Rao, "Performance of a reduced feedback OFDMA system employing joint scheduling and diversity", *VTC Spring*, May 2011.

S. H. Hur, M. J. Rim, B. D. Rao, and J. R. Zeidler, "Determination of cyclic delay for CDD utilizing RMS delay spread in OFDMA multiuser scheduling systems", *ASILOMAR Conference*, Nov. 2010, pp.506-510.

S. H. Hur, B. C. Jung, and B. D. Rao, "Sum rate enhancement by maximizing DSINR in an opportunistic interference alignment scheme", submitted to *Asilomar Conference*, 2011.

S. H. Hur and B. D. Rao, "Sum rate analysis of an OFDMA system employing joint scheduling and diversity with reduced feedback", in revision for *IEEE Trans. on Signal Processing*.

S. H. Hur, M. J. Rim, B. D. Rao, and J. R. Zeidler, "On the optimal frequency selectivity to multiuser diversity in OFDMA scheduling systems", in preparation.

S. H. Hur, B. C. Jung, and B. D. Rao, "Joint User Scheduling and Beamforming in Uplink Interference-Limited Multi-Cell Environments", in preparation.

ABSTRACT OF THE DISSERTATION

The Effect of Joint Scheduling and Diversity on a Multi-user Wireless Communication System

by

Seong-Ho Hur

Doctor of Philosophy in Electrical Engineering
(Communication Theory and Systems)

University of California, San Diego, 2011

Professor Bhaskar D. Rao, Chair

Multiuser diversity gain usually increases with the number of independent users in a system and with the dynamic range of the channel fluctuation. To enhance the sum rate of a system, joint consideration of scheduling and traditional diversity schemes such as selection diversity, combining diversity, and coded diversity is addressed in past works. The basic principle of joint consideration is to enhance multiuser diversity gain by increasing the number of independent candidates for selection in direct proportion to the number of transmit or receive antennas, or by increasing the variation in the channels between the transmitter and receivers.

In the first part of the dissertation, we consider joint scheduling and diversity with low feedback requirements to enhance the benefits of multiuser diversity in an

orthogonal frequency division multiple access (OFDMA) system. The OFDMA spectrum is assumed to consist of N_{RB} resource blocks and the reduced feedback scheme consists of each user feeding back channel quality information (CQI) for only the best-N_{FB} resource blocks. Assuming largest normalized CQI scheduling and a general value for N_{FB}, we develop a unified framework to analyze the sum rate of the system for both the quantized and non-quantized CQI feedback schemes. Based on this framework, we provide closed-form expressions for the sum rate for three different multi-antenna transmitter schemes; Transmit antenna selection, orthogonal space time block codes and cyclic delay diversity (CDD). Furthermore, we approximate the sum rate expression and determine the feedback ratio ($\frac{N_{\mathrm{FB}}}{N_{\mathrm{RB}}}$) required to achieve a sum rate comparable to the sum rate obtained by a full feedback scheme.

In the second part of the dissertation, we examine the interplay between frequency selectivity and multiuser diversity in an OFDMA scheduling system. A scheduling unit block consists of contiguous multiple subcarriers. Users are scheduled based on their block average throughput in a proportional fair way. Multiuser diversity gain increases with the degree and dynamic range of channel fluctuations. However, a decrease of the block average throughput in a highly selective channel can lower the sum rate as well. In this part, we first study channel selectivity that is desirable for maximizing the maximum of the block average throughput of an arbitrary user. Based on this study, we then propose a method to determine per-user optimal cyclic delay when CDD is used to enhance the sum rate by increasing channel selectivity for a channel with limited frequency selectivity. We show that the throughput by the proposed technique is very close to the optimal sum rate possible with CDD.

In the third part of the dissertation, we consider joint user scheduling and beamforming to enhance sum-rate performance in an interference-limited uplink cellular network, and propose three schemes for this purpose. Specifically, one method is to maximize the signal to generated interference and noise ratio and another is to maximize the signal to interference and noise ratio in the dual network. To improve the user-orthogonality between selected users, we also propose two-step user-selection procedure. We compare the proposed schemes with a conventional scheme which maximizes the signal to noise ratio or minimizes generated interference to other cells. We show that the proposed schemes outperform the conventional ones in most cases, and better exploit multiuser diversity in reducing inter-cell interference.

Chapter 1

Introduction

Improving the reliability of communication and providing high data rate services has been the main pursuit throughout each generation of wireless networks. A fundamental characteristic of a wireless channel is *fading*, the received signal power fluctuation due to multipath. In particular, *deep fading* severely reduces the reliability of a received signal. To mitigate the harmful effects of fading in the traditional point-to-point wireless communication scenario, *diversity* has been used. The basic principle of diversity is to *avoid* deep fading by creating and combining independent multiple copies of a signal between a transmitter and a receiver over various dimensions such as time, frequency, and space. In a multiuser context, the impact of fading can be quite different. Consider the multiuser communication scenario where channels are independent across users and a transmitter can track the channel fluctuations of users. When there are many users in the system, it is highly probable that there exists a user whose channel gain is near its own *maximum*. Then, the selection of a user with the largest channel gain for communication leads to large throughput of the system, which is called *multiuser diversity* gain. The basic principle of multiuser diversity gain is to *exploit* fading.

Multiuser diversity gain usually increases with the number of candidates for selection and the dynamic range of the channel fluctuation. In a condition that the number of candidates is small or that the channel fluctuation is limited, joint consideration of user scheduling and traditional diversity techniques has been utilized since some diversity techniques can boost multiuser diversity gain. This dissertation deals with several topics in the context of joint consideration of user scheduling and diversity.

The first topic is feedback reduction. When there are multiple users, multiple antennas, and multiple frequency blocks as in an orthogonal frequency division multiple access (OFDMA) system, the amount of feedback would be very large. As a feedback reduction scheme, we consider *best-N_{FB} feedback* in an OFDMA system, where a user sends back the best subset of the available total information and N_{FB} denotes the size of the subset. Then we asked how much can the amount of feedback be reduced without sacrificing the sum rate of the case wherein all the information is sent back to the transmitter. To answer this question, we derive the exact sum rate of the best-N_{FB} feedback system and provide an expression for the required amount of feedback.

The second topic is the relationship between frequency diversity and multiuser diversity in an OFDMA scheduling system. Frequency diversity is usually due to resolvable multipaths in a fading channel. As frequency diversity increases, the channel fluctuation in the frequency domain increases, which leads to a decrease of correlation between frequency components, that is, *subcarriers*. When the scheduling unit is an individual subcarrier, multiuser diversity gain would increase with frequency diversity because the equivalent number of candidates for selection in the frequency domain increases due to low correlation. However, when the scheduling unit is a *block* of consecutive subcarriers, as is the general case in an OFDMA system, too much frequency diversity inside a block may decrease the block average throughput itself. To investigate this situation, we derive the analytical relationship between frequency diversity and multiuser diversity in an OFDMA scheduling system and show that there exists optimal frequency diversity that is desirable to maximize multiuser diversity gain.

The third topic is to design a scheduling policy and beamforming strategy in an uplink cellular network. In a cellular network, a signal received in one cell is likely to be interfered with by signals transmitted from other cells. Thus, a key challenge in the cellular network is to reduce inter-cell interference. In uplink communication, the signal to interference and noise ratio (SINR) in one cell is affected by user selection in a neighboring cell, which will be elaborated in Section 1.1.5. Due to this *coupled nature* in uplink user scheduling, we asked which users should be selected in each cell and how beamforming vectors should be designed. Since no optimal solution is known even for the simplest two-user interference channel, we focus on proposing a suboptimal solution with low complexity.

This chapter is organized as follows. In Section 1.1, we provide the background of

the thesis such as fading channels, multiuser diversity, joint consideration of scheduling and diversity, orthogonal frequency division multiple access, and interference-limited cellular network. In Section 1.2, we describe the contributions of the thesis. Finally, in Section 1.3, we summarize the organization of the thesis.

1.1 Background

1.1.1 Fading Channels

In a wireless communication channel, there are scatterers located at random points along the signal propagation path. These scatterers reflect a transmitted signal and cause various time-delayed versions of a transmitted signal to be received at the receiver. If the delays of received versions are all small relative to the inverse of the bandwidth of a transmitted signal, a composite received signal can be modeled as

$$y(t) = h(t)x(t) + z(t) \tag{1.1}$$

where $y(t)$ denotes the received signal at time t, $x(t)$ denotes the transmitted signal, $z(t)$ denotes an additive white Gaussian noise (AWGN), and $h(t)$ denotes the sum of all the multipath gains. This $h(t)$ causes a received signal to take a random phase and an amplitude, which is called *fading*. Formally, fading refers to the fluctuation of the received signal power in a wireless communication channel. When all the delay values are similar around one dominant value as in (1.1), this is called *frequency flat fading*. Depending on the distribution of $h(t)$, fading is classified as Rayleigh fading, Ricean fading, Nakagami fading, Weibull fading, and so on. To combat flat fading in a received signal, a channel equalization technique can be utilized to compensate for the distorted amplitude and to correct the shifted phase at the received signal.

When scatterers are moving or either a transmitter or a receiver is moving, it is less probable that there may be only one dominant delay value in a received signal. In fact, four or six dominant meaningful multipaths are considered for an indoor, a pedestrian, or a vehicular channel model in the wideband code division multiple access (WCDMA) technology. The fading channel consisting of meaningful multipaths with different delay values is called a *frequency selective fading* channel. The received signal for the frequency selective channel is given by

$$y(t) = h(t) * x(t) + z(t), \tag{1.2}$$

where the operator * denotes a convolution. If a fading channel consists of L paths, $h(t)$ is given by

$$h(t) = \sum_{i=1}^{L} \alpha_i h_i \delta(t - \tau_i) \tag{1.3}$$

where α_i denotes an amplitude of a waveform of path-i such that $\sum_{i=1}^{L} \alpha_i^2 = 1$, h_i denotes a fading coefficient of path-i, τ_i denotes a delay value for path-i, and $\delta(t)$ denotes a dirac-delta function. Note that a channel model in (1.1) can be regarded as a special case of (1.2) when $\alpha_1 = 1$, $L = 1$ and $\tau_1 = 0$.

The term *flat* and *selective* when we describe a fading channel makes more intuitive sense when the power spectrum of the received signal is considered. The received signal power spectrum $\mathcal{S}_Y(\omega)$ for (1.2) is given by

$$\mathcal{S}_Y(\omega) = |H(i\omega)|^2 \mathcal{S}_X(\omega), \tag{1.4}$$

where $\mathcal{S}_X(\omega)$ denotes the transmitted signal power spectrum and $H(i\omega)$ denotes the Fourier transform of the fading channel $h(t)$. The Fourier transform of the channel in (1.3) is given by

$$H(i\omega) = \int_{-\infty}^{\infty} h(t) e^{-i\omega t} dt = \sum_{i=1}^{L} \alpha_i h_i e^{-i\omega\tau_i}. \tag{1.5}$$

For a flat channel with $\alpha_1 = 1$, $L = 1$ and $\tau_1 = 0$ in (1.5), we have that $H(i\omega) = h_1$. Thus, we have

$$|H(i\omega)|^2 = |h_1|^2, \tag{1.6}$$

and this is flat in the entire frequency band, which explains the description, *flat* fading channel. For a simple example for a frequency selective channel, suppose that $L = 2$, $\alpha_1 = \alpha_2 = 1/\sqrt{2}$ and $h_1 = h_2$ in (1.3) and (1.5). Then, we have

$$|H(i\omega)|^2 = \frac{|h_1|^2 |1 + e^{i\omega(\tau_1 - \tau_2)}|^2}{2}, \tag{1.7}$$

and this depends on a specific frequency ω, which explains the description, *frequency selective* channel. The examples for a flat channel and frequency selective channel with $L = 4$ are shown in Fig. 1.1.

1.1.2 Multiuser Diversity in a Multiuser Communication System

In view of point-to-point communication, fading is regarded as a main source of impairment in a communication system. Specifically, deep fading, as in Fig. 1.2(a), has

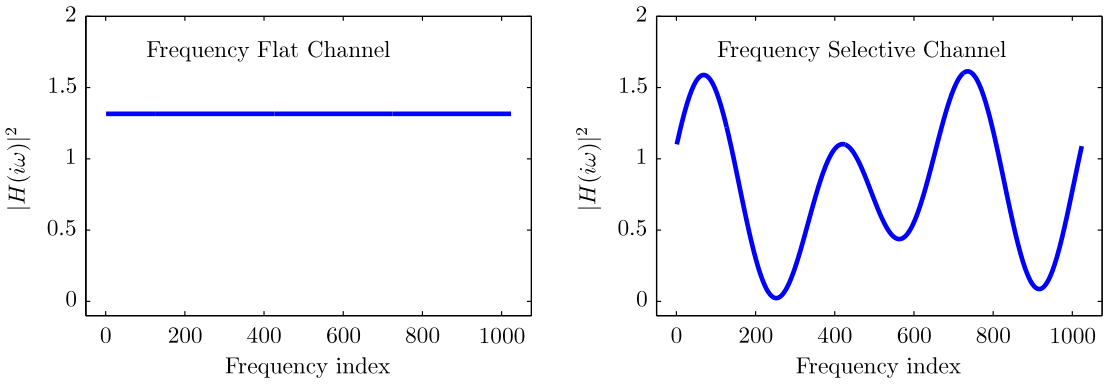

(a) (b)

Figure 1.1: Example of the power spectrum for a fading channel with the FFT size of 1024. (a) Frequency flat channel ($L = 1$). (b) Frequency selective channel ($L = 4$).

a very harmful effect on the system performance. Thus, it is important to mitigate fading in a channel. For this purpose, traditional diversity techniques are utilized over time, frequency, phase, and space [1–3]. For example in a frequency diversity technique, suppose that there is a channel with L independent multipaths in (1.3), each of which follows a complex Gaussian distribution with zero mean and unit variance (*i.e.,* $h_i \sim \mathcal{CN}(0, 1)$). If those paths are combined in an optimal way as in a maximal ratio combining (MRC) scheme, the equivalent channel gain is given by

$$|h_{\mathrm{MRC}}|^2 = \sum_{i=1}^{L} \alpha_i^2 |h_i|^2. \tag{1.8}$$

Then, variance of $|h_{\mathrm{MRC}}|^2$ is given by $\sum_{i=1}^{L} \alpha_i^4$ since $|h_i|^2$ is assumed to be independent across i. If all the paths have the same gain value (*i.e.,* $\alpha_i = \frac{1}{\sqrt{L}}$), then the variance is $\frac{1}{L}$. Note that variance reduces by a factor of L compared to the original flat fading channel gain, as in Fig. 1.2(b) where $L = 5$. Thus, deep fading is less probable, which leads to improving the system performance, usually lowering the bit error rate in a system. The fundamental idea of diversity techniques is to create independent multiple copies of signal paths between a transmitter and a receiver and to reduce the possibility of deep fading [1–3].

On the other hand, in view of multiuser communication, we can exploit fading through channel quality feedback from receivers to a transmitter and user scheduling at a transmitter [4, 5]. If there are three users, as in Fig. 1.3(a), where channels are independent across users and the average channel gain of each user is one. If a transmitter

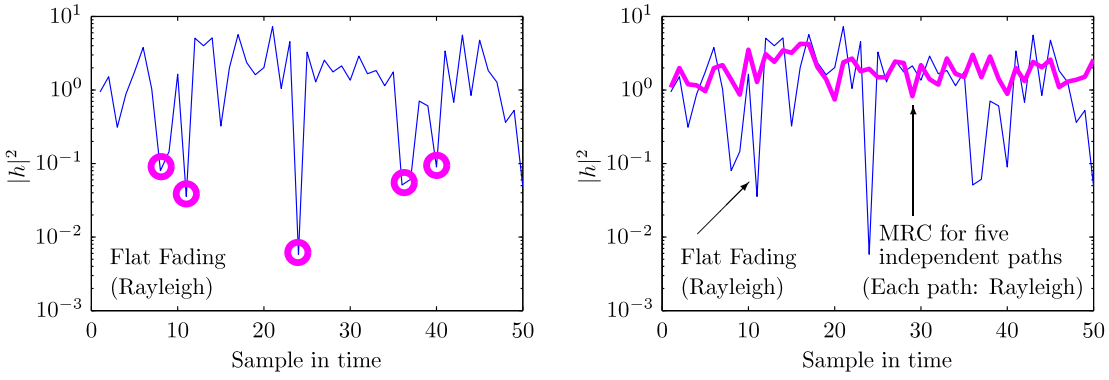

(a) (b)

Figure 1.2: Example of channel gain. (a) Frequency flat channel. (b) Equivalent channel after maximal ratio combining for $L = 5$.

schedules a user with the largest channel gain at any scheduling time instant, the channel gain of a selected user is depicted in Fig. 1.3(b). The average channel gain by maximum user scheduling, as in Fig. 1.3(b), is larger than the average channel gain of individual users, as in Fig. 1.3(a), which usually improves the sum rate of the system. This gain is called *multiuser diversity gain*.

Multiuser diversity gain follows from selection of the maximum. The relationship between multiuser diversity gain and the individual users' channel statistics can be found through the upper bound from order statistics. Suppose that there are N independent and identically distributed (*i.i.d.*) random variables X_i. Then, the upper bound for the average of the maximum is given by

$$\mathbb{E}\left[\max_{1\leq i\leq N} X_i\right] \leq \mathbb{E}[X_i] + \frac{N-1}{\sqrt{2N-1}}\sqrt{\mathrm{var}[X_i]} \tag{1.9}$$

where $\mathbb{E}[\cdot]$ denotes the expectation and $\mathrm{var}[\cdot]$ denotes variance. We note from (1.9) that multiuser diversity gain increases with

- the expectation of individual users' channel gain (corresponding to $\mathbb{E}[X_i]$),
- the number of users for selection (corresponding to N), and
- the dynamic range of the fluctuation of the individual users' channel gain (corresponding to $\mathrm{var}[X_i]$).

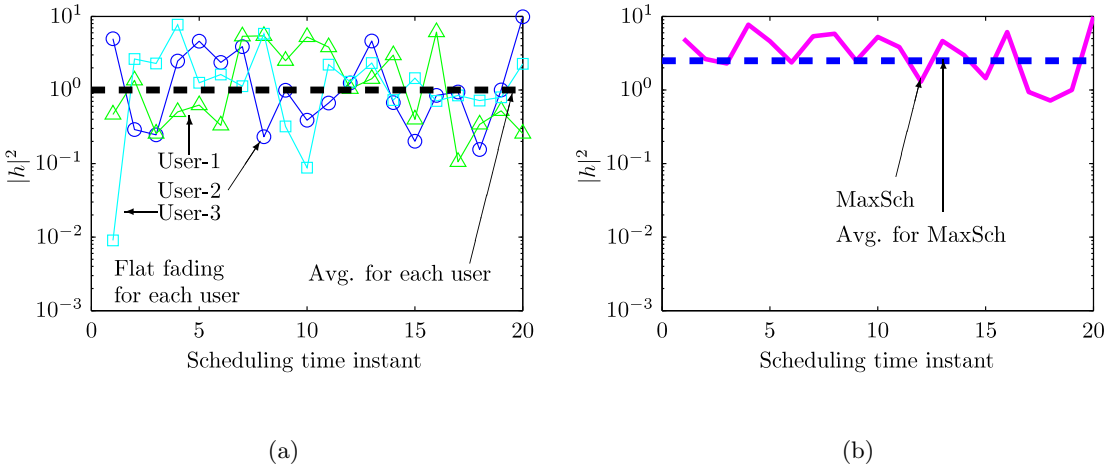

(a) (b)

Figure 1.3: Example of multiuser diversity gain. (a) Channel gain of three individual users. The black dotted line depicts the average channel gain. (b) Channel gain of a selected user from maximum user scheduling.

1.1.3 Joint Consideration of Scheduling and Diversity

As seen in Section 1.1.2, multiuser diversity gain increases with the number of users for selection, and the expectation and the dynamic range of the fluctuation of the individual users' channel gain [5, 6]. In a condition that the number of users in a system is small or that a channel shows the limited fluctuation, joint consideration of scheduling and diversity has been utilized.

For one example, suppose that there is N_{US} users in a system, which is relatively small for exploiting multiuser diversity. If maximum user scheduling is used, there are only N_{US} candidates for selection. Suppose that a transmitter has N_{T} transmit antennas and that a transmit antenna selection (TAS) scheme is combined with maximum user scheduling at the transmitter. When channels from transmit antennas to each user are assumed to be independent, each transmitter has N_{T} candidates for selection in each user. Thus, the total number of candidates is $N_{\mathrm{T}} \times N_{\mathrm{US}}$, which may greatly enhance multiuser diversity gain [7, 8].

For another example, suppose that users have N_{R} antennas. Similar to a TAS scheme, a receive antenna selection (RAS) scheme can greatly enhance multiuser diversity gain by increasing the number of candidates for selection. Instead of using RAS, the MRC scheme can be used to combine all the signals received at the receive antennas. The equation for a received signal in receive antenna-i is given by

$$y_i(t) = h_i x(t) + z_i(t), \tag{1.10}$$

where h_i is assumed to be a frequency flat fading channel. When all the received signals are combined in the optimal way for MRC, the average channel gain is given by

$$|h_{\mathrm{MRC}}|^2 = \sum_{i=1}^{N_{\mathrm{R}}} |h_i|^2. \tag{1.11}$$

If $\mathbb{E}[|h_i|^2] = \alpha$ and $\mathrm{var}[|h_i|^2] = \beta$, then $\mathbb{E}[|h_{\mathrm{MRC}}|^2] = N_{\mathrm{R}}\alpha$ and $\mathrm{var}[|h_{\mathrm{MRC}}|^2] = N_{\mathrm{R}}\beta$. Thus, note that multiuser diversity gain will be greatly enhanced as well. More examples can be found in [5–8].

In summary, the fundamental principle of joint consideration is to enhance multiuser diversity by increasing the number of independent candidates for selection in direct proportion to the number of transmit antennas or receive antennas [7, 8], or by increasing the variation in the channels between the transmitter and receivers as in MRC, or the opportunistic beamforming methods [5, 6].

1.1.4 Orthogonal Frequency Division Multiple Access

As seen in Section 1.1.1, multipaths in a fading channel cause frequency selectivity in the frequency domain. Usually, the hardware complexity to implement a system to combat a frequency flat fading channel is lower than that for a system to deal with a frequency selective fading channel. Thus, an effort to convert a frequency selective fading channel into a frequency flat fading channel has been made through an orthogonal frequency division multiplexing (OFDM) scheme.

For a frequency selective fading channel in (1.3), the discrete-time model at time m is given by

$$y[m] = \sum_{i=1}^{L} \alpha_i h_i[m] x[m-i+1] + z[m]. \tag{1.12}$$

The smearing of the previous symbol (*i.e.,* $x[m-i+1]$ for $i \neq 1$) is due to the filtering results in inter-symbol interference (ISI). The effect of ISI becomes more serious as the period of the symbol decreases, and thus ISI is a major obstacle to achieve high data-rate communication. By taking the discrete Fourier transform (DFT) of (1.12), the received signal at the frequency component-n is given by

$$Y[n] = H[n]X[n] + Z[n], \quad 1 \leq n \leq N_{\mathrm{SC}} \tag{1.13}$$

where $Y[n]$, $X[n]$, and $Z[n]$ denote the DFT of $y[m]$, $x[m]$ and $z[m]$ respectively, and N_{SC} denotes the size of DFT. $H[n]$ is given by

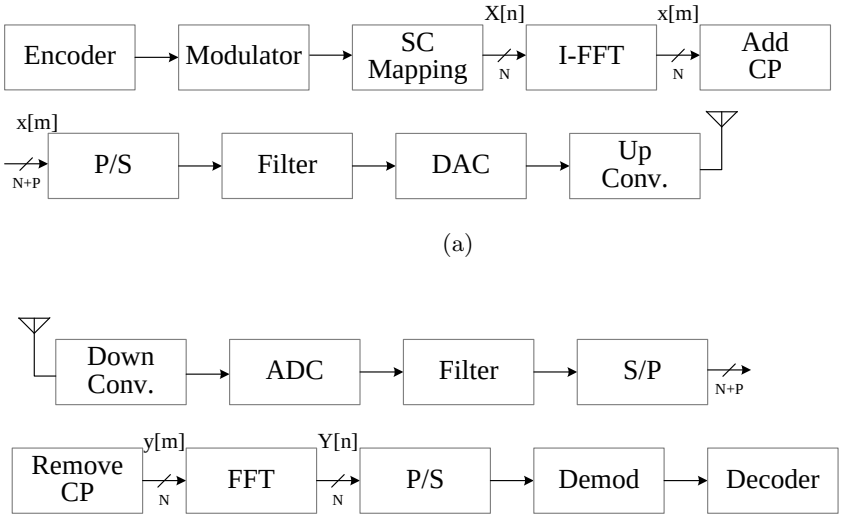

Figure 1.4: Block diagram of an OFDM system. 'SC' stands for the subcarrier and 'CP' stands for the cyclic prefix. (a) Transmitter. (b) Receiver.

$$H[n] = \sum_{i=1}^{L} \alpha_i h_i e^{-j\frac{2\pi(i-1)n}{N_{\mathrm{SC}}}}. \tag{1.14}$$

Each frequency index n is called *subcarrier-n*. In (1.13), the received signal $Y[n]$ experiences frequency flat fading since this takes the same form in (1.1), which also implies that there is no ISI in the frequency domain. The DFT operation that leads to this benefit is made possible because of adding and removing the cyclic prefix (CP) in an OFDM system. Thus, the biggest benefit of the OFDM scheme is that there is no requirement for the complicated filter bank to combat ISI or multipaths. The block diagram of a transmitter and a receiver is depicted in Fig. 1.4, where FFT stands for the fast Fourier transform.

Since the entire bandwidth of an OFDM system is usually much larger than the coherent bandwidth, there exists frequency selectivity among the channel gains of the orthogonal subcarriers. In many systems, subcarriers are grouped into multiple blocks which are used as the basic scheduling unit to allow multiple users to share the common frequency resource. This is called an *orthogonal frequency division multiple access (OFDMA)* system [9]. The construction of blocks of subcarriers is pursued in two ways to utilize frequency selectivity existing in the entire band. One method is to make up blocks using distributed subcarriers in the band. Since subcarriers inside a block

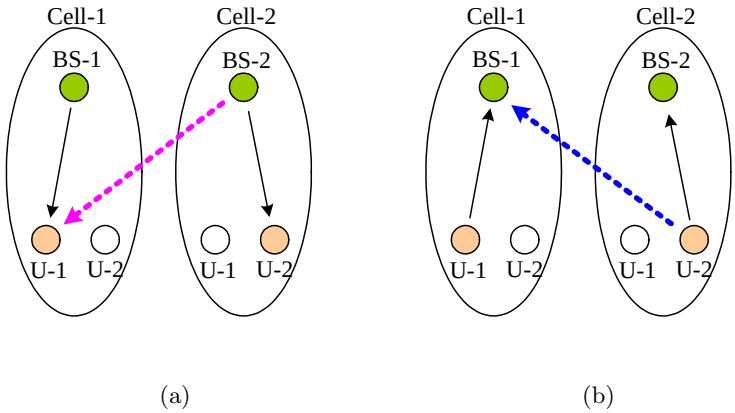

Figure 1.5: Simple diagram of a two-cell system. BS stands for a base station and 'U' stands for a user. (a) Downlink. (b) Uplink.

are likely to experience independent fading, frequency diversity gain can be achieved for each user in this approach. The other method is to make up blocks using consecutive subcarriers within the coherence bandwidth [10]. When this method is combined with frequency domain opportunistic user scheduling, multiuser diversity can be enhanced, since frequency selectivity across blocks can be utilized by scheduling the best user for each block.

1.1.5 Interference-limited Cellular Network

A cellular network is a radio network distributed over land areas to support wireless communication. The land areas are divided into many cells and each cell has at least one fixed-location transceiver known as a cell site or base station (BS). Each cell accommodates many portable terminals, such as mobile phones and laptops. The network enables these portable terminals to communicate with other terminals of any type which belongs to other networks. Depending on the extent of coverage of the cell, the cell is classified into macro cell, pico cell, and femto cell. The biggest advantage of the cellular network is that it enables moving terminals to communicate in a seamless way by what is called a handover operation. One example of a two-cell system is depicted in Fig. 1.5.

As seen in Fig. 1.5, a signal received in one cell can be interfered with by signals transmitted from other cells. Thus, the most important performance measure in a cellular network is the SINR. Suppose that there are two cells and that only one user is selected out of two users in each cell. Multiple antennas are assumed to be used at the BS and

by users. In downlink, the received signal equation in user-1 in cell-1 is given by

$$\mathbf{y}_1 = H_1\mathbf{w}_1x_1 + H_2\mathbf{w}_2x_2 + \mathbf{z}_1, \tag{1.15}$$

where H_i denotes a channel matrix from BS-i, $\mathbf{w}_i$ denotes a beamforming vector used at BS-i, x_i denotes a transmitted signal from BS-i and $\mathbf{z}_1$ denotes AWGN with an identity covariance matrix (*i.e.,* $\mathbf{I}$). Then, SINR of user-1 after multiplying with a receive beamforming vector $\mathbf{v}_1$ is given by

$$\text{SINR}_1 = \frac{P_1|\mathbf{v}_1H_1\mathbf{w}_1|^2}{\mathbf{I} + P_2|\mathbf{v}_1H_2\mathbf{w}_2|^2}, \tag{1.16}$$

where P_i denotes a transmitted power from BS-i. Note that H_2 is not dependent on a selected user in cell-2. Thus, SINR_1 is not affected by whatever user is selected in cell-2 if BS-2 does not use beamforming (*i.e.,* $\mathbf{w}_2 = [1, \cdots, 1]^T$) or BS-2 always uses the pre-determined set of beamforming vectors as in a random beamforming scheme [11]. Thus, independent user scheduling is possible in downlink without consideration of who would be selected in other cells.

Consider the uplink communication scenario, where H_i denotes a channel matrix from a selected user in cell-i to BS-1, $\mathbf{w}_i$ denotes a transmit beamforming vector used by a selected user in cell-i, and x_i denotes a transmitted signal from a selected user in cell-i. Then, the received signal equation at BS-1 is the same as (1.15) and SINR_1 at BS-1 the same as (1.16). Contrary to downlink, H_2 is dependent on a selected user in cell-2. Thus, SINR_1 is always affected by which user is selected in other cells. This makes the user scheduling problem in uplink more difficult and we address this issue in Chapter 4.

1.2 Contributions of the Thesis

The main contributions of this dissertation are contained in Chapter 2–4. In Chapter 2 and Chapter 3, we consider an OFDMA system employing joint scheduling and diversity. In Chapter 2, we focus on reduced feedback and find the exact sum rate in the ideal channel environment. In Chapter 3, we develop the relationship between frequency diversity and multiuser diversity in a frequency selective channel. Based on the relationship, we find the channel selectivity that is desirable to maximize multiuser diversity gain. In Chapter 4, we consider an interference-limited uplink multi-cell system and propose techniques to enhance the sum rate of the system by utilizing scheduling and beamforming. The three parts are summarized below.

1.2.1 Reduced Feedback in an OFDMA System Employing Scheduling and Diversity Jointly

High data rate services are the main pursuit of next-generation wireless networks. The orthogonal frequency division multiple access (OFDMA) has emerged as a key technology for delivering high data rates for next generation networks [10, 12, 13]. This is mainly because the inherent OFDM technology has the ability to combat frequency selective fading as seen in Section 1.1.4. In addition, it offers flexibility in radio resource management (RRM), since the large total bandwidth is divided into many orthogonal subcarriers, and groups of them are used to allocate different portions of radio resources to different users in both the frequency and time domains.

As seen in Section 1.1.2, to exploit multiuser diversity inherent in a wireless network with multiple users, it is necessary to schedule a transmission, at any scheduling instant, to a user with the best channel condition [4, 5], which is also known as *opportunistic scheduling* [14]. In order to provide fairness, in addition to exploiting multiuser diversity, a normalized signal to noise ratio (SNR)-based or channel quality information (CQI)-based scheduling scheme is considered [15]. This can be regarded as a form of proportional fair scheduling [16, 17].

For the purpose of user scheduling and rate adaptation at the transmitter, information about the channel quality has to be fed back to the transmitter by the receivers. In joint scheduling and diversity in OFDMA systems, feedback may be needed for all the resource blocks as well as the antennas, which may easily overwhelm the feedback link traffic, even for a system with a small number of users. This motivates research into reduced feedback [18]. In the area of feedback reduction research, there are two main methods: feedback rate reduction related to quantization and feedback number reduction related to reducing the number of parameters being fed back. For an example, see [19, 20] and references therein. One way to obtain the feedback number reduction is what is called best feedback where a user sends back the best subset of the available whole information [21–30]. Specifically, let N_{RB} denote the total number of resource blocks in an OFDMA system or spatial degrees of freedom in a space division multiple access system. The feedback number reduction in best feedback can be obtained by letting users feed back information about only the best-N_{FB} blocks or fewer modes where N_{FB} is smaller than N_{RB} [21–30].

In this dissertation, we consider an OFDMA system employing joint scheduling

and transmit diversity techniques. Consecutive subcarriers are assumed to make up resource blocks which are the basic scheduling resource unit. An ideal channel model is assumed for each resource block, that is, flat inside a block and independent across blocks. The transmitter schedules a transmission in each resource block to a user with largest normalized channel quality information among users who provided feedback, where normalization is considered to assure fairness across users.

We focus on feedback reduction, specifically best-N_{FB} feedback. Regarding best-N_{FB} feedback, researches have been limited to investigate the asymptotic sum rate scaling of a system or to take approximation for the sum rate or to consider only quantized feedback information or to analyze the exact sum rate only for $N_{\mathrm{FB}} = 1$ and $N_{\mathrm{FB}} = N_{\mathrm{RB}}$ [21–30]. Thus, we asked if the exact sum rate of a system with best-N_{FB} feedback can be obtained for general values of N_{FB}, various diversity techniques, and both non-quantized and quantized feedback information. To answer this question, we develop a unified framework consisting of four steps to analyze the sum rate of a system with best-N_{FB} feedback. The framework is developed in detail with an application to TAS both for non-quantized quantized channel quality information in Section 2.3, and then to other diversity techniques in Section 2.4. We consider a general value of N_{FB}, and present closed-form expressions.

In best-N_{FB} feedback, we asked how much feedback is required to make the sum rate gap between a full feedback scheme and a best-N_{FB} feedback scheme negligible while minimizing uplink feedback overhead. To answer this question, we approximate the sum rate ratio, *i.e.,* the ratio of the sum rate obtained by a partial feedback scheme to the sum rate obtained by a full feedback scheme in Section 2.5. We express the sum rate ratio as a function of the feedback ratio ($\frac{N_{\mathrm{FB}}}{N_{\mathrm{RB}}}$), that is, the amount of feedback normalized by the total number of blocks. This enables us to provide a simple equation to determine the required feedback ratio for a pre-determined sum rate ratio. In the case of quantized CQI feedback, we also discuss a feedback design strategy to enhance the sum rate under a fixed feedback load. The details of this topic can be found in Chapter 2.

1.2.2 Relationship between Frequency Diversity and Multiuser Diversity in an OFDMA System Employing Joint Scheduling and Diversity

As seen in Section 1.1.1, frequency selectivity of a fading channel is usually due to resolvable multipaths in a channel and provides frequency diversity benefits [31]. Frequency selectivity controls the degree of correlation between subcarriers in an OFDMA system. Meanwhile, multiuser diversity gain increases with the number of candidates for selection as in (1.9). However, the relationship between multiuser diversity gain and the degree of correlation between subcarriers has not been well investigated. To give an idea for this question, suppose that there are N_{SC} identically distributed random variables X_i's and that N_{SC}, $\mathbb{E}[X_i]$ and $\mathrm{var}[X_i]$ are fixed. We assume that correlation between X_i's is a function of index difference as in Fig. 1.6(a). That is, $\rho_\ell = \mathbb{E}[(X_i - \mathbb{E}[X_i])(X_{i+\ell} - \mathbb{E}[X_{i+\ell}])]$. Now, two cases are considered regarding maximum selection.

First, suppose in Fig. 1.6(a) that the selection unit is an individual X_i and that Y is a maximum of X_i's as follows:

$$Y = \max_{1 \le i \le N_{\mathrm{SC}}} X_i. \tag{1.17}$$

In general, derivation of $\mathbb{E}[Y]$ is involved or not tractable. Instead, if all X_i's are *i.i.d.*, one idea for $\mathbb{E}[Y]$ can be given from (1.9). However, when $\rho_\ell \neq 0$ as in Fig. 1.6(a), we cannot directly use the relation in (1.9). To have some idea, consider a case that $\rho_\ell = 1$ for all ℓ, which means that all X_i's take the same values in each realization. Thus, in every selection, this case is equivalent to the case that there is only one random variable. This means that the equivalent number of candidates for selection is only one. Thus, $\mathbb{E}[Y]$ may have the smaller value than that for the case where all X_i's are independent (*e.g.,* $\rho_\ell = 0$). This shows that correlation between subcarriers decreases $\mathbb{E}[Y]$. Thus, multiuser diversity gain related to $\mathbb{E}[Y]$ may decrease with correlation ρ_ℓ. This is corresponding to the case where all the subcarriers are *dependent* and the scheduling unit is an individual subcarrier, where X_i denotes the SINR of each subcarrier.

Second, a random variable Z_b is defined as follows:

$$Z_b \triangleq \frac{1}{S_{\mathrm{RB}}} \sum_{i=(b-1)S_{\mathrm{RB}}+1}^{bS_{\mathrm{RB}}} \log_2(1 + X_i), \quad 1 \le b \le N_{\mathrm{RB}}, \tag{1.18}$$

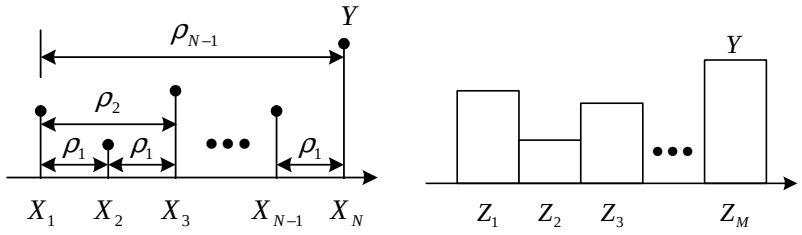

(a) (b)

Figure 1.6: Selection of maximum. (a) From identically distributed but *dependent* random variables. ρ_ℓ denotes correlation between two subcarriers. (b) From identically distributed but *dependent* random *blocks*.

where $S_{\mathrm{RB}} \times N_{\mathrm{RB}} = N_{\mathrm{SC}}$. Suppose in Fig. 1.6(b) that the selection unit is Z_b and Y is the maximum of Z_b's as follows:

$$Y = \max_{1 \le b \le N_{\mathrm{RB}}} Z_b. \tag{1.19}$$

Then, Z_b's are also dependent blocks when X_i's are dependent. To investigate the relationship between correlation ρ_ℓ and the maximum Y, consider a case that $\rho_\ell = 1$ for all ℓ. The correlation between Z_b's is also one, which means that Z_b's have the same value in each realization. Thus, $\mathbb{E}[Y]$ might be small in this case because the equivalent number of candidates for selection is one in (1.19). On another hand, when X_i's are independent, all Z_b's are also independent, which leads that the equivalent number of candidates for selection in (1.19) is N_{RB}, the maximum. However, Z_b itself would be small because of concavity of $\log(1+x)$. For example, suppose two set of numbers with the identical sum of elements as, $\mathfrak{S}_1 = \{1, 1, 1\}$ and $\mathfrak{S}_2 = \{\frac{3}{2}, 1, \frac{1}{2}\}$. Then, $Z_1 = \frac{1}{3}(\log_2(1+1) + \log_2(1+1) + \log_2(1+1)) = 1$, and $Z_2 = \frac{1}{3}(\log_2(1+\frac{3}{2}) + \log_2(1+1) + \log_2(1+\frac{1}{2})) = 0.9690$. This implies that variation of X_i's is not good for Z_b. Thus, $\mathbb{E}[Y]$ might not be large either. Therefore, there can be optimal correlation to maximize $\mathbb{E}[Y]$ between $\rho_\ell = 0$ and $\rho_\ell = 1$. This is corresponding to the case where subcarriers are dependent and the scheduling unit is *blocks* of subcarriers. Z_b denotes the block average throughput.

In [32], the interaction between multiuser diversity and frequency diversity was studied. However, the scheduling unit block was assumed to be the whole frequency band, which is the special case of Fig. 1.6(c) when $N_{\mathrm{RB}} = 1$. It was shown that the flat fading channel is the best in view of SNR-based selection of the users. However, a sub-block of the whole frequency band is considered as a scheduling unit, that is, $N_{\mathrm{RB}} > 1$, as is the general scheme in OFDMA systems, and throughput-based selection

of the users and fair scheduling are considered as well, the flat fading channel may not be best because the lack of diversity between blocks is likely to decrease the sum rate.

In this dissertation, to understand the interplay between frequency selectivity and multiuser diversity, we investigate the effect of frequency selectivity on an OFDMA multiuser system, where proportional fair scheduling is employed for user fairness. We assume that the scheduling unit is a block of contiguous subcarriers. We define intra-block sum correlation and inter-block sum correlation to characterize frequency selectivity in a frequency block-based scheduling system. We develop approximate expressions to the maximum of the block average throughput of an arbitrary user, and use the expressions to show that there exists an optimal frequency selectivity profile which maximizes multiuser diversity. We then propose two techniques to optimally add frequency selectivity, that is, determine per-user optimal cyclic delay for CDD, in a limited fluctuating channel. The details of this topic can be found in Chapter 2.

1.2.3 Joint Scheduling and Beamforming in an Uplink Cellular Network

As seen in Section 1.1.5, a signal received in one cell is interfered with by signal transmitted from other cells in a cellular network. A key challenge in the cellular network is handling of inter-cell interference [33,34]. In uplink communication, the received SINR in a cell is affected by which users are selected in other cells as in Fig. 1.5(b). This coupled nature makes the problem of user scheduling in uplink communication more difficult than in downlink communication. Then, we asked how the SINR of selected users in uplink communication can be enhanced. Specifically, the first issue is which users should be selected for communication and the second issue is how to design the beamforming vectors.

The cellular network is one of the most common systems with an interference channel. Although the capacity and the optimal schemes are already known for the Gaussian broadcast channel, neither the capacity nor an optimal scheme for the interference channel is fully known, even in the simplest two-user interference channel. In uplink communication, the best user sets for each cell might be able to be found through full cooperation between base stations and exhaustive search. However, this could be too complicated, and even seem infeasible, for a system with many users. An interference alignment scheme found recently might be an alternative answer. However,

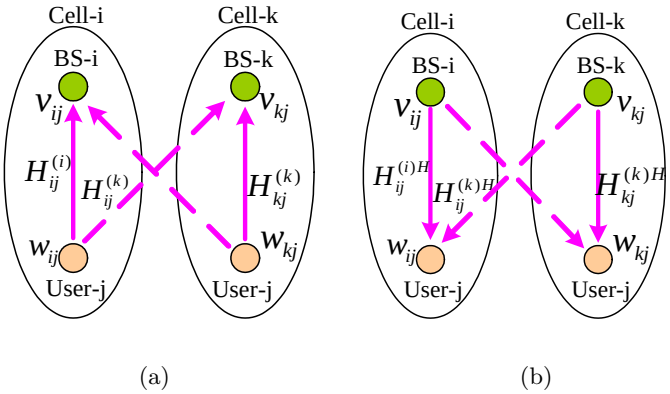

(a) (b)

Figure 1.7: (a) Primal network for an uplink communication system. (b) Dual network for an uplink communication system.

this requires that every transmitter should know the channel information for all the links in a system, which also seems too complicated. For this reason, we focus on finding a suboptimal scheme with low complexity to enhance the sum rate of the uplink communication system.

A transmit beamforming vector in a system usually affects all the receivers in a system. For example, consider an uplink communication system in Fig. 1.7(a). If we change a transmit beamforming vector $\mathbf{w}_{ij}$ for user-j in cell-i, both BS-i and BS-k are affected by the change. On the other hand, if we change a receive beamforming vector $\mathbf{v}_{ij}$ at BS-i, only BS-i is affected by the change. This implies that a receive beamforming vector in a system affects only the receiver employing the vector. Thus, the problem of designing a transmit beamforming vector is more challenging than designing a receive beamforming vector. Therefore, conversion of the problem of transmit beamforming vector design into that of receive beamforming vector design has been given through the dual network where the roles of a transmitter and a receiver are switched as in Fig. 1.7(b) [35, 36].

In this dissertation, we utilize the dual network to handle inter-cell interference in the uplink. Specifically, we propose a scheme to enhance the sum rate of a system by maximizing the SINR in a dual network through joint user scheduling and beamforming to exploit multiuser diversity as well as signal processing benefits. Users are required to compute a transmit beamforming vector and to feedback a metric which will be used as a user-scheduling metric in a base station (BS). One of the benefits of this procedure is that users use only local channel information to compute a transmit beamforming vector

and user-scheduling metric in a decoupled manner [37–39]. In addition to reducing inter-cell interference, we also propose a two-step user-selection procedure to improve the orthogonality of selected users in each cell to reduce intra-cell interference. The details of this topic can be found in Section 4.2.

Recently, an opportunistic interference alignment technique was proposed to enhance the sum rate in uplink communication [40]. Using local information at each user, authors try to align interference from other cells as much as possible. However, the scheme does not sufficiently exploit the signal dimension. Utilizing the developed principle based on maximizing the SINR in a dual network, we also propose a new scheme for opportunistic interference alignment. The details of this topic can be found in Section 4.3.

1.3 Thesis Organization

In Chapter 2 and Chapter 3, we consider an OFDMA system employing joint scheduling and diversity.

In Chapter 2, we focus on reduced feedback and find the exact sum rate for the ideal channel environment. For this purpose, we provide a unified framework consisting of four steps. The details of the technical content in Chapter 2 are as follows. In Section 2.2, we give the system model and provide an overview of the unified framework for the analysis. In Section 2.3, we develop a unified framework to analyze the sum rate of the TAS scheme. In Section 2.4, we analyze the sum rate for both OSTBC and CDD schemes utilizing the framework. In Section 2.5, we develop the relation between the sum rate ratio and feedback ratio, and derive the expression for the required number of feedback. In Section 2.6, we show numerical results which support the analytical results.

In Chapter 3, we develop the relationship between frequency diversity and multiuser diversity. Based on the relationship, we find the channel selectivity that is desirable to maximize multiuser diversity gain. Utilizing the finding, we propose two CDD-based schemes to optimally control the frequency selectivity of a channel. The details of the technical content in Chapter 3 are as follows. In Section 3.2, we give the channel and system model. In Section 3.3, we analyze the nature of the optimal frequency selectivity structure for maximizing the maximum of the block average throughput of an arbitrary user. In Section 3.4, we develop two CDD-based techniques to control frequency selectivity of a channel by determining the proper cyclic delay value utilizing either power

delay profile (PDP) or RMS delay spread. In Section 3.5, we provide numerical results to support the developed theory.

In Chapter 4, we consider an interference-limited uplink multi-cell system and propose techniques to enhance the sum rate of the system. The details of the technical content in Chapter 4 are as follows. In Section 4.2, we exploit network duality and propose two schemes to enhance the sum rate from joint scheduling and transmit beamforming. In Section 4.2.1, we give the system model. In Section 4.2.2, we develop the sum rate of the system. In Section 4.2.3, we describe the conventional user selection schemes. In Section 4.2.4, we propose two schemes to enhance the sum rate of the system by utilizing network duality. In Section 4.2.5, we compare the proposed beamforming strategy with the conventional ones. In Section 4.2.6, we show numerical results and compare the sum rate of the proposed schemes with the conventional one.

In Section 4.3, we propose a scheme in opportunistic interference alignment to enhance the sum rate. In Section 4.3.1, we give the system model. In Section 4.3.2, we develop the sum rate of the system. In Section 4.3.3, we explain the conventional opportunistic interference alignment scheme. In Section 4.3.4, we propose a scheme to enhance the sum rate by maximizing SINR in a dual network. In Section 4.3.5, we present numerical results and compare the sum rate with that of conventional schemes.

Finally, in Chapter 5, we summarize our contributions and outline the possible extensions of our work.

Chapter 2

Sum Rate Analysis of a Reduced Feedback OFDMA System Employing Joint Scheduling and Diversity

2.1 Introduction

Diversity is a common technique employed to mitigate the harmful effects of fading in a wireless channel and to achieve reliable communication [1–3]. This is achieved by creating and combining independent multiple copies of a signal between a transmitter and a receiver over various dimensions such as time, frequency and space [1–3]. On the other hand, when fading is viewed in a multiuser communication context and scheduling of users is introduced for sharing the common resources, multiuser diversity can be exploited to significantly increase the system throughput [4, 5]. To exploit multiuser diversity inherent in a wireless network with multiple users, it is necessary to schedule a transmission, at any scheduling instant, to a user with the best channel condition [4, 5], which is also known as opportunistic scheduling [14]. However, fairness becomes an issue in a system with asymmetric user fading statistics which leads to channel resources being dominated by strong users [5]. In order to provide fairness, in addition to exploiting multiuser diversity, a normalized signal to noise ratio (SNR)-based or channel quality information (CQI)-based scheduling scheme is considered [15]. This can be regarded as

a form of proportional fair scheduling [16].

The gain from multiuser diversity usually increases with the number of independent users in a system and with a large dynamic range for the channel fluctuation within the time of the scheduling window [5, 6]. To enhance the sum rate of a system, joint consideration of scheduling and traditional diversity schemes such as transmit antenna selection (TAS) and maximal ratio combining (MRC) at a receiver is addressed in [7, 8] and the references therein. The basic principle of joint consideration is to enhance multiuser diversity by increasing the number of independent candidates for selection directly proportional to the number of transmit antennas [7, 8], or by increasing the variation in the channels between the transmitter and receivers as in the opportunistic beamforming methods [5, 6]. For the purpose of user scheduling and rate adaptation at the transmitter, information about the channel quality has to be fed back to the transmitter by the receivers. As the number of users as well as the antennas at the transmitter increases, the amount of feedback becomes large placing an enormous burden on the feedback link traffic. In particular, the amount of feedback may become prohibitive when we consider OFDMA systems which have emerged as the basic physical layer communication technology to meet the high data rate services in future wireless communication standards [10]. With the goal of exploiting frequency diversity in user scheduling, subcarriers in OFDMA systems are grouped into resource blocks and used as the basic unit for user scheduling [10]. When we consider joint scheduling and diversity in OFDMA systems, feedback may be needed for all the resource blocks as well as the antennas, which may easily overwhelm the feedback link traffic even for a system with a small number of users. This motivates our research into schemes with reduced feedback.

Feedback reduction has received much interest in wireless communication research [18]. There are two main methods: feedback rate reduction related to quantization, and feedback number reduction related to reducing the number of parameters being fed back. See, for example, [19, 20] and references therein. For the feedback number reduction, a threshold-based technique is usually considered, so that only the users with a large probability of being scheduled feedback their information [41]. Let N_{RB} denote the total number of resource blocks in OFDMA systems or spatial degrees of freedom in a space division multiple access system. The feedback number reduction can be obtained by letting users feed back information about only the best-N_{FB} blocks or fewer modes when N_{FB} is smaller than N_{RB} [8, 24, 28, 29]. For OFDMA systems employing

joint scheduling and diversity, the performance of schemes employing feedback about the best-N_{FB} blocks, for a general N_{FB}, has not been rigorously studied. Only the performance for a best-1 feedback ($N_{\mathrm{FB}} = 1$) or a full feedback scheme ($N_{\mathrm{FB}} = N_{\mathrm{RB}}$) without consideration of diversity options are given in [29]. The analysis in [28] is for a general N_{FB}. However, it deals with a single-input single-output (SISO) system with quantized CQI feedback and consequently does not consider the various multi-antenna diversity techniques.

In this chapter, we consider an OFDMA system employing joint scheduling as well as using a multi-antenna transmit diversity technique. Various diversity options are considered in this work; Transmit antenna selection (TAS), orthogonal space time block codes (OSTBC) and cyclic delay diversity (CDD). For rate adaptation and user scheduling, we assume that users feedback to the transmitter the CQI values of the best-N_{FB} resource blocks out of a total of N_{RB} values. For a practical variant of the feedback system, we also consider quantized CQI. The transmitter schedules a transmission in each resource block to a user with largest normalized CQI among users who provided feedback, where normalization is considered to assure fairness across users. We develop a unified framework consisting of four steps to analyze the sum rate of the system with partial feedback of either non-quantized or quantized CQI for a general N_{FB}, and present closed-form expressions.

Our results show that the performance gap between a full feedback scheme and a best-1 ($N_{\mathrm{FB}} = 1$) feedback scheme is not negligible even when there are a moderate number of users. Then the question arises as to how many CQI values should be fed back to the transmitter to make the gap negligible while minimizing uplink feedback overhead. This issue is also addressed in our work based on the derived equations for the sum rate. Specifically, we approximate the sum rate ratio, *i.e.,* the ratio of the sum rate obtained by a partial feedback scheme to the sum rate obtained by a full feedback scheme. We express the sum rate ratio as a function of the feedback ratio ($\frac{N_{\mathrm{FB}}}{N_{\mathrm{RB}}}$), *i.e.,* the amount of feedback normalized by the total number of blocks. We show that the sum rate ratio is approximately the same as the probability of the complement of a scheduling outage which corresponds to the case that no user provides CQI to the transmitter for a certain block. This enables us to provide a simple equation to determine the required feedback ratio for a pre-determined sum rate ratio. In the case of quantized CQI feedback, we also discuss a feedback design strategy to enhance the sum rate under a fixed feedback

load.

In summary, the chapter has three main contributions. First, we present the cumulative distribution function (CDF) for the SNR of a selected user in the best-N_{FB} feedback system. This result has a convenient form in terms of a *polynomial* of the CDF of each user's CQI, which is *amenable* to further analytical evaluation. Second, we develop a unified framework to analyze the sum rate of a reduced feedback OFDMA system employing joint scheduling and diversity, and derive closed-form expressions for both the non-quantized and quantized CQI feedback schemes. Third, we approximate the sum rate result and develop an analytical and simple expression for the required feedback ratio to achieve a pre-determined sum rate ratio.

This chapter is organized as follows. In Section 2.2, we describe the system model and provide an overview of the unified framework for the analysis. In Section 2.3, we develop the framework and analyze the sum rate of the TAS scheme. In Section 2.4, we analyze the sum rate for both OSTBC and CDD schemes employing the framework. In Section 2.5, we develop the relation between the sum rate ratio and feedback ratio, and derive the expression for the required feedback ratio. In Section 2.6, we show numerical results and they support the analytical results. We conclude in Section 2.7.

2.2 System Model and Overview of the Framework

In this section, we first describe the system model and then provide an overview of the unified framework for the sum rate analysis.

2.2.1 System Model

We consider a multiple-input single-output (MISO) complex Gaussian broadcast channel with one base station equipped with N_{T} transmit antennas and N_{US} users each equipped with a single antenna, as shown in Fig. 2.1. An OFDMA system is assumed. In a multiuser OFDMA system the throughput is larger when the resource allocation is flexible and has high granularity, *e.g.,* assignment at the individual subcarrier level. However, the complexity and feedback overhead can be prohibitive, calling for simpler approaches. In our work, the overall subcarriers are grouped into N_{RB} resource blocks (RB), and each block contains contiguous subcarriers. The assignment is done at the block level, *i.e.,* a resource block is assigned to a user. The block size is assumed to be known and in practice can be determined at the medium access control (MAC)

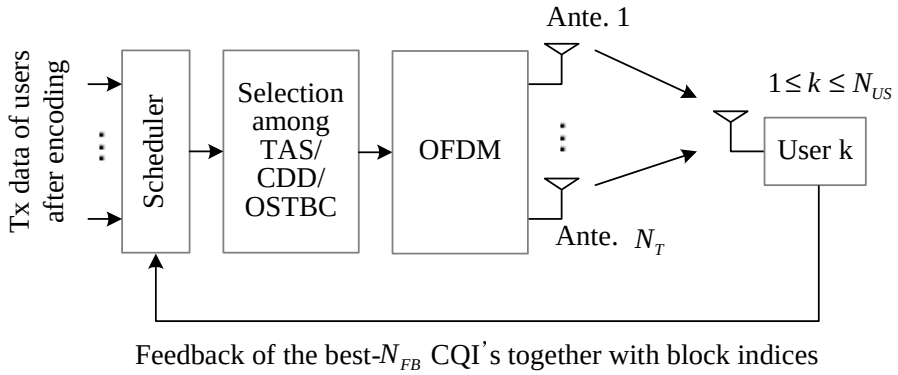

Figure 2.1: System block diagram of a multiuser OFDMA system. Best-N_{FB} CQIs are sent to the transmitter.

layer taking into account the number of users. For this system, we showed in [6] that the optimal channel selectivity maximizing the sum rate is flat within each block and independent across blocks. We assume the optimal channel selectivity condition in our analysis of the system performance.

Let $H_{k,r,i}$ denote the channel between transmit antenna-i and the receive antenna of user-k for resource block-r, where $1 \le k \le N_{\mathrm{US}}$, $1 \le r \le N_{\mathrm{RB}}$ and $1 \le i \le N_{\mathrm{T}}$. We assume that $H_{k,r,i}$ follows a complex Gaussian distribution, *i.e.,* $\mathcal{CN}(0, c_k)$,[1] where c_k denotes the average channel power of user-k and reflects the fact that the users are distributed asymmetrically. We assume that c_k for each user is known to the transmitter by infrequent feedback from users. We also assume that $H_{k,r,i}$ is independent across users (k), blocks (r) and transmit antennas (i). Then, the received signal of user-k at block-r satisfies the equation

$$y_{k,r} = H_{k,r}\ s_{k,r} + n_{k,r} \tag{2.1}$$

where $s_{k,r}$ is the transmitted symbol and $n_{k,r}$ is additive white Gaussian noise (AWGN) with $\mathcal{CN}(0, \sigma_w^2)$. We note that $H_{k,r}$ is the equivalent channel depending on the specific diversity technique and is a function of $H_{k,r,i}$, which will be shown in later sections.

For reliable and adaptive communication, the knowledge of the channel between the transmitter and receiver is required at the transmitter. For this purpose, we assume that channel quality information (CQI) of resource blocks is fed back from users to the transmitter. The feedback policy is that users measure CQI for each block at their

[1] $\mathcal{CN}(\mu,\sigma^2)$ denotes a circularly symmetric complex Gaussian distribution with mean μ and variance σ^2.

receiver and feed back the CQI values of the best-N_{FB} resource blocks from among the total N_{RB} values [29]. Since we assume that the users are asymmetrically distributed in their average SNR, scheduling is based on CQI normalized by each user's mean value at the transmitter. For each block, the user with largest normalized CQI is chosen from among the users who fed back CQI to the transmitter for that block. If no user provides CQI for a certain block, *i.e.,* the case of a scheduling outage in the block [29], we assume that the transmitter does not utilize that block. However, one can easily incorporate other variations such as round-robin scheduling or a scheduling scheme which maintains the previously assigned user. For diversity, we consider three different multiple transmit antenna techniques; transmit antenna selection (TAS) [42], cyclic delay diversity (CDD) [43],[2] and orthogonal space time block codes (OSTBC) [44]. Let $Z_{k,r}$ denote CQI of user-k at block-r, which will be the starting point of the analysis. Then, $Z_{k,r}$ depends on the diversity technique, the noise variance and channel $H_{k,r,i}$.

As the number of users increases, the amount of feedback will be prohibitive for a full feedback scheme, *i.e.,* CQI feedback for all the resource blocks, so that we focus on the sum rate for partial feedback schemes with a general N_{FB}. Instead of investigating the asymptotic property of the sum rate for a very large or infinite number of users [11, 45], we focus on the exact sum rate for the system with a finite number of users. Specifically, we develop a unified framework consisting of four steps to analyze the sum rate of this system with partial feedback of either non-quantized or quantized CQI, and present closed-form expressions. An overview of the framework is provided next.

2.2.2 Overview of the Unified Framework

The framework for the sum rate analysis consists of four steps, where the n-th step is denoted as Step-n. We first discuss the analysis in the non-quantized CQI case. We find F_{Z_k} in Step-1, *i.e.,* the CDF of $Z_{k,r}$ which is the CQI of user-k at block-r at a receiver.[3] This depends on the choice of the diversity technique. We find F_{Y_k} in Step-2, *i.e.,* the CDF of $Y_{k,r}$ denoting the SNR of user-k for resource block-r as seen by the transmitter as a consequence of partial feedback. We find $F_{X|\mathrm{cond}}$ in Step-3, *i.e.,*

[2]For CDD, we consider that phases are multiplied on the basis of a block to maintain the characteristic of flat fading inside a block. In a strict sense, the scheme we consider is classified as CDD when the block consists of a single subcarrier, and as the frequency domain opportunistic beamforming when the block consists of more than one subcarriers [5].

[3]Since we assume that blocks are identically distributed, for notational simplicity, we omit r in $F_{Z_{k,r}}$, which is also the case for other notations of CDFs.

the conditional CDF of X_r denoting the SNR of a selected user as a consequence of scheduling. The conditioning in Step-3 is related to the asymmetric user distribution in their average SNR and the number of contending users for the block. The important characteristics of $F_{X|\text{cond}}$ is that it has a convenient form in terms of a *polynomial in* F_{Z_k}, which is *amenable* to further integration to obtain the sum rate in Step-4. Thus, once we find F_{Z_k} and we have the integration result for a throughput equation with respect to an arbitrary power of $F_{Z_k}(x)$, *i.e.,* $\int_0^\infty \log_2(1+x)\, d\{F_{Z_k}(x)\}^n$ for an arbitrary positive integer n, we can obtain closed-form sum rate expressions in a straightforward manner.

In the quantized CQI case, following the same approach as the first two steps in the non-quantized case, we find F_W, the CDF of $W_{k,r}$ denoting the normalized CQI at a receiver and F_U, the CDF of $U_{k,r}$ denoting the normalized CQI as seen by the transmitter. Then, we find $P_{X^{\text{Q}}|\text{cond}}$ in Step-3, *i.e.,* the conditional probability mass function (PMF) of X_r^{Q}, the SNR of a selected user. By taking an average of throughputs over the PMF found, we can obtain closed-form sum rate expressions in Step-4. For easy reference, we summarize the steps in Table 2.1.

Table 2.1: The main steps for the unified framework to obtain the sum rate for both non-quantized CQI and quantized CQI.

Framework	Non-quantized CQI feedback	
	Random variable	Output
Step-1	$Z_{k,r}$: CQI at a receiver	F_{Z_k}
Step-2	$Y_{k,r}$: SNR seen at a transmitter	F_{Y_k}
Step-3	X_r: SNR of a selected user	$F_{X\|\text{cond}}$
Step-4	$\mathbb{E}_{\text{cond}}\mathbb{E}_{X_r}[\log_2(1+X_r)\|\text{cond}]$	
Framework	Quantized CQI feedback	
	Random variable	Output
Step-1	$W_{k,r}$: Normalized CQI at a receiver	F_W
Step-2	$U_{k,r}$: Normalized CQI seen at a transmitter	F_U
Step-3	X_r^{Q}: SNR of a selected user	$P_{X^{\text{Q}}\|\text{cond}}$
Step-4	$\mathbb{E}_{\text{cond}}\mathbb{E}_{X_r^{\text{Q}}}[\log_2(1+X_r^{\text{Q}})\|\text{cond}]$	

k: user index, r: block index.

In summary, Step-1 of the unified framework depends on the diversity technique. The next two steps (Step-2 and Step-3) depend on the feedback and scheduling policy.

Step-4 involves evaluating the performance measure. We explain the procedure by providing details of the four steps for the TAS scheme in Section 2.3. Then in Section 2.4, we focus on finding the CDF of $Z_{k,r}$ in Step-1 for OSTBC and CDD. Step-2 and Step-3 do not require much additional effort, and we provide the sum rate result utilizing Step-4.

2.3 Sum Rate Analysis with Application to TAS

In this section, we explain the details of the framework, consisting of the four steps in Table 2.1, with application to the transmit antenna selection (TAS)-based diversity scheme for both non-quantized CQI and quantized CQI.

2.3.1 Sum Rate Analysis for Non-quantized CQI

Step-1, Finding $F_{Z_k}(x)$

This step consists of finding the distribution of CQI. In TAS, a transmit antenna with the best channel condition among all the transmit antennas is selected for transmission [42]. Thus, the equivalent channel at block-r of user-k is a channel with maximum CQI across transmit antennas, *i.e.,* $H_{k,r} = H_{k,r,i^*}$ where $i^* = \arg\max_{1\le i\le N_{\mathrm{T}}} |H_{k,r,i}|^2$. Since we assume that $H_{k,r,i}$ follows $\mathcal{CN}(0, c_k)$, $|H_{k,r,i}|^2$ follows the Gamma distribution $\mathcal{G}(1, \frac{1}{c_k})$ [46, (17.6)]. Here, $\mathcal{G}(\alpha, \beta)$ denotes the Gamma distribution whose CDF is given by [46, (17.3)]

$$F(x) = \widetilde{\Gamma}(\alpha, \beta x) = \frac{1}{\Gamma(\alpha)} \int_0^{\beta x} t^{\alpha-1} e^{-t} dt, \tag{2.2}$$

where $\widetilde{\Gamma}(\cdot,\cdot)$ is the incomplete Gamma function ratio given by $\widetilde{\Gamma}(a, x) = \frac{1}{\Gamma(a)} \int_0^x t^{a-1} e^{-t} dt$ [46, (17.3)] and $\Gamma(\cdot)$ is the Gamma function given by $\Gamma(a) = \int_0^\infty t^{a-1} e^{-t} dt$ [47]. Then, equivalent CQI in TAS is $Z_{k,r} = |H_{k,r}|^2 = \max_{1\le i\le N_{\mathrm{T}}} |H_{k,r,i}|^2$. From the assumption of the independent and identical distribution (*i.i.d.*) for $H_{k,r,i}$'s in i, the CDF of $Z_{k,r}$ is given by

$$F_{Z_k}(x) = \Pr\left\{ Z_{k,r} \le x \right\} \overset{(a)}{=} \left[\Pr\left\{ |H_{k,r,i}|^2 \le x \right\} \right]^{N_{\mathrm{T}}} \overset{(b)}{=} \left[\widetilde{\Gamma}(1, \tfrac{x}{c_k}) \right]^{N_{\mathrm{T}}} \tag{2.3}$$

where (a) follows from the order statistics [48, 2.1.1] that $Z_{k,r}$ is the maximum of independent $|H_{k,r,i}|^2$s, and (b) follows from the fact that $|H_{k,r,i}|^2$ has the distribution $\mathcal{G}(1, \frac{1}{c_k})$. We note that the SNR at block-r of user-k is $\mathrm{SNR}_{k,r} = \rho Z_{k,r}$ where $\rho = P/\sigma_w^2$ when the total transmit power is P.

Step-2, Finding $F_{Y_k}(x)$

This step considers the distribution of CQI as a result of partial feedback. As a reminder, each user feeds back the best-$N_{\rm FB}$ CQI values to the transmitter. Let $Z_{k,(\ell)}$ denote the order statistics of $Z_{k,r}$'s of user-k, where $Z_{k,(1)} \leq \cdots \leq Z_{k,(N_{\rm RB})}$. Then, the feedback scheme is equivalent to each user determining the order statistics for its CQI and feeding back CQI $Z_{k,(\ell)}$'s, for $N_{\rm RB} - N_{\rm FB} + 1 \leq \ell \leq N_{\rm RB}$ and the corresponding resource block indices. Let $Y_{k,r}$ denote the SNR corresponding to received CQI at the transmitter for user-k at block-r through feedback. If user-k provides feedback containing CQI for block-r, then based on the *i.i.d.* assumption of $Z_{k,r}$'s in r, the SNR $Y_{k,r}$ viewed from the transmitter can be interpreted as any one of the best-$N_{\rm FB}$ values multiplied by ρ. To capture this aspect, let $R_{k,r}$ denote a random variable with a probability mass function of $\Pr\{R_{k,r} = \ell\} = \frac{1}{N_{\rm FB}}$, for $N_{\rm RB} - N_{\rm FB} + 1 \leq \ell \leq N_{\rm RB}$. Then $Y_{k,r}$ is given by

$$Y_{k,r} = \rho Z_{k,(R_{k,r})}. \tag{2.4}$$

The CDF of $Y_{k,r}$, $F_{Y_k}(x)$, is given in the following lemma.

Lemma 1. For $F_{Z_k}(x)$ in (2.3), the CDF of $Y_{k,r}$ in (2.4) is given by

$$F_{Y_k}(x) = \sum_{m=0}^{N_{\rm FB}-1} e_1(N_{\rm RB}, N_{\rm FB}, m)\{F_{Z_k}(\tfrac{x}{\rho})\}^{N_{\rm RB}-m} \tag{2.5}$$

where

$$e_1(N_{\rm RB}, N_{\rm FB}, m) = \sum_{\ell=m}^{N_{\rm FB}-1} \tfrac{N_{\rm FB}-\ell}{N_{\rm FB}} \tbinom{N_{\rm RB}}{\ell} \tbinom{\ell}{m} (-1)^{\ell-m}. \tag{2.6}$$

Proof: See Appendix A.1.

Corollary 1. When $N_{\rm FB} = N_{\rm RB}$ (*i.e.,* full feedback), $e_1(N_{\rm RB}, N_{\rm RB}, m) = 1$ for $m = N_{\rm RB} - 1$, and 0 otherwise.

Proof: See Appendix A.2.

For example in best-1 feedback ($N_{\rm FB} = 1$), since $e_1(N_{\rm RB}, 1, m)$ is only non-zero for $m = 0$ and the value is 1, we can verify that (2.5) reduces to $F_{Y_k}(x) = \{F_{Z_k}(\frac{x}{\rho})\}^{N_{\rm RB}}$, which confirms $Y_{k,r} = \rho \times \max_{1 \leq r' \leq N_{\rm RB}} Z_{k,r'}$ [48, 2.1.1]. In full feedback ($N_{\rm FB} = N_{\rm RB}$), since $e_1(N_{\rm RB}, N_{\rm RB}, m) = 1$ for $m = N_{\rm RB} - 1$ and zero otherwise from Corollary 1, we can verify that (2.5) reduces to $F_{Y_k}(x) = F_{Z_k}(\frac{x}{\rho})$, which confirms that $Y_{k,r} = \rho Z_{k,r}$. That is, $Y_{k,r}$ has the same statistics as $\mathrm{SNR}_{k,r}$ for full feedback.

Step-3, Finding the Conditional CDF of X_r

This step involves finding the distribution of the SNR of the channel of the user selected in the scheduling step based on partial feedback. Since a channel is assumed to be *i.i.d.* across the resource blocks for each user, the probability that a user provides the transmitter with CQI for block-r is $\frac{N_{\mathrm{FB}}}{N_{\mathrm{RB}}}$. Let S_r denote a set of users who provided CQI to the transmitter for block-r. Since the channel is independent across users, the number of users who provided CQI at block-r, *i.e.,* $|S_r|$, follows the binomial distribution with the probability mass function [49]

$$\Pr\{|S_r| = n\} = \binom{N_{\mathrm{US}}}{n} \left(\frac{N_{\mathrm{FB}}}{N_{\mathrm{RB}}}\right)^n \left(1 - \frac{N_{\mathrm{FB}}}{N_{\mathrm{RB}}}\right)^{N_{\mathrm{US}}-n}, \; 0 \le n \le N_{\mathrm{US}}. \tag{2.7}$$

For Step-3 related to the *user selection* in Table 2.1, let $U_{k,r} = \frac{Y_{k,r}}{\rho c_k}$, *i.e.,* normalized CQI of user-k in block-r viewed at the transmitter. Based on the scheduling policy, a user with the largest $U_{k,r}$ among users in S_r is scheduled on block-r by the transmitter. In our assumption, $Y_{k,r}$'s are independent but not identically distributed in k due to the different average SNR distribution (*i.e.,* different c_k) across users. However, $U_{k,r}$'s are *i.i.d.* in k as well because they are normalized by their average SNR, *i.e.,* ρc_k. Let k_r^* denote a random variable representing a selected user for transmission on block-r by the transmitter and X_r be the SNR of the selected user. Since, in our model we do not utilize a block when $|S_r| = 0$, we concentrate on the case $|S_r| \neq 0$. Note that $|S_r| = 0$ corresponds to a scheduling outage. Then, it is shown in Appendix A.3 that the conditional CDF of X_r is given by

$$F_{X|\; k_r^*=k,|S_r|=n}(x) = \left\{F_{Y_k}(x)\right\}^n. \tag{2.8}$$

Since $F_{Y_k}(x) = F_{Z_k}(\frac{x}{\rho})$ for full feedback ($N_{\mathrm{FB}} = N_{\mathrm{RB}}$) and $F_{Y_k}(x) = \{F_{Z_k}(\frac{x}{\rho})\}^{N_{\mathrm{RB}}}$ for best-1 feedback ($N_{\mathrm{FB}} = 1$), for these two special cases we have

$$F_{X|\; k_r^*=k,|S_r|=n}(x) = \begin{cases} \left[F_{Z_k}(\frac{x}{\rho})\right]^n & : \text{Full FB} \\ \left[F_{Z_k}(\frac{x}{\rho})\right]^{nN_{\mathrm{RB}}} & : \text{Best-1 FB} \end{cases} \tag{2.9}$$

with $F_{Z_k}(x)$ given in (2.3). For the general case, substituting $F_{Y_k}(x)$ from Lemma 1 into (2.8), we have the following result.

Lemma 2. For $F_{Z_k}(x)$ in (2.3), the conditional CDF of X_r in (2.8) is given by

$$F_{X|\; k_r^*=k,|S_r|=n}(x) = \sum_{m=0}^{n(N_{\mathrm{FB}}-1)} e_2(N_{\mathrm{RB}}, N_{\mathrm{FB}}, n, m)\left\{F_{Z_k}(\tfrac{x}{\rho})\right\}^{nN_{\mathrm{RB}}-m} \tag{2.10}$$

where $e_2(N_{\rm RB}, N_{\rm FB}, n, m)$ is given by

$$\begin{cases} \{e_1(N_{\rm RB}, N_{\rm FB}, 0)\}^n, \quad m = 0 \\ \sum_{\ell=1}^{\min\{m, N_{\rm FB}-1\}} \frac{\{(n+1)\ell - m\}}{m e_1(N_{\rm RB}, N_{\rm FB}, 0)}\, e_1(N_{\rm RB}, N_{\rm FB}, \ell) \\ \qquad \times e_2(N_{\rm RB}, N_{\rm FB}, n, m-\ell), \quad 1 \le m < n(N_{\rm FB}-1) \\ \{e_1(N_{\rm RB}, N_{\rm FB}, N_{\rm FB}-1)\}^n, \quad m = n(N_{\rm FB}-1). \end{cases} \tag{2.11}$$

Proof: See Appendix A.4.

Step-4, Finding the Sum Rate

Now we use the derived CDF to obtain the sum rate of the OFDMA system. Since blocks are identically distributed, the sum rate is $R_{\rm SUM} = \frac{1}{N_{\rm RB}} \sum_{r=1}^{N_{\rm RB}} \mathbb{E}[\log(1+X_r)] = \mathbb{E}[\log(1+X_r)]$. From the property of the conditional expectation [49], we have

$$R_{\rm SUM} = \mathbb{E}_{k_r^*}\, \mathbb{E}_{|S_r|}\Big[\, \mathbb{E}_{X_r}\Big[\log(1+X_r) \mid |S_r| = 0\Big] + \mathbb{E}_{X_r}\Big[\log(1+X_r) \mid |S_r| \neq 0\Big]\, \Big]. \tag{2.12}$$

Since $X_r = 0$ when $|S_r| = 0$, the first term is zero and does not contribute to the sum rate. Other variations on the scheduling when there is a scheduling outage, as mentioned in Section 2.2.1, can be readily incorporated into the first term. Concentrating on the second term, the sum rate is further developed as follows:

$$\begin{aligned} R_{\rm SUM} &= \mathbb{E}_{k_r^*}\, \mathbb{E}_{|S_r|}\left[\int_0^\infty \log(1+x)\, d\Big\{F_{X|\ k_r^*=k, |S_r|=n}(x)\Big\} \;\Big|\; |S_r| = n \neq 0\right] \\ &\overset{(a)}{=} \mathbb{E}_{k_r^*}\, \mathbb{E}_{|S_r|}\left[\sum_{m=0}^{n(N_{\rm FB}-1)} e_2(N_{\rm RB}, N_{\rm FB}, n, m) \times \right. \\ &\qquad \left. \int_0^\infty \log(1+x)\, d\Big\{F_{Z_k}(\tfrac{x}{\rho})\Big\}^{nN_{\rm RB}-m} \;\Big|\; |S_r| = n \neq 0\right] \\ &\overset{(b)}{=} \frac{1}{N_{\rm US}} \sum_{k=1}^{N_{\rm US}} \sum_{n=1}^{N_{\rm US}} \binom{N_{\rm US}}{n} \left(\frac{N_{\rm FB}}{N_{\rm RB}}\right)^n \left(1 - \frac{N_{\rm FB}}{N_{\rm RB}}\right)^{N_{\rm US}-n} \times \\ &\qquad \sum_{m=0}^{n(N_{\rm FB}-1)} e_2(N_{\rm RB}, N_{\rm FB}, n, m) I_1(1, \tfrac{1}{\rho c_k}, (nN_{\rm RB} - m)N_{\rm T}), \end{aligned} \tag{2.13}$$

where (a) follows from the conditional CDF of X_r in (2.10); (b) follows from the fact that the PMF $\Pr\{k_r^* = k\} = \frac{1}{N_{\rm US}}$, because $U_{k,r}$ for user selection is *i.i.d.* in k, and

$\Pr\{|S_r| = n\}$ is given by (2.7), and that we have the following integration identity for the CDF $F_Z(x)$ with the form given in (2.2) [7]

$$\int_0^\infty \log(1+x)\, d\{F_Z(x)\}^n = I_1(\alpha, \beta, n). \tag{2.14}$$

It is shown in Appendix A.5 that $I_1(x, y, z)$ is given by

$$\tfrac{z}{(x-1)!\ln 2} \sum_{k=0}^{z-1} (-1)^k \tbinom{z-1}{k} \sum_{i=0}^{k(x-1)} b_{k,i}\, \tfrac{(x+i-1)!}{(k+1)^{x+i}} \sum_{\ell=0}^{x+i-1} \{(k+1)y\}^\ell\, \Gamma(-\ell, (k+1)y) e^{(k+1)y} \tag{2.15}$$

where $\Gamma(a, x) = \int_x^\infty t^{a-1} e^{-t} dt$ is the incomplete Gamma function [47, 8.350.2] and

$$b_{k,i} = \begin{cases} 1, & i = 0 \\ \frac{1}{i} \sum_{n=1}^{\min\{i, x-1\}} \frac{n(k+1)-i}{n!}\, b_{k,i-n}, & 1 \le i < k(x-1) \\ \frac{1}{[(x-1)!]^k}, & i = k(x-1) \end{cases}. \tag{2.16}$$

When $x = 1$, $I_1(x, y, z)$ is further reduced to [7, 17]

$$I_1(1, y, z) = \tfrac{1}{\ln 2} \sum_{k=1}^{z} (-1)^{k-1} \tbinom{z}{k} \Gamma(0, ky) e^{ky}. \tag{2.17}$$

We note that the conditional CDF of X_r in (2.10) is amenable to the integration since it is represented in terms of a polynomial in $F_{Z_k}(x)$ and we have the integration result in (2.14). Although we can represent the incomplete Gamma function in (2.15) using a finite summation as in [7] and [50], *i.e.,* $\Gamma(-\ell, (k+1)y) = \frac{(-1)^\ell}{\ell!}\Big[\Gamma(0, (k+1)y) - e^{-(k+1)y} \sum_{m=0}^{\ell-1} \frac{(-1)^m m!}{\{(k+1)y\}^{m+1}}\Big]$, we note that the form in (2.15) is much more appropriate for easy, fast and precise evaluation especially for large z, which is related to $N_{\rm RB}$, $N_{\rm US}$, and $N_{\rm T}$.

The expression can be simplified to obtain the sum rate for the special cases of best-1 and full feedback.

$$R_{\rm SUM} = \begin{cases} \frac{1}{N_{\rm US}} \sum_{k=1}^{N_{\rm US}} I_1(1, \frac{1}{\rho c_k}, N_{\rm US} N_{\rm T}) & : \text{Full FB} \\ \frac{1}{N_{\rm US}} \sum_{k=1}^{N_{\rm US}} \sum_{n=1}^{N_{\rm US}} \binom{N_{\rm US}}{n} \left(\frac{1}{N_{\rm RB}}\right)^n \left(1 - \frac{1}{N_{\rm RB}}\right)^{N_{\rm US}-n} & \\ \qquad \times I_1(1, \frac{1}{\rho c_k}, n N_{\rm RB} N_{\rm T}) & : \text{Best-1 FB.} \end{cases} \tag{2.18}$$

2.3.2 Sum rate analysis for Quantized CQI

In this subsection, we provide the sum rate for the partial feedback TAS-system with quantized CQI.

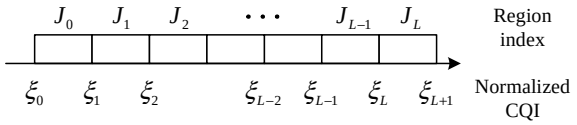

Figure 2.2: Quantization region for normalized CQI. ($\xi_0 = 0,\ \xi_{L+1} = \infty$) J_ℓ denotes a quantization region index.

Feedback Procedure and Scheduling for the Quantized System

For quantization purposes, it is useful to work with normalized CQI defined as $W_{k,r} = \frac{Z_{k,r}}{c_k}$. Each user computes $W_{k,r}$ for all the resource blocks and finds the best-N_{FB} $W_{k,r}$'s. Then, each user quantizes the selected $W_{k,r}$ values using a quantization policy depicted in Fig. 2.2. In the figure, J_ℓ for $0 \le \ell \le L$ denotes the quantization region index and ξ_ℓ denotes the boundary value between regions. More specifically, quantization is done as follows:

$$q_{k,r} = Q(W_{k,r}) = J_\ell, \quad \text{if} \quad \xi_\ell \le W_{k,r} < \xi_{\ell+1}. \tag{2.19}$$

Then, each user feeds back the quantized region indices $q_{k,r}$'s for the selected best-N_{FB} blocks to the transmitter together with the corresponding resource block indices. To exploit multiuser diversity as in the non-quantized CQI case, we assume for the scheduling policy that the transmitter schedules a transmission for each block to a user with the largest quantization region index. When multiple users provide the same quantization index, the transmitter randomly selects a user.

Step-1, Finding $F_W(x)$

The step is related to determining the distribution of normalized CQI. Since normalized CQI is $W_{k,r} = \frac{Z_{k,r}}{c_k}$ and $\Pr\{W_{k,r} \le x\} = \Pr\{Z_{k,r} \le c_k x\}$, the CDF of $W_{k,r}$ with the TAS diversity scheme is given from (2.3) by

$$F_W(x) = F_{Z_k}(c_k x) = \{\widetilde{\Gamma}(1, x)\}^{N_{\mathrm{T}}}. \tag{2.20}$$

Step-2, Finding $F_U(x)$

The step is related to the feedback policy and involves determining the order statistics for normalized CQI, $W_{k,(1)} \le \cdots \le W_{k,(N_{\mathrm{RB}})}$, quantizing $W_{k,(\ell)}$ for $N_{\mathrm{RB}} - N_{\mathrm{FB}} + 1 \le \ell \le N_{\mathrm{RB}}$, and sending back the corresponding quantized region indices together with block indices. Defining $U_{k,r} = \frac{Y_{k,r}}{\rho c_k}$, from Section 2.3.1 it denotes normalized CQI as seen

by the transmitter. Since $\Pr\{U_{k,r} \le x\} = \Pr\{Y_{k,r} \le \rho c_k x\}$, the CDF of $U_{k,r}$ in TAS is given by

$$F_U(x) = F_{Y_k}(\rho c_k x) \overset{(a)}{=} \sum_{m=0}^{N_{\mathrm{FB}}-1} e_1(N_{\mathrm{RB}}, N_{\mathrm{FB}}, m)\{\widetilde{\Gamma}(1,x)\}^{(N_{\mathrm{RB}}-m)N_{\mathrm{T}}} \tag{2.21}$$

where (a) follows from (2.5) and (2.20), and $e_1(N_{\mathrm{RB}}, N_{\mathrm{FB}}, m)$ is given in (2.6).[4] For the two special cases, we have $F_U(x) = \{\widetilde{\Gamma}(1,x)\}^{N_{\mathrm{T}}}$ for full feedback ($N_{\mathrm{FB}} = N_{\mathrm{RB}}$) from Corollary 1 and $F_U(x) = \{\widetilde{\Gamma}(1,x)\}^{N_{\mathrm{RB}}N_{\mathrm{T}}}$ for best-1 feedback ($N_{\mathrm{FB}} = 1$).

Let $U_{k,r}^{\mathrm{Q}}$ denote the quantization index received at the transmitter through feedback, which is equivalent to quantizing $U_{k,r}$ based on the policy in (2.19). The distribution of $U_{k,r}^{\mathrm{Q}}$ can be readily determined from the distribution of $U_{k,r}$ given above. It is shown in Appendix A.6 that $U_{k,r}^{\mathrm{Q}}$ is *i.i.d.* in k and r. Then, a user with the largest $U_{k,r}^{\mathrm{Q}}$ is selected for block-r by the transmitter in the next step.

Step-3, Finding the Conditional PMF of X_r^{Q}

Let X_r^{Q} denote the SNR of a user selected for a transmission in block-r. Suppose that n users provided the quantization index for block-r, *i.e.,* $|S_r| = n$ recalling that S_r denotes the set of those users. We note that the probability for each user to be selected is equal since $U_{k,r}^{\mathrm{Q}}$'s are *i.i.d.* across users. For the selected quantization index to be J_ℓ, no one should provide a larger quantization index than J_ℓ (*i.e.,* $U_{k,r}^{\mathrm{Q}} \le J_\ell$) and at least one user should provide the quantization index equal to J_ℓ. Thus, for $1 \le k \le N_{\mathrm{US}}$ and $0 \le \ell \le L$, it is shown in Appendix A.7 that the conditional PMF of X_r^{Q} is given by

$$\Pr\{X_r^{\mathrm{Q}} = \rho c_k \xi_\ell \Big| |S_r| = n\} = \tfrac{1}{N_{\mathrm{US}}}\left[\{F_U(\xi_{\ell+1})\}^n - \{F_U(\xi_\ell)\}^n\right]. \tag{2.22}$$

Step-4, Finding the Sum Rate

To calculate the sum rate, we assume that the modulation level for the transmission to the selected user-k is assumed to be determined as $\log(1+\rho c_k \xi_\ell)$ so as to prevent an outage of the link when user-k with a quantization level J_ℓ is selected. It is shown in Appendix A.8 that the sum rate is given by

$$R_{\mathrm{SUM}} = \mathbb{E}[\log(1+X_r^{\mathrm{Q}})] = \sum_{k=1}^{N_{\mathrm{US}}}\sum_{\ell=1}^{L} \frac{\log_2(1+\rho c_k \xi_\ell)}{N_{\mathrm{US}}}$$

[4] $F_U(x) \triangleq F_{U_{k,r}}(x)$ for notational simplicity since $U_{k,r}$'s are *i.i.d.* in k and r.

$$\times I_2(F_U(\xi_\ell), F_U(\xi_{\ell+1}), N_{\rm US}, N_{\rm FB}/N_{\rm RB}), \tag{2.23}$$

where $I_2(x, y, z, r)$ is given by

$$I_2(x, y, z, r) = \{1 - r\,(1 - y)\}^z - \{1 - r\,(1 - x)\}^z\,. \tag{2.24}$$

For full feedback as a special case, we have

$$R_{\rm SUM} = \tfrac{1}{N_{\rm US}} \sum_{k=1}^{N_{\rm US}} \sum_{\ell=0}^{L} \log(1 + \rho c_k \xi_\ell) \left[\{F_W(\xi_{\ell+1})\}^{N_{\rm US}} - \{F_W(\xi_\ell)\}^{N_{\rm US}} \right]. \tag{2.25}$$

2.4 Sum Rate Analysis with Application to OSTBC and CDD

Since the diversity technique affects the distribution of $Z_{k,r}$ or $W_{k,r}$ in Step-1, we focus in this section on deriving F_{Z_k} and F_W for OSTBC and CDD. Step-2 and Step-3 from the TAS analysis can be adopted with no change. Then, we can obtain the sum rate by carrying out Step-4.

2.4.1 Sum Rate for the Orthogonal Space Time Block Codes (OSTBC) Scheme

Sum Rate for Non-quantized CQI Feedback

For the equal power transmission from each antenna in OSTBC, effective CQI of user-k at block-r is given by the square of the 2-norm of a channel vector from the transmit antennas normalized by the number of transmit antennas [17, 44], *i.e.,*

$$Z_{k,r} = |H_{k,r}|^2 = \frac{1}{N_{\rm T}} \sum_{i=1}^{N_{\rm T}} |H_{k,r,i}|^2. \tag{2.26}$$

Since we assume that $H_{k,r,i}$ follows $\mathcal{CN}(0, c_k)$, $|H_{k,r,i}|^2$ follows the Gamma distribution $\mathcal{G}(1, \frac{1}{c_k})$ [46, (17.6)]. The sum of n *i.i.d.* random variables with $\mathcal{G}(\alpha, \beta)$ follows the Gamma distribution $\mathcal{G}(n\alpha, \beta)$ [51, 2-1-110] and a Gamma distributed random variable with $\mathcal{G}(\alpha, \beta)$ multiplied by a constant c follows the distribution of $\mathcal{G}(\alpha, \frac{\beta}{c})$.[5] Therefore, CQI $Z_{k,r}$ in (2.26) follows the Gamma distribution with $\mathcal{G}(N_{\rm T}, \frac{N_{\rm T}}{c_k})$. Thus, the CDF of $Z_{k,r}$ for Step-1 is given from (2.2) by

$$F_{Z_k}(x) = \widetilde{\Gamma}\Big(N_{\rm T}, \tfrac{N_{\rm T} x}{c_k}\Big). \tag{2.27}$$

[5]For $Y = cX$ where X follows $\mathcal{G}(\alpha, \beta)$, since $F_X(x) = \widetilde{\Gamma}(\alpha, \beta x)$ from (2.2), $F_Y(x) = \Pr\{cX \le x\} = \Pr\{X \le \frac{x}{c}\} = F_X(\frac{x}{c}) = \widetilde{\Gamma}(\alpha, \frac{\beta x}{c})$, which means that Y follows $\mathcal{G}(\alpha, \frac{\beta}{c})$.

Since the feedback policy and the scheduling policy in OSTBC are the same as in TAS, we can follow the same next two steps, specifically Step-2 in Section 2.3.1 and Step-3 in Section 2.3.1. Then, we obtain the conditional CDF of X_r, the SNR of a selected user in block-r, which is given for the general case in (2.10) and for two special cases in (2.9) where $F_{Z_k}(x)$ is to be replaced by (2.27).

We can carry out Step-4 by again exploiting the fact that the conditional CDF in (2.10) is represented in terms of a polynomial in $F_{Z_k}(x)$ in (2.27) and using the integration identity in (2.14). The sum rate $\mathbb{E}[\log(1+X_r)]$ of OSTBC for the general case of $N_{\rm FB}$ can be shown to be given by

$$R_{\rm SUM} = \frac{1}{N_{\rm US}} \sum_{k=1}^{N_{\rm US}} \sum_{n=1}^{N_{\rm US}} \binom{N_{\rm US}}{n} \left(\frac{N_{\rm FB}}{N_{\rm RB}}\right)^n \left(1-\frac{N_{\rm FB}}{N_{\rm RB}}\right)^{N_{\rm US}-n} \times \sum_{m=0}^{n(N_{\rm FB}-1)} e_2(N_{\rm RB}, N_{\rm FB}, n, m) I_1(N_{\rm T}, \tfrac{N_{\rm T}}{\rho c_k}, nN_{\rm RB}-m). \tag{2.28}$$

From (2.9) and (2.14), we have the sum rate for two special cases (*i.e.,* $N_{\rm FB}=N_{\rm RB}$ and $N_{\rm FB}=1$) as

$$R_{\rm SUM} = \begin{cases} \frac{1}{N_{\rm US}} \sum_{k=1}^{N_{\rm US}} I_1(N_{\rm T}, \frac{N_{\rm T}}{\rho c_k}, N_{\rm US}) & : \text{Full FB} \\ \frac{1}{N_{\rm US}} \sum_{k=1}^{N_{\rm US}} \sum_{n=1}^{N_{\rm US}} \binom{N_{\rm US}}{n} \left(\frac{1}{N_{\rm RB}}\right)^n \left(1-\frac{1}{N_{\rm RB}}\right)^{N_{\rm US}-n} & \\ \quad \times I_1(N_{\rm T}, \frac{N_{\rm T}}{\rho c_k}, nN_{\rm RB}) & : \text{Best-1 FB.} \end{cases} \tag{2.29}$$

Since the maximum code rate for complex OSTBC is 1 only for $N_{\rm T}=2$ and less than 1 otherwise [52], we note that the exact sum rate can be obtained by multiplying the code rate, *i.e.,* multiplying $\frac{3}{4}$ for $N_{\rm T}=3$ and 4.

Sum rate for Quantized CQI Feedback

We consider the same policy for quantization, feedback, and scheduling as that in Section 2.3.2. Since normalized CQI is $W_{k,r}=\frac{Z_{k,r}}{c_k}$ and $\Pr\{W_{k,r}\le x\}=\Pr\{Z_{k,r}\le c_k x\}$, the CDF of $W_{k,r}$ in OSTBC for Step-1 is given from (2.27) by

$$F_W(x) = F_{Z_k}(c_k x) = \widetilde{\Gamma}(N_{\rm T}, N_{\rm T}x). \tag{2.30}$$

Normalized CQI viewed at the transmitter for user-k at block-r is $U_{k,r}=\frac{Y_{k,r}}{\rho c_k}$. As in Step-2 in Section 2.3.2, the CDF of $U_{k,r}$ for OSTBC is given by

$$F_U(x) = F_{Y_k}(\rho c_k x) \overset{(a)}{=} \sum_{m=0}^{N_{\rm FB}-1} e_1(N_{\rm RB}, N_{\rm FB}, m) \{\widetilde{\Gamma}(N_{\rm T}, N_{\rm T}x)\}^{N_{\rm RB}-m} \tag{2.31}$$

where (a) follows from (2.5) and (2.30), and $e_1(N_{\mathrm{RB}}, N_{\mathrm{FB}}, m)$ is given in (2.6). For the two special cases, we have $F_U(x) = \widetilde{\Gamma}(N_{\mathrm{T}}, N_{\mathrm{T}}x)$ for full feedback ($N_{\mathrm{FB}} = N_{\mathrm{RB}}$), and $\{\widetilde{\Gamma}(N_{\mathrm{T}}, N_{\mathrm{T}}x)\}^{N_{\mathrm{RB}}}$ for best-1 feedback ($N_{\mathrm{FB}} = 1$). Since the conditional PMF of the SNR for a selected user for Step-3 is the same as (2.22), the sum rate of OSTBC has the same form as (2.23) where $F_U(x)$ in (2.31) is to be substituted.

2.4.2 Sum Rate for the Cyclic Delay Diversity (CDD)

Sum Rate for Non-quantized CQI Feedback

As in OSTBC and TAS, we derive the sum rate for CDD by first obtaining the CDF of $Z_{k,r}$ for Step-1 and then using the same remaining 3-steps of the framework in Table 2.1. For equal power transmission from each antenna, the equivalent channel of CDD with cyclic delay D_i at each transmit antenna is a dot product of a channel vector and complex phases determined by the cyclic delays [43], *i.e.*, $H_{k,r} = \frac{1}{\sqrt{N_{\mathrm{T}}}} \sum_{i=1}^{N_{\mathrm{T}}} H_{k,r,i} e^{j\frac{2\pi}{N} D_i}$. The resulting channel follows $\mathcal{CN}(0, c_k)$ since $H_{k,r}$ is a linear combination of complex Gaussian random variables [49]. Thus, CQI for the equivalent channel of user-k at block-r is given by

$$Z_{k,r} = |H_{k,r}|^2 = \frac{1}{N_{\mathrm{T}}} \left| \sum_{i=1}^{N_{\mathrm{T}}} H_{k,r,i} e^{j\frac{2\pi}{N} D_i} \right|^2, \tag{2.32}$$

which follows the Gamma distribution with $\mathcal{G}\left(1, \frac{1}{c_k}\right)$ [46, (17.6)]. From (2.2), the CDF of $Z_{k,r}$ for Step-1 is given by

$$F_{Z_k}(x) = \widetilde{\Gamma}\left(1, \frac{x}{c_k}\right). \tag{2.33}$$

We can see that $F_{Z_k}(x)$ in (2.33) for CDD is the same as that in (2.3) for TAS and in (2.27) for OSTBC where $N_{\mathrm{T}} = 1$. Thus, the sum rate of CDD is exactly the same as that in (2.13) and (2.18) for TAS and in (2.28) and (2.29) for OSTBC where $N_{\mathrm{T}} = 1$.

We note in [5, 43] that CDD or opportunistic beamforming is a technique to enhance the frequency diversity in a given channel by multiplying a gain to the channel randomly but in a controlled manner. We also note that the diversity gain increases with the number of the transmit antennas. However, since blocks are assumed to be already independent in our channel model, CDD does not have a room to increase frequency diversity even though we increase the number of the transmit antennas. Thus, we verify that the distribution of CQI of CDD in (2.33) does not depend on N_{T}.

Sum Rate for Quantized CQI Feedback

Since normalized CQI is $W_{k,r} = \frac{Z_{k,r}}{c_k}$ and $\Pr\{W_{k,r} \le x\} = \Pr\{Z_{k,r} \le c_k x\}$, the CDF of $W_{k,r}$ in CDD for Step-1 is given from (2.33) by

$$F_W(x) = F_{Z_k}(c_k x) = \widetilde{\Gamma}(1, x). \tag{2.34}$$

Normalized CQI viewed at the transmitter for user-k at block-r is $U_{k,r} = \frac{Y_{k,r}}{\rho c_k}$. Through the same step as Step-2 in Section 2.3.2, the CDF of $U_{k,r}$ for Step-2 is given by

$$F_U(x) = F_{Y_k}(\rho c_k x) \overset{(a)}{=} \sum_{m=0}^{N_{\mathrm{FB}}-1} e_1(N_{\mathrm{RB}}, N_{\mathrm{FB}}, m)\{\widetilde{\Gamma}(1, x)\}^{N_{\mathrm{RB}}-m} \tag{2.35}$$

where (a) follows from (2.5) and (2.34), and $e_1(N_{\mathrm{RB}}, N_{\mathrm{FB}}, m)$ is given in (2.6). Since the conditional PMF of the SNR for a selected user for Step-3 is the same as (2.22), the sum rate of CDD is given by (2.23) with $F_U(x)$ in (2.35). We can verify that the sum rate of CDD does not depend on N_{T} since blocks are assumed to be independent.

2.5 Relation between Probability of Normal Scheduling and the Sum Rate Ratio

In this section, we investigate the problem of minimizing the amount of feedback in the system by examining how much feedback is required to maintain the sum rate comparable to the sum rate obtained by a full feedback scheme. Let $R_{\mathrm{FB}} = \frac{N_{\mathrm{FB}}}{N_{\mathrm{RB}}}$ denote the feedback ratio, *i.e.,* the ratio of the number of feedback blocks to the total number of blocks. The design objective is to find the minimum feedback ratio while the achieved sum rate is above a certain fraction of the sum rate obtained by a full feedback scheme, *i.e.,*

$$\text{Find the minimum } R_{\mathrm{FB}}, \;\; s.t. \;\; R_{\mathrm{SUM}}^{\mathrm{ratio}} = \frac{R_{\mathrm{SUM}} \text{ by partial feedback}}{R_{\mathrm{SUM}} \text{ by full feedback}} \ge \eta. \tag{2.36}$$

Since we have the expressions for the sum rate for both partial and full feedback schemes, they can be substituted in the above equation and one can solve for N_{FB}. Here we make two simplifications and obtain a more tractable expression. We carry this out for the OSTBC diversity scheme.

First we note from (2.10) that we have

$$\sum_{m=0}^{n(N_{\mathrm{FB}}-1)} e_2(N_{\mathrm{RB}}, N_{\mathrm{FB}}, n, m) = 1, \tag{2.37}$$

since $F_{X|\ k_r^*=k,|S_r|=n}(\infty)=1$ and $F_{Z_k}(\infty)=1$ by the CDF property [49]. Second we note that $I_1(x,y,z)$ in (2.15) has almost the same value for large z when x and y are fixed. This is graphically illustrated in Fig. 2.3. We assume that $I_1(x,y,z_1)\simeq I_1(x,y,z_2)$ for large z_1 and z_2. More specifically, when we assume that $I_1(N_{\mathrm{T}},\frac{N_{\mathrm{T}}}{\rho c_k},nN_{\mathrm{RB}}-m)\simeq I_1(N_{\mathrm{T}},\frac{N_{\mathrm{T}}}{\rho c_k},N_{\mathrm{US}})$ in (2.28) and using (2.37), the sum rate of OSTBC for partial feedback in (2.28) reduces to

$$\begin{aligned} R_{\mathrm{SUM}} &\simeq \tfrac{1}{N_{\mathrm{US}}}\sum_{k=1}^{N_{\mathrm{US}}} I_1(N_{\mathrm{T}},\tfrac{N_{\mathrm{T}}}{\rho c_k},N_{\mathrm{US}})\sum_{n=1}^{N_{\mathrm{US}}}\binom{N_{\mathrm{US}}}{n}\left(\tfrac{N_{\mathrm{FB}}}{N_{\mathrm{RB}}}\right)^n\left(1-\tfrac{N_{\mathrm{FB}}}{N_{\mathrm{RB}}}\right)^{N_{\mathrm{US}}-n} \\ &\overset{(a)}{=} \tfrac{1}{N_{\mathrm{US}}}\sum_{k=1}^{N_{\mathrm{US}}} I_1(N_{\mathrm{T}},\tfrac{N_{\mathrm{T}}}{\rho c_k},N_{\mathrm{US}})\ \left(1-(1-\tfrac{N_{\mathrm{FB}}}{N_{\mathrm{RB}}})^{N_{\mathrm{US}}}\right), \end{aligned} \tag{2.38}$$

where (a) follows from the binomial theorem [49]. From the sum rate obtained by a full feedback scheme in (2.29) and the sum rate obtained by partial feedback in (2.38), we have

$$R_{\mathrm{SUM}}^{\mathrm{ratio}}=\frac{R_{\mathrm{SUM}}\text{ by partial feedback}}{R_{\mathrm{SUM}}\text{ by full feedback}}\simeq 1-(1-\tfrac{N_{\mathrm{FB}}}{N_{\mathrm{RB}}})^{N_{\mathrm{US}}}. \tag{2.39}$$

This approximation is well supported by the numerical results in Section 2.6. We note that the right-hand side in (2.39) is exactly the same as the probability that at least one user provides CQI to the transmitter in a block, *i.e.,* a probability of the complement of a scheduling outage.[6] From (2.36) and (2.39), the required feedback ratio is given by

$$R_{\mathrm{FB}}=\tfrac{N_{\mathrm{FB}}}{N_{\mathrm{RB}}}\geq 1-(1-\eta)^{\frac{1}{N_{\mathrm{US}}}}. \tag{2.40}$$

We note here that the required feedback ratio does not depend on the number of antennas and user distribution in the average SNR but on the number of users. In the same way, we compute the required feedback ratio for TAS making the same assumption about $I_1(x,y,z)$ and obtain the same result as (2.40). It is useful to note that the required feedback ratio in our system with fixed amount of feedback can be derived from the scheduling outage probability using the approximation above. This has similarities to the problem of determining the required threshold in a threshold-based feedback system considering a scheduling outage as in [41].

The above analysis was conducted assuming unquantized CQI. A similar analysis can be carried out assuming quantized CQI and employing some approximations one can obtain the same result as (2.39) and (2.40). We omit the details.

[6] Since a scheduling outage in a block happens when no user provides CQI for that block, its probability is $(1-\frac{N_{\mathrm{FB}}}{N_{\mathrm{RB}}})^{N_{\mathrm{US}}}$.

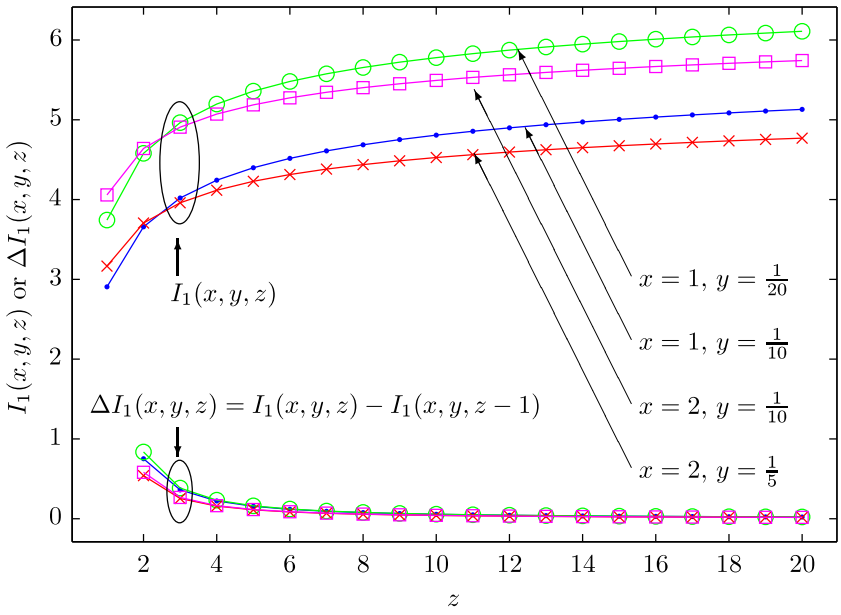

Figure 2.3: $I_1(x,y,z)$ and its slope. We note that when x and y are fixed, the rate of increase in $I_1(x,y,z)$ is very small when z is large.

2.6 Numerical Results

In this section, we conduct a numerical study of the analytical results to obtain some insight. To reflect asymmetrical user distribution in their average SNR, we use the exponential decay model for the average channel power of users [17]:

$$c_k = c\, e^{-\lambda k}, \quad s.t. \quad \sum_{k=1}^{N_{\mathrm{US}}} c_k = N_{\mathrm{US}}. \tag{2.41}$$

We can see that $\lambda = 0$ corresponds to *i.i.d.* users and that user asymmetry increases with λ.

2.6.1 Effect of Partial Feedback on the Sum Rate

In Fig. 2.4, we show the sum rate results computed using the analytical expressions and the simulation results as a function of the number of users. In the figure, TAS with $N_{\mathrm{T}} = 2$ is used and the average channel power is identical across users (*i.e.*, $\lambda = 0$) in Fig. 2.4(a) and different in Fig. 2.4(b). We can see that both analytic and simulation results are well matched. We can also see the effect of the feedback ratio (R_{FB}) on the sum rate. As we expect, the sum rate increases with the feedback ratio for both choices of λ. We note that the throughput gap between best-1 feedback ($R_{\mathrm{FB}} = 0.1$) and full

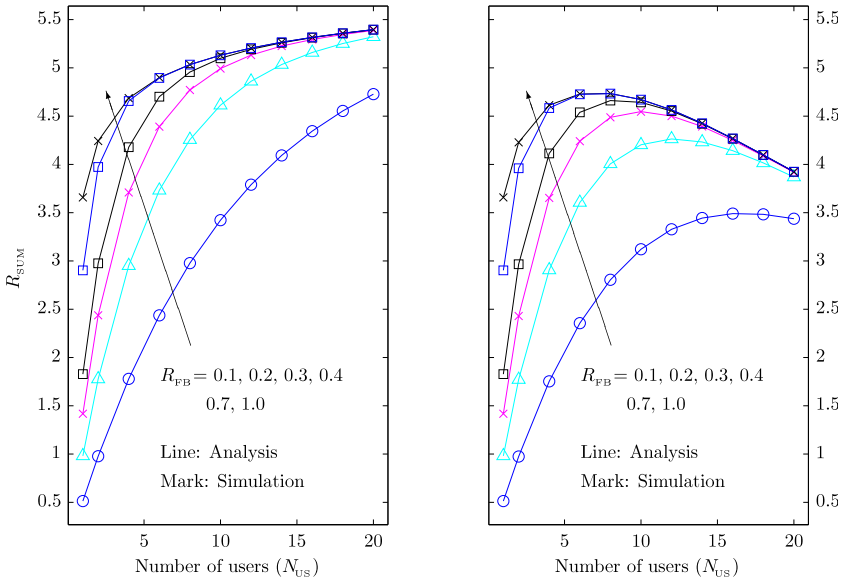

(a) $\lambda = 0$ (b) $\lambda = 0.3$

Figure 2.4: Effect of feedback ratio ($R_{\mathrm{FB}} = \frac{N_{\mathrm{FB}}}{N_{\mathrm{RB}}}$) on the sum rate for different λ in (2.41). (TAS, $N_{\mathrm{RB}} = 10$, $N_{\mathrm{T}} = 2$, and Tx SNR= 10dB)

feedback ($R_{\mathrm{FB}} = 1.0$) is large even when the number of users is 20. When the number of users is smaller than 10, we need $R_{\mathrm{FB}} \geq 0.4$ to attain a throughput comparable to a full feedback scheme. For $\lambda \neq 0$, we also note that fairness provided by proportional fair scheduling decreases the sum rate when the number of users is large, because the throughput variation is larger in the larger population and the throughput function ($\log_2(1+x)$) is concave, which is known as the fairness-capacity trade-off in [17].

In Fig. 2.5, we show the effect of the number of antennas for both TAS and OSTBC schemes with partial feedback. Users are asymmetrically distributed (*i.e.*, $\lambda \neq 0$). In general, multiuser diversity increases with the number of users, as well as the mean and the variance of the signal quality [6]. Since selection of antennas in TAS can be regarded as an increase of the number of users due to the increase of candidate channels for communication, the sum rate of TAS increases with N_{T}. However, since OSTBC decreases the variance of the signal quality by the averaging effect shown in (2.26), the sum rate of OSTBC decreases with N_{T}. In both feedback ratio of $R_{\mathrm{FB}} = 0.1$ and $R_{\mathrm{FB}} = 0.5$, we can verify this effect of the number of antennas on the sum rate for each transmit antenna scheme.

We show in Fig. 2.6 the sum rate result for partial feedback with quantized CQI. For the quantized CQI case, we consider $L = 1, 3, 7$ and 15 in Fig. 2.2, each of which

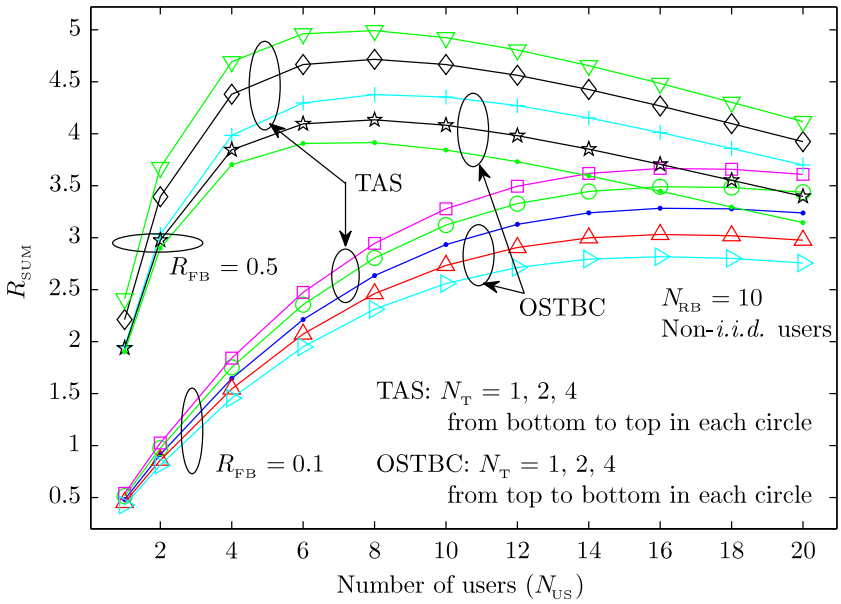

Figure 2.5: Effect of the number of antennas on the sum rate with partial feedback. (TAS and OSTBC, $N_{\mathrm{RB}} = 10$, λ in (2.41)= 0.3, and Tx SNR= 10dB.)

corresponds to $1, 2, 3$ and 4 bits in quantization ($N_{\mathrm{QB}} \triangleq \lceil \log_2(L+1) \rceil$). We show both the analytical and simulation results for the quantized CQI case. We find that both results are well matched. As we can expect, the sum rate increases as the number of bits for quantization increases. Since we focus on the analytic derivation of the sum rate for partial feedback, we do not optimize the quantization region but use the uniform quantization region, *i.e.*, $F_W(\xi_\ell) = \frac{\ell}{L+1}$ for $F_W(x)$ of TAS and OSTBC in Section 2.3.2 and Section 2.4.1. Finding the optimal region to maximize the sum rate considering system parameters including diversity type, the number of antennas and users, and the feedback ratio is left as future work.

In Fig. 2.7, we show the sum rate for quantized CQI with varying feedback loads. The feedback load is defined as the number of bits to be sent back from each user, *i.e.*, $L_{\mathrm{FB}} = N_{\mathrm{FB}}(\lceil \log_2 N_{\mathrm{RB}} \rceil + \lceil \log_2 N_{\mathrm{T}} \rceil + N_{\mathrm{QB}})$. In the figure, we compare two cases for every fixed L_{FB} at $12, 24$ and 64 where one of N_{FB}, N_{T} or N_{QB} is additionally fixed. Specifically, when N_{FB} is fixed at 8 in case of $L_{\mathrm{FB}} = 64$, we note that the larger N_{T} is always preferable to the larger N_{QB}. When N_{FB} is made variable, for both $L_{\mathrm{FB}} = 12$ and $L_{\mathrm{FB}} = 24$ we note that the larger N_{FB} is preferable for the small population and the larger N_{T} or N_{QB} is preferable for the large population. This suggests that N_{FB} should be first determined based on the number of users as in (2.36) and then based on the value for N_{T} the number

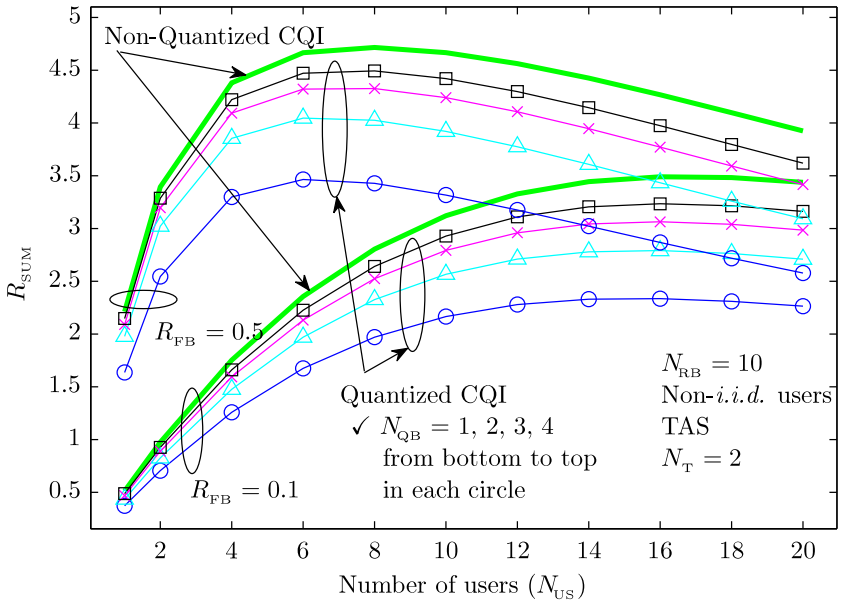

Figure 2.6: Comparison of the sum rate for non-quantized CQI and quantized CQI for the different feedback ratio. (TAS, $N_{\mathrm{RB}} = 10$, λ in (2.41)= 0.0, and Tx SNR= 10dB.)

of feedback bits N_{QB} should be determined.

2.6.2 The Sum Rate Ratio and Required Feedback Ratio

In Fig. 2.8, we study the $R_{\mathrm{SUM}}^{\mathrm{ratio}}$, *i.e.,* the sum rate normalized by that of a full feedback scheme as a function of the feedback ratio. As we expect, the feedback ratio required to achieve a large sum rate ratio decreases with increasing number of users. We note that the sum rate ratio does not depend on the transmit antenna scheme (*i.e.,* TAS or OSTBC) and user distribution (*i.e.,* λ). In Fig. 2.9, we can verify the tight relation between the sum rate ratio and the probability of the complement of a scheduling outage when the number of users is not so small. These two figures support the approximation for the sum rate ratio in Section 2.5, which states that the sum rate ratio is affected mainly by a scheduling outage which is caused when no user provides CQI for a block and that the probability of a scheduling outage depends only on the number of users and the feedback ratio as in (2.39). In Fig. 2.9, we also note that the sum rate ratio in the small population (*i.e.,* $N_{\mathrm{US}} = 2$) moves toward the approximation when the number of antennas increases since the approximation for $I_1(x, y, z)$ holds better for larger N_{T} especially for TAS.

In Fig. 2.10, we show the required feedback ratio to achieve a pre-determined

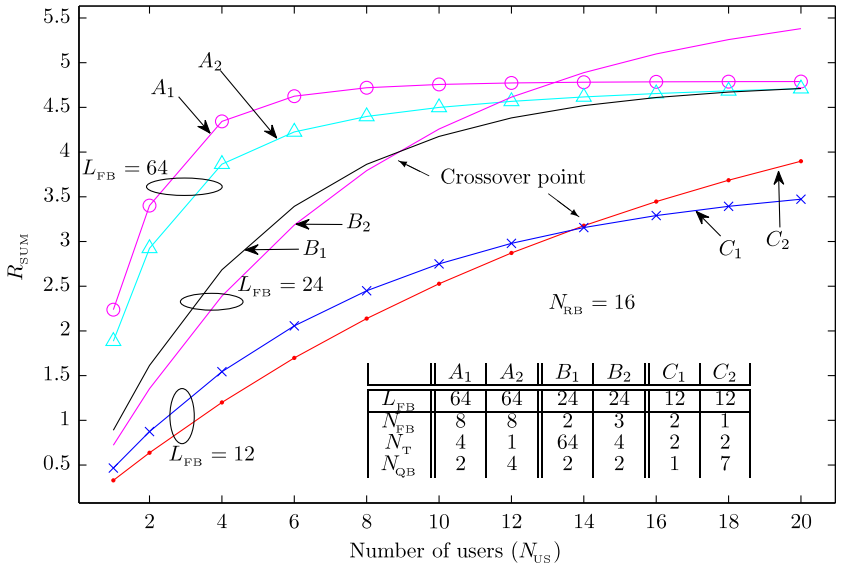

	A_1	A_2	B_1	B_2	C_1	C_2
$L_{\rm FB}$	64	64	24	24	12	12
$N_{\rm FB}$	8	8	2	3	2	1
$N_{\rm T}$	4	1	64	4	2	2
$N_{\rm QB}$	2	4	2	2	1	7

Figure 2.7: Comparison of the sum rate for the fixed feedback load where $L_{\rm FB} = N_{\rm FB}(4 + \lceil \log_2 N_{\rm T} \rceil + N_{\rm QB})$. (TAS, $N_{\rm RB} = 16$, λ in (2.41)= 0.0, and Tx SNR= 10dB.)

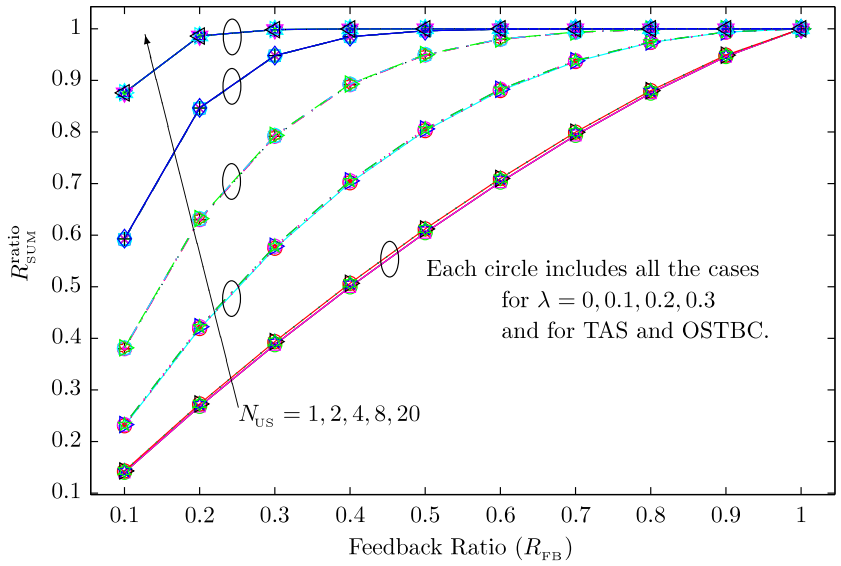

Figure 2.8: $R_{\rm SUM}$ normalized by that of a full feedback scheme vs. feedback ratio. We note that the normalized values are independent of transmit antenna scheme (TAS or OSTBC) and user distribution (Slopes).

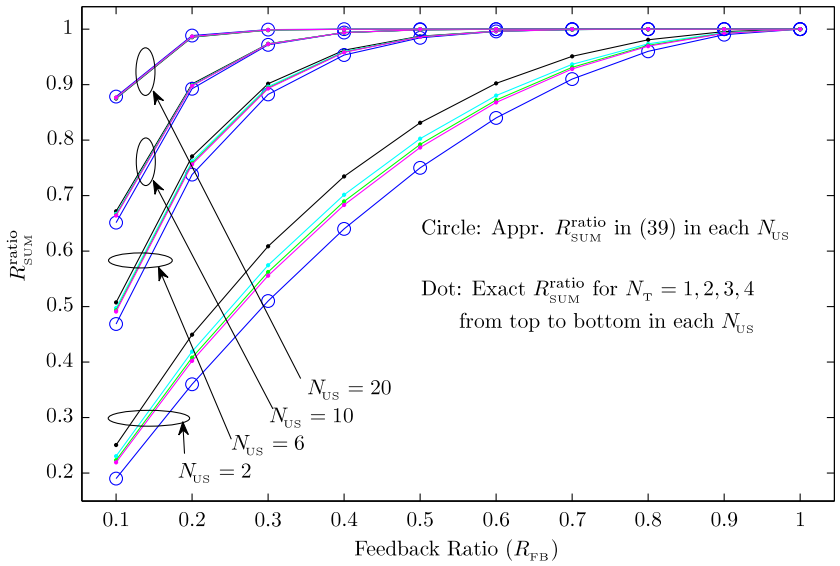

Figure 2.9: R_{SUM} normalized by that of a full feedback scheme and the probability of normal scheduling vs. feedback ratio.

sum rate ratio. As the number of users increases, the required feedback ratio decreases because the number of CQI values from all users increases and the scheduling outage probability decreases. On the other hand, we see that the required feedback ratio increases with the threshold for the smaller scheduling outage probability. We also note that the required feedback ratio is nearly independent of the transmit antenna scheme and the user distribution. That is, the required feedback ratio is mainly dependent on the number of users. Consequently, using this relation, we can determine the appropriate feedback ratio in designing a system.

2.7 Conclusion

We considered joint scheduling and diversity to enhance the benefits of multiuser diversity in a multiuser OFDMA scheduling system. We considered the role of partial feedback and developed a unified framework to analyze the sum rate of reduced feedback schemes employing three different multi-antenna transmitter schemes; Transmit antenna selection (TAS), orthogonal space time block codes (OSTBC) and cyclic delay diversity (CDD). Specifically, for the reduced feedback scheme wherein each user feeds back the best-N_{FB} CQI values out of a total of N_{RB} CQI values, both quantized and non-quantized CQI feedback were addressed. Considering largest normalized CQI scheduling in each

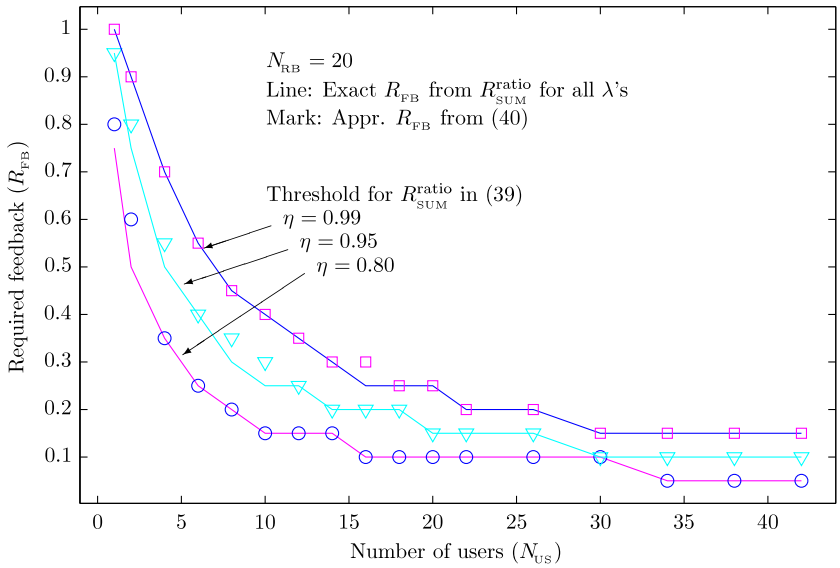

Figure 2.10: Required feedback ratio to achieve a pre-determined sum rate compared to that by a full feedback scheme.

block, closed-form expressions were derived for the sum rate for all the three multi-antenna transmitter schemes. Further, by approximating the sum rate expression, we derived a simple expression for the minimum required feedback ratio ($\frac{N_{FB}}{N_{RB}}$) to achieve a sum rate comparable to the sum rate obtained by a full feedback scheme.

This chapter, in full, is a reprint of "*Sum rate analysis of a reduced feedback OFDMA system employing joint scheduling and diversity*," which is in revision for publication in IEEE Transactions on Signal Processing. Sections of this chapter also appear in Vehicular Technology Conference 2011 Spring under the title "*Performance of a reduced feedback OFDMA system employing joint scheduling and diversity*". Both of these works are co-authored with Professor Bhaskar D. Rao. The dissertation author was the primary investigator and author of this paper.

Chapter 3

Optimal Frequency Selectivity to Multiuser Diversity in an OFDMA Scheduling System

3.1 Introduction

Multiuser diversity is inherent in all multiuser wireless networks with independent fading among users [4, 5, 53]. This diversity is exploited by scheduling the user with the best channel in a given time slot. It leads to an increase of the system sum rate as the number of users increases [4, 5, 53]. In a single-input single-output (SISO) system, this scheme is known to be optimal in the sense of maximizing the sum rate [4]. Meanwhile, user unfairness can result from the asymmetric user fading statistics wherein a channel resource is likely to be dominated by strong users [5]. To provide user fairness in addition to achieving multiuser diversity, fair schedulers employing a proportional fair or one-round-robin schemes are used [17]. The main idea of such fair schedulers is to schedule users on their own maximum/optimum channel [5, 17].

Frequency selectivity of a fading channel is usually due to resolvable multipaths in a channel which controls the degree of channel fluctuation in the frequency domain and provides frequency diversity benefits [31]. While frequency selectivity complicates channel estimation, this form of diversity can be exploited by employing advanced techniques at a receiver such as maximal ratio combining (MRC) or minimum mean squared estimation (MMSE) [54,55]. It improves the bit error rate (BER) in single carrier

systems [55] and increases outage capacity in multicarrier systems such as orthogonal frequency division multiplexing (OFDM) [56].

In particular, for an OFDM system operating in a channel with limited fluctuations, cyclic delay diversity (CDD) was proposed to increase frequency selectivity and achieve the better BER or outage performance [43, 56, 57]. This is an extension of conventional delay diversity in [58] to OFDM systems. Cyclic delay provides a mechanism to increase frequency selectivity by increasing the effective number of paths in the resulting channel. Based on results in [59] where it is shown that more frequency selective channels result in the lower BER, it is advantageous to have larger cyclic delays in a channel when channel estimation is ideal [43]. In [56], the outage performance with respect to frequency selectivity was investigated showing that larger selectivity, as measured by the root mean square (RMS) delay spread, leads to the better outage performance. In [59, 60], a new measure of frequency selectivity was proposed, *i.e.,* the inverse of the sum correlation of frequency components of a channel. They showed that the measure correlates with BER performance in a channel better than the conventional measure, the RMS delay spread.

In [7, 61], the relation between multiuser diversity and spatial diversity using multiple antennas is explored in the flat fading channel context. However, multiuser diversity has not been well studied with respect to the multipath channel, *i.e.,* frequency selectivity. In [32], the interaction between multiuser diversity and frequency diversity was studied when the scheduling unit block is the whole frequency band and when the maximum signal to noise ratio (SNR) user scheduling is employed. It was shown that the flat fading channel is the best in view of SNR-based selection of the users. However, if we consider a sub-block of the whole frequency band as a scheduling unit, as is the general scheme in orthogonal frequency division multiple access (OFDMA) systems, and consider fair scheduling as well, we show that the flat fading channel is not the best because the lack of diversity between blocks is likely to decrease the sum rate. Alternately, too large frequency selectivity is likely to decrease the block average throughput, which also leads to a decrease of the sum rate indicating that there is an optimal interplay between multiuser diversity and frequency diversity.

In this chapter, to understand the interplay between frequency selectivity and multiuser diversity, we investigate the effect of frequency selectivity on an OFDMA multiuser system, where proportional fair scheduling is employed for user fairness. We

assume that the scheduling unit is a block of contiguous subcarriers. As a measure of system performance, we choose the maximum of the block average throughput, and we show that this measure is a function of both intra-block and inter-block subcarrier correlation. We develop approximate expressions to the maximum of the block average throughput of an arbitrary user, and use them to show that there exists an optimal frequency selectivity profile which maximizes multiuser diversity. Utilizing the insights from this study, we then show how CDD techniques can be used to effectively control frequency selectivity. We propose two techniques to optimally add frequency selectivity, *i.e.,* determine per-user optimal cyclic delay for CDD, in a limited fluctuating channel. We show that our techniques achieve the large gain compared to the standard SISO technique and that the throughput is very close to the optimal sum rate possible with CDD.

In summary, the chapter has two main contributions. First, we provide an analytical relationship between multiuser diversity and frequency selectivity, and characterize optimal frequency selectivity. Second, we develop two CDD-based techniques to optimally control frequency selectivity in a given channel to maximize system throughput.

This chapter is organized as follows. In Section 3.2, we describe the channel and system model. In Section 3.3, we study the nature of the optimal frequency selectivity structure for maximizing the maximum of the block average throughput of an arbitrary user. In Section 3.4, we develop two CDD-based techniques to control frequency selectivity of the channel by determining the proper value for the cyclic delay based on a power delay profile (PDP) and an RMS delay spread, respectively. In Section 3.5, we provide numerical results to support the theory developed. They confirm the interplay between frequency selectivity and system throughput, and desirable frequency selectivity for maximizing throughput. They also document the effectiveness of our CDD-based techniques to add frequency selectivity. We conclude in Section 3.6.

3.2 System Model

We consider a single-input single-output (SISO) complex Gaussian broadcast channel with one base station and K users as shown in Fig. 3.1. An OFDMA system is assumed where N_{SC} and T denote the length (in samples) and the time interval respectively of the FFT (Fast Fourier Transform) used in the OFDM system. N_{SC} also equals the total number of subcarriers. A frequency selective channel is assumed and

the discrete time channel is given by

$$h(t) = \sum_{m=1}^{L} \alpha_m h_m \delta\left(t - \tfrac{(m-1)T}{N_{\mathrm{SC}}}\right), \tag{3.1}$$

where L is the number of paths, α_m is the average gain of path-m (*i.e.,* $\sum_{m=1}^{L} \alpha_m^2 = 1$), and h_m is the fading coefficient of path-m, which is modeled as $\mathcal{CN}(0,1)$, *i.i.d.* in m.[1] The frequency response at subcarrier-n is given by

$$H_n = \sum_{m=1}^{L} \alpha_m h_m e^{-j\frac{2\pi(m-1)n}{N_{\mathrm{SC}}}}, \quad 1 \le n \le N_{\mathrm{SC}} \tag{3.2}$$

Then, the received signal at subcarrier-n satisfies the equation $Y_n = H_n X_n + W_n$, where X_n is the transmitted symbol and W_n is additive white Gaussian noise (AWGN) with $\mathcal{CN}(0, \sigma_w^2)$. The received SNR on subcarrier-n, denoted by γ_n, is given by $\gamma_n = P|H_n|^2/\sigma_w^2$, where $\mathbb{E}[|X_n|^2] = P$. Based on the assumptions on h_m, the H_n's are jointly Gaussian with the marginal density of H_n being $\mathcal{CN}(0,1)$. The SNR γ_n follows a Gamma distribution $\mathcal{G}(1, \frac{\sigma_w^2}{P})$.[2]

In a multiuser system, the throughput is larger when the resource allocation is flexible and has high granularity, *e.g.,* assignment at the individual subcarrier level. However, the complexity and feedback overhead can be prohibitive calling for simpler approaches. In our work, the overall N_{SC} subcarriers are grouped into N_{RB} number of resource blocks (RB), and each block contains contiguous S_{RB} subcarriers as in Fig. 3.2, where N_{SC}=$N_{\mathrm{RB}} \times S_{\mathrm{RB}}$. The assignment is done at the block level, *i.e.,* a resource block is assigned to a user. The block size (S_{RB}) is assumed to be known and in practice can be determined at the medium access control (MAC) layer taking into account the number of users. A measure used for resource allocation is the block average throughput C_b, which for block-b of a user is given by

$$C_b \triangleq \frac{1}{S_{\mathrm{RB}}} \sum_{n=1+(b-1)S_{\mathrm{RB}}}^{bS_{\mathrm{RB}}} \log_2(1+\gamma_n). \tag{3.3}$$

For scheduling purposes, it is assumed that each user feeds back the ordered best-N_{FB} block average throughput values (C_b) together with the block indices to the transmitter. The feedback is assumed to be error-free and with no-delay.

[1] $\mathcal{CN}(\mu,\sigma^2)$ denotes a circularly symmetric complex Gaussian distribution with mean μ and variance σ^2.

[2] $\mathcal{G}(\alpha,\beta)$ denotes a Gamma distribution with PDF [49], $f_{\gamma_n}(\gamma) = \frac{\beta^\alpha}{\Gamma(\alpha)}\gamma^{\alpha-1}e^{-\beta\gamma}$, where $\Gamma(\alpha) = \int_0^\infty t^{\alpha-1}e^{-t}dt$.

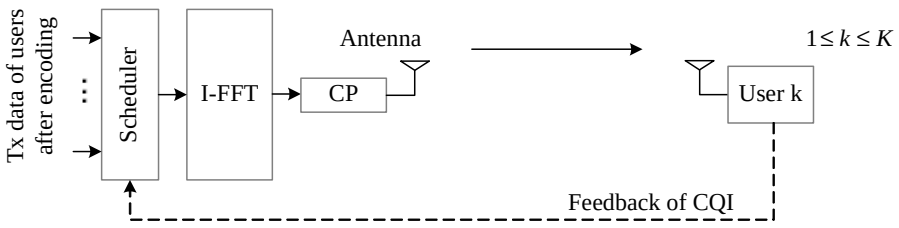

Figure 3.1: System block diagram of a multiuser OFDMA system. Channel quality information is sent back to a transmitter.

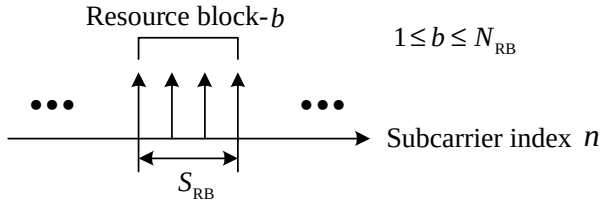

Figure 3.2: Subcarrier grouping. Consecutive subcarriers are grouped into resource blocks.

3.2.1 Proportional Fair Scheduling

To prevent a user with a good channel from being allocated a disproportionate number of resource blocks, the transmitter schedules users employing a proportional fair scheme based on the feedback information provided by them [5]. Since we have N_{RB} blocks and a grouping scheme is used, there are N_{RB} steps in the assignment of blocks to users at each time t. In this approach, user k_ℓ^* is scheduled to a block b_ℓ^* at ℓ-th assignment in time t as follows ($1 \le \ell \le N_{\mathrm{RB}}$):

$$(k_\ell^*, b_\ell^*) = \arg \max_{k \in \{\text{all users}\}} \max_{b \in \{\text{remaining blocks}\}} R_{k,b}^{\mathrm{PFM}}\Big(t + \tfrac{\ell}{N_{\mathrm{RB}}}\Big), \tag{3.4}$$

where $R_{k,b}^{\mathrm{PFM}}$ denotes the proportional fair metric in block-b of user-k, and is given by $C_{k,b}/R_k^{\mathrm{AVG}}$, where $C_{k,b}$ denotes the block average throughput of user-k as per (3.3) and R_k^{AVG} denotes the average throughput of user-k. Once a user is scheduled in ℓ-th assignment, the average throughputs for all users are updated in the following manner.

$$R_k^{\mathrm{AVG}}\Big(t + \tfrac{\ell}{N_{\mathrm{RB}}}\Big) = \begin{cases} \Big(1 - \frac{1}{t_c}\Big) R_k^{\mathrm{AVG}}\Big(t + \frac{\ell-1}{N_{\mathrm{RB}}}\Big) + \frac{1}{t_c} C_{k_\ell^*, b_\ell^*}, & k = k_\ell^* \\ \Big(1 - \frac{1}{t_c}\Big) R_k^{\mathrm{AVG}}\Big(t + \frac{\ell-1}{N_{\mathrm{RB}}}\Big), & k \neq k_\ell^* \end{cases}. \tag{3.5}$$

Here t_c is the length of scheduling window [5]. The sum rate of the system is given by

$$R_{\text{SUM}} = \frac{1}{N_{\text{RB}}} \sum_{\ell=1}^{N_{\text{RB}}} \mathbb{E}[C_{k_\ell^*, b_\ell^*}]. \tag{3.6}$$

This sort of proportional fair scheduling is highly likely to schedule users to their own maximum block with the largest block average throughput across the entire frequency band for the selected user [5]. This situation becomes more lively when the number of users increases as well as when the number of feedback is one (*i.e.,* $N_{\text{FB}} = 1$). *This leads us to assume that the sum rate gain (multiuser diversity) is directly related to maximizing the maximum of the block average throughput of an arbitrary user in the entire band (i.e., maximizing* $\max_b C_b$*).* We now focus on how frequency selectivity affects the maximum of the block average throughput in OFDMA multiuser scheduling systems.

3.3 Optimal Frequency Selectivity Regarding the Maximum of the Block Average Throughput

When we consider a system without feedback, frequency selectivity improves the bit error rate [59] or outage performance [56]. However, when we consider a scheduling system with feedback based on a block of subcarriers, frequency selectivity will not always improve the sum rate. To study this more analytically, we first examine a measure for frequency selectivity. We then provide an approach to investigate the relation between the maximum of the block average throughput $\mathbb{E}[\max_b C_b]$ and frequency selectivity of a channel. Finally, we show that there exists optimal frequency selectivity that maximizes the maximum of the block average throughput. For this purpose we define useful functions below, which are also shown in Table 3.1 for easy reference.

3.3.1 Characterization of Frequency Selectivity of a Channel

Some of Useful Functions

Since frequency selectivity of a channel indicates similarity or difference between subcarriers, it can be described by the statistical correlation property between subcarriers. As a basic measure characterizing frequency selectivity, we first define the correlation

Table 3.1: Notation summary of useful functions. ρ denotes correlation and Ψ denotes the sum of correlation.

Notation	Definition
$\rho_{\mathrm{SC}}(\lvert\Delta_n\rvert)$	CC-SC: Correlation coefficient of the SNR between two subcarriers apart by Δn.
$\Psi_{\mathrm{SC}}(r, \lvert\Delta_b\rvert, S_{\mathrm{RB}})$	Sum of $\rho_{\mathrm{SC}}(\lvert\Delta_n\rvert)$ between every possible two subcarriers each in two blocks apart by Δ_b.
	$\Psi_{\mathrm{SC}}(1, 0, S_{\mathrm{RB}})$: *Intra-block sum correlation.*
	$\frac{1}{\Psi_{\mathrm{SC}}(1,0,N_{\mathrm{SC}})}$: *Frequency selectivity measure.*
$\rho_{\mathrm{RB}}(\lvert\Delta_b\rvert)$	CC-RB: Correlation coefficient of the block average throughput between two blocks apart by Δ_b.
$\Psi_{\mathrm{RB}}(S_{\mathrm{RB}})$	*Inter-block sum correlation*: Sum of $\rho_{\mathrm{RB}}(\lvert\Delta_b\rvert)$ between every possible two blocks in the whole band.
	$\frac{1}{\Psi_{\mathrm{RB}}(S_{\mathrm{RB}})}$: Effective number of blocks.

coefficient of the SNR between two subcarriers indexed by n_1 and n_2 (CC-SC) as [49]

$$\rho_{\mathrm{SC}}(|\Delta_n|) \triangleq \frac{\mathrm{cov}(\gamma_{n_1}, \gamma_{n_2})}{\sqrt{\mathrm{var}[\gamma_{n_1}]}\sqrt{\mathrm{var}[\gamma_{n_2}]}} \tag{3.7}$$

where $\Delta_n = n_2 - n_1$ and 'SC' stands for the 'subcarrier'. 'cov' and 'var' denote covariance and variance respectively. It is shown in Appendix B.1 that for the channel in (3.1), we have

$$\rho_{\mathrm{SC}}(|\Delta_n|) = |\mathrm{cov}(H_{n_1}, H_{n_2})|^2, \tag{3.8}$$

where it can be shown from (3.2) that

$$\mathrm{cov}(H_{n_1}, H_{n_2}) = \sum_{m=1}^{L} \alpha_m^2 e^{-j\frac{2\pi}{N_{\mathrm{SC}}}(m-1)(n_2-n_1)}. \tag{3.9}$$

We note from (3.8) and (3.9) that ρ_{SC} is a function of $|\Delta_n|$, and that ρ_{SC} is periodic with a period N_{SC}, *i.e.*, $\rho_{\mathrm{SC}}(|\Delta_n|) = \rho_{\mathrm{SC}}(|\Delta_n - N_{\mathrm{SC}}|)$. By the nonnegativity of $\rho_{\mathrm{SC}}(|\Delta_n|)$ in (3.8) and the magnitude property of the correlation coefficient [49] (*i.e.*, $-1 \le \rho_{\mathrm{SC}}(|\Delta_n|) \le 1$), we find that $0 \le \rho_{\mathrm{SC}}(|\Delta_n|) \le 1$.

Since the scheduling unit is a subcarrier block in OFDMA systems, we need to know frequency selectivity between blocks. To state the correlation between blocks, we define the sum of correlation coefficients of the SNR between subcarriers in each of the

two blocks indexed by b_1 and b_2 as

$$\Psi_{\mathrm{SC}}(r,|\Delta_b|,S_{\mathrm{RB}}) \triangleq \frac{1}{S_{\mathrm{RB}}^2} \sum_{\substack{n_1=1+\\(b_1-1)S_{\mathrm{RB}}}}^{b_1 S_{\mathrm{RB}}} \sum_{\substack{n_2=1+\\(b_2-1)S_{\mathrm{RB}}}}^{b_2 S_{\mathrm{RB}}} [\rho_{\mathrm{SC}}(|\Delta_n|)]^r. \tag{3.10}$$

where $\Delta_b = b_2 - b_1$ and r is a free parameter related to the order of expansion of $\log_2(1+\gamma_n)$ in (3.3). In our analysis, $r = 1$ for the measure of frequency selectivity in (3.13). The case that $r = 2$ is shown in (B.14) of Appendix B.2 for the second order approximation of the variance of the block average throughput. We note in (3.10) that sum is over every possible combination of subcarriers from blocks b_1 and b_2 respectively. By replacing the summation index, we can rewrite (3.10) as

$$\Psi_{\mathrm{SC}}(r,|\Delta_b|,S_{\mathrm{RB}}) = \frac{1}{S_{\mathrm{RB}}^2} \sum_{n_1'=1}^{S_{\mathrm{RB}}} \sum_{n_2'=1}^{S_{\mathrm{RB}}} [\rho_{\mathrm{SC}}(|\Delta_b S_{\mathrm{RB}} + n_2' - n_1'|)]^r, \tag{3.11}$$

where we can verify that Ψ_{SC} depends on $|\Delta_b|$ utilizing (3.8) and (3.9). For $\Psi_{\mathrm{SC}}(r,|\Delta_b - N_{\mathrm{RB}}|,S_{\mathrm{RB}})$, we note in the argument of ρ_{SC} in (3.11) that $|(\Delta_b - N_{\mathrm{RB}})S_{\mathrm{RB}} + n_2' - n_1'| = |(\Delta_b)S_{\mathrm{RB}} + n_2' - n_1' - N_{\mathrm{SC}}| \overset{(a)}{\equiv} |(\Delta_b)S_{\mathrm{RB}} + n_2' - n_1'|$, where the last equivalence (a) follows from the periodicity of ρ_{SC}. Thus, we can find that Ψ_{SC} is also periodic with a period of N_{RB}, *i.e.,* $\Psi_{\mathrm{SC}}(r,|\Delta_b|,S_{\mathrm{RB}}) = \Psi_{\mathrm{SC}}(r,|\Delta_b - N_{\mathrm{RB}}|,S_{\mathrm{RB}})$.

As a special case, for the same block ($\Delta_b = 0$) and for the first order ($r = 1$), we have

$$\Psi_{\mathrm{SC}}(1,0,S_{\mathrm{RB}}) = \frac{1}{S_{\mathrm{RB}}^2} \sum_{n_1=1}^{S_{\mathrm{RB}}} \sum_{n_2=1}^{S_{\mathrm{RB}}} \rho_{\mathrm{SC}}(|\Delta_n|). \tag{3.12}$$

Since this sum is for subcarriers within an identical block, it is referred to as *intra-block sum correlation.* Since $0 \le \rho_{\mathrm{SC}}(|\Delta_n|) \le 1$ and $\rho_{\mathrm{SC}}(0) = 1$, we find from (3.12) that $\frac{1}{S_{\mathrm{RB}}} \le \Psi_{\mathrm{SC}}(1,0,S_{\mathrm{RB}}) \le 1$ where the minimum is for a channel with independent subcarriers, and the maximum is for a flat channel.

Measure of Frequency Selectivity of a Channel

As one measure to characterize frequency selectivity, the inverse of the intra-block sum correlation in (3.12) for the whole band (*i.e.,* $S_{\mathrm{RB}} = N_{\mathrm{SC}}$) is used in [59, 60]. Considering $\rho_{\mathrm{SC}}(|\Delta_n|) = \rho_{\mathrm{SC}}(|\Delta_n - N_{\mathrm{SC}}|)$, we have from (3.12) that $\Psi_{\mathrm{SC}}(1,0,N_{\mathrm{SC}}) = \frac{1}{N_{\mathrm{SC}}} \sum_{n=0}^{N_{\mathrm{SC}}-1} \rho_{\mathrm{SC}}(n)$. Thus, its inverse is given by

$$\frac{1}{\Psi_{\mathrm{SC}}(1,0,N_{\mathrm{SC}})} = \frac{1}{\frac{1}{N_{\mathrm{SC}}} \sum_{n=0}^{N_{\mathrm{SC}}-1} \rho_{\mathrm{SC}}(n)}. \tag{3.13}$$

We note in (3.13) that the frequency selectivity is inversely proportional to the average correlation coefficient in the whole band. This agrees with the intuition that an increase of frequency selectivity makes a channel more fluctuating, which leads to a decrease of the correlation coefficient of the SNR between subcarriers [59] and the sum correlation in (3.12), and an increase of its inverse $\frac{1}{\Psi_{\mathrm{SC}}(1,0,N_{\mathrm{SC}})}$ in (3.13). Thus, we regard large frequency selectivity (*i.e.,* $\frac{1}{\Psi_{\mathrm{SC}}(1,0,N_{\mathrm{SC}})}$) as the small intra-block sum correlation and vice versa throughout the chapter.

In addition to being used as a measure for frequency selectivity, $\frac{1}{\Psi_{\mathrm{SC}}(1,0,N_{\mathrm{SC}})}$ is used as the effective number of paths in a channel [59,60,62,63]. Providing some intuition about this relationship, we first check the following equation from [56, (11)] and [63, (9)].

$$\frac{1}{\Psi_{\mathrm{SC}}(1,0,N_{\mathrm{SC}})} = \frac{\mathrm{var}[\gamma_1]}{\mathrm{var}\left[\frac{1}{N_{\mathrm{SC}}}\sum_{n=1}^{N_{\mathrm{SC}}}\gamma_n\right]} = \frac{1}{\sum_{m=1}^{L}\alpha_m^4}. \tag{3.14}$$

This indicates the effective number of paths in a channel when the gains of the paths are made equal (*i.e.,* $\frac{1}{\Psi_{\mathrm{SC}}(1,0,N_{\mathrm{SC}})} = L$ when $\alpha_m = \sqrt{1/L}$). For example, for two equal paths ($\alpha_1 = \alpha_2 = \sqrt{1/2}$), $\frac{1}{\Psi_{\mathrm{SC}}(1,0,N_{\mathrm{SC}})}$ is exactly 2. However, when $\alpha_1 = \sqrt{2/3}$ and $\alpha_2 = \sqrt{1/3}$, $\frac{1}{\Psi_{\mathrm{SC}}(1,0,N_{\mathrm{SC}})}$ is $\frac{9}{5}$. The conventional diversity order for these two cases is the same value of 2 since diversity is a high SNR measure [64, (9.3)]. However, $\frac{1}{\Psi_{\mathrm{SC}}(1,0,N_{\mathrm{SC}})}$ can differentiate.

When frequency diversity provided by the multipaths is exploited in the frequency domain of OFDM systems, the order of frequency diversity, *i.e.,* the effective number of independent subcarriers, is the same as the effective number of paths. Thus, the effective number of independent subcarriers is the same as $\frac{1}{\Psi_{\mathrm{SC}}(1,0,N_{\mathrm{SC}})}$. For example, suppose that all the subcarriers are completely correlated. Then, $\rho_{\mathrm{SC}}(|\Delta_n|) = 1$ for any $\Delta_n = n_2 - n_1$. Thus, $\frac{1}{\Psi_{\mathrm{SC}}(1,0,N_{\mathrm{SC}})} = 1$ in (3.13). Since all subcarriers have the same value in each channel realization, the frequency diversity order is one and the effective number of independent subcarriers is one. Thus, the effective number of independent subcarriers matches with $\frac{1}{\Psi_{\mathrm{SC}}(1,0,N_{\mathrm{SC}})}$. For another example of all independent subcarriers, we have $\rho_{\mathrm{SC}}(|\Delta_n|) = 0$ for different subcarriers ($\Delta_n \neq 0$) and $\rho_{\mathrm{SC}}(|\Delta_n|) = 1$ for itself ($\Delta_n = 0$). Thus, $\frac{1}{\Psi_{\mathrm{SC}}(1,0,N_{\mathrm{SC}})} = N_{\mathrm{SC}}$, which is the same as the effective number of independent subcarriers.

3.3.2 Development of the Relation between $\mathbb{E}[\max_b C_b]$ and Frequency Selectivity

Function Definitions for Inter-block Frequency Selectivity and Effective Number of Resource Blocks

As we briefly mentioned in Section 3.3.1, we need to characterize inter-block frequency selectivity since we consider a block-based OFDMA system. As a basic measure for this purpose, we define the correlation coefficient of the block average throughput between two blocks indexed by b_1 and b_2 (CC-RB) as [49]

$$\rho_{\mathrm{RB}}(|\Delta_b|) \triangleq \frac{\mathrm{cov}(C_{b_1}, C_{b_2})}{\sqrt{\mathrm{var}[C_{b_1}]}\sqrt{\mathrm{var}[C_{b_2}]}} \tag{3.15}$$

where 'RB' stands for the 'resource block' and we follow the same notations in Section 3.3.1. For the first order approximation of C_b, it is shown in Appendix B.2 that we have

$$\rho_{\mathrm{RB}}(|\Delta_b|) = \frac{\Psi_{\mathrm{SC}}(1, |\Delta_b|, S_{\mathrm{RB}})}{\Psi_{\mathrm{SC}}(1, 0, S_{\mathrm{RB}})} \tag{3.16}$$

where we verify that this is a function of $|\Delta_b|$. We can easily verify that $0 \leq \rho_{\mathrm{RB}}(|\Delta_b|) \leq 1$ from the nonnegativity of Ψ_{SC} in (3.10) and the magnitude property of the correlation coefficient and that $\rho_{\mathrm{RB}}(|\Delta_b|) = \rho_{\mathrm{RB}}(|\Delta_b - N_{\mathrm{RB}}|)$ from the periodicity of $\Psi_{\mathrm{SC}}(1, |\Delta_b|, S_{\mathrm{RB}})$ in (3.10).

In the same line of context for (3.12), we define the sum of correlation coefficients of the block average throughput between every possible two blocks in the whole band as

$$\Psi_{\mathrm{RB}}(S_{\mathrm{RB}}) \triangleq \frac{1}{N_{\mathrm{RB}}^2} \sum_{b_1=1}^{N_{\mathrm{RB}}} \sum_{b_2=1}^{N_{\mathrm{RB}}} \rho_{\mathrm{RB}}(|\Delta_b|). \tag{3.17}$$

Since this sum is for all the blocks in the whole band, it is referred to as *inter-block sum correlation*. From the periodicity of $\rho_{\mathrm{RB}}(|\Delta_b|)$, (3.17) is reduced to

$$\Psi_{\mathrm{RB}}(S_{\mathrm{RB}}) = \frac{1}{N_{\mathrm{RB}}} \sum_{b=0}^{N_{\mathrm{RB}}-1} \rho_{\mathrm{RB}}(b). \tag{3.18}$$

We note that the inter-block sum correlation is the average correlation among blocks in the whole band.

The discussion about effective number of subcarriers (*i.e.*, $\frac{1}{\Psi_{\mathrm{SC}}(1,0,N_{\mathrm{SC}})}$) in Section 3.3.1 motivates defining the effective number of independent blocks as $\frac{1}{\Psi_{\mathrm{RB}}(S_{\mathrm{RB}})}$, which is the inverse of the inter-block sum correlation in (3.18). We can verify from (3.18)

that $1 \leq \frac{1}{\Psi_{\mathrm{RB}}(S_{\mathrm{RB}})} \leq N_{\mathrm{RB}}$ where the minimum is for a flat channel (*i.e.,* $\rho_{\mathrm{RB}}(|\Delta_b|) = 1$ for all Δ_b), and the maximum is for a channel with independent blocks (*i.e.,* $\rho_{\mathrm{RB}}(|\Delta_b|) = 0$ for $\Delta_b \neq 0$ and $\rho_{\mathrm{RB}}(|\Delta_b|) = 1$ for $\Delta_b = 0$). In these both extreme cases of frequency selectivity of a channel, we can easily verify that the effective number $\frac{1}{\Psi_{\mathrm{RB}}(S_{\mathrm{RB}})}$ is the same as the number of independent blocks. Noting (3.14) and the analogy between $\frac{1}{\Psi_{\mathrm{SC}}(1,0,N_{\mathrm{SC}})}$ and $\frac{1}{\Psi_{\mathrm{RB}}(S_{\mathrm{RB}})}$, we can verify for the first order approximation of C_b that

$$\frac{1}{\Psi_{\mathrm{RB}}(S_{\mathrm{RB}})} = \frac{\mathrm{var}[\sum_{n=1}^{S_{\mathrm{RB}}} \frac{\gamma_n}{S_{\mathrm{RB}}}]}{\mathrm{var}\left[\frac{1}{N_{\mathrm{RB}}} \sum_{b=1}^{N_{\mathrm{RB}}} \left(\sum_{n=1+(b-1)S_{\mathrm{RB}}}^{bS_{\mathrm{RB}}} \frac{\gamma_n}{S_{\mathrm{RB}}}\right)\right]}. \tag{3.19}$$

Considering from (3.14) that $\frac{1}{\Psi_{\mathrm{SC}}(1,0,S_{\mathrm{RB}})} = \frac{\mathrm{var}[\gamma_1]}{\mathrm{var}\left[\frac{1}{S_{\mathrm{RB}}} \sum_{n=1}^{S_{\mathrm{RB}}} \gamma_n\right]}$, we have from (3.14) and (3.19) as

$$\frac{1}{\Psi_{\mathrm{SC}}(1,0,N_{\mathrm{SC}})} = \frac{1}{\Psi_{\mathrm{SC}}(1,0,S_{\mathrm{RB}})} \times \frac{1}{\Psi_{\mathrm{RB}}(S_{\mathrm{RB}})}. \tag{3.20}$$

This gives the idea that the effective number of subcarriers in the whole band at the left-hand side is the same as the product of the effective number of blocks in the whole band and the effective number of subcarriers in each effective block at the right-hand side.

Approximations of $\mathbb{E}[\max_b C_b]$ and Optimality in Frequency Selectivity that Maximizes $\mathbb{E}[\max_b C_b]$

Suppose that we have N *i.i.d.* random variables of X_i $(1 \leq i \leq N)$ and that Y is the maximum of X_i's. That is, $Y = \max_{1 \leq i \leq N} X_i$. When a probability density function (PDF) of X_i is not given in a closed-form,[3] it is usually not tractable to compute $\mathbb{E}[Y]$. However, we can obtain some insight about the relation between $\mathbb{E}[Y]$ and $\{\mathbb{E}[X_i], \mathrm{var}[X_i], N\}$ from a simple upper bound of the order statistics [48]

$$\mathbb{E}[Y] \leq \mathbb{E}[X_i] + \frac{N-1}{\sqrt{2N-1}} \sqrt{\mathrm{var}[X_i]}. \tag{3.21}$$

While this bound is good for the small N, it becomes loose when N becomes larger. In a special case that X_i is Gaussian random variable, the weak law of large number gives an approximation of $\mathbb{E}[Y]$ as [65]

$$\mathbb{E}[Y] \simeq \mathbb{E}[X_i] + \sqrt{2\mathrm{var}[X_i] \ln N}. \tag{3.22}$$

[3]For example, suppose that X_i is the sum of dependent random variables, say Z_j for $1 \leq j \leq m$ and that we know only PDF of Z_j and their correlation. It is usually hard or intractable to obtain the PDF of X_i. However, we can compute $\mathbb{E}[X_i]$ and $\mathrm{var}[X_i]$.

This approximation is better for large N. We note in (3.21) and (3.22) that the expectation of the maximum of X_i (*i.e.,* $\mathbb{E}[Y]$) increases with two moments of X_i (*i.e.,* $\mathbb{E}[X_i]$ and $\mathrm{var}[X_i]$) and the number of X_i (*i.e.,* N).

From the assumption in Section 3.2.1 that the sum rate gain (multiuser diversity) is directly related to the maximum of the block average throughput by the proportional fair scheduling, we focus on approximating $\mathbb{E}[\max_b C_b]$. Using $\mathbb{E}[C_b]$ in (B.3) and $\mathrm{var}[C_b]$ in (B.8) in Appendix B.2, we can approximate $\mathbb{E}[\max_b C_b]$ by replacing N in (3.21) with the effective number of blocks $\frac{1}{\Psi_{\mathrm{RB}}(S_{\mathrm{RB}})}$ in (3.18) as

$$\mathbb{E}[\max_b C_b] \leq E_1 + \frac{\left(\frac{1}{\Psi_{\mathrm{RB}}(S_{\mathrm{RB}})}-1\right)\sqrt{\Psi_{\mathrm{SC}}(1,0,S_{\mathrm{RB}})}}{\sqrt{\frac{2}{\Psi_{\mathrm{RB}}(S_{\mathrm{RB}})}-1}}\sqrt{V_1}. \tag{3.23}$$

where $E_1 = \mathbb{E}[\log_2(1+\gamma_1)]$ and $V_1 = \frac{\mathrm{var}[\gamma_1]}{\{(1+\mathbb{E}[\gamma_1])\ln 2\}^2}$ for notational simplicity.

In [56, 62], Gaussian approximation of C_b in (3.3) is suitable for identically distributed γ_n when the system bandwidth is large. Since we consider a block of wideband systems, we can apply this theorem for the reasonable block size. We will show the justification of this assumption in the numerical results. Thus, we can assume that C_b follows $\mathcal{N}(\mathbb{E}[C_b], \mathrm{var}[C_b])$.[4] Using (B.3), (B.8), and the effective number of blocks $\frac{1}{\Psi_{\mathrm{RB}}(S_{\mathrm{RB}})}$ in (3.18), we can approximate $\mathbb{E}[\max_b C_b]$ using the relation in (3.22) as

$$\mathbb{E}[\max_b C_b] \simeq E_1 + \sqrt{\Psi_{\mathrm{SC}}(1,0,S_{\mathrm{RB}})\ln\frac{1}{\Psi_{\mathrm{RB}}(S_{\mathrm{RB}})}}\sqrt{2V_1}. \tag{3.24}$$

We note that the second order expansion of $\mathrm{var}[C_b]$ in (B.14) in Appendix B.2 can be used in (3.21) and (3.22) to obtain more accurate approximations.

From (3.23) and (3.24), we can note two important facts when a marginal distribution of the SNR (γ_n) is fixed. First, the maximum C_b of a user increases with $\Psi_{\mathrm{SC}}(1,0,S_{\mathrm{RB}})$, *intra-block sum correlation.* This means that subcarriers within a block should be highly correlated to increase the maximum of C_b. Thus, the flat fading is the best case in this view. On the other hand, the maximum C_b of a user increases with $\frac{1}{\Psi_{\mathrm{RB}}(S_{\mathrm{RB}})}$, the inverse of *inter-block sum correlation.* This means that blocks should be lowly correlated to increase the maximum of C_b. Thus, frequency selective fading with larger $\frac{1}{\Psi_{\mathrm{RB}}(S_{\mathrm{RB}})}$ is preferred in this view. Thus, for larger $\mathbb{E}[\max_b C_b]$, we need the large intra-block sum correlation and the small inter-block sum correlation. As the number of paths in a channel increases, $\Psi_{\mathrm{SC}}(1,0,S_{\mathrm{RB}})$ decreases but $\frac{1}{\Psi_{\mathrm{RB}}(S_{\mathrm{RB}})}$ increases. Thus,

[4] $\mathcal{N}(\mu,\sigma^2)$ denotes a Gaussian distribution with mean μ and variance σ^2.

we note that there exists a trade-off between these two factors, *i.e.,* intra-block sum correlation and inter-block sum correlation.

To find an optimality of frequency selectivity for $\mathbb{E}[\max_b C_b]$, let us look at $\mathcal{E} \triangleq \sqrt{\Psi_{\mathrm{SC}}(1,0,S_{\mathrm{RB}}) \ln \frac{1}{\Psi_{\mathrm{RB}}(S_{\mathrm{RB}})}}$ in (3.24). We note that $\mathcal{E}$ indicates the additional gain of expectation by the maximum selection compared to the individual one (*i.e.,* E_1 in (3.24)). We consider $\mathcal{E}$ for three types of channels. One is a flat channel (CH_A), other is a channel with independent subcarriers (CH_B) and another is an ideal channel which is flat within a block and mutually independent between blocks (CH_C). Following the discussion in Section 3.3.1 and Section 3.3.2, we have $\Psi_{\mathrm{SC}}(1,0,S_{\mathrm{RB}})$ and $\frac{1}{\Psi_{\mathrm{RB}}(S_{\mathrm{RB}})}$ in Table 3.2 for each channel. We note that $\frac{1}{\Psi_{\mathrm{SC}}(1,0,N_{\mathrm{SC}})}$ can be computed from (3.20). From the table, we can find that CH_C has the largest $\mathcal{E}$, which leads to the largest $\mathbb{E}[\max_b C_b]$ in (3.24). However, frequency selectivity of CH_C is less than CH_B (a channel with independent subcarriers). We note that both extreme cases of a channel, *i.e.,* flat or fully independent, are not good for maximizing $\mathbb{E}[\max_b C_b]$. This tells us that there may exist optimal frequency selectivity between a flat channel and an independent channel. Further, a channel with optimal selectivity should be like CH_C, *i.e.,* as flat as possible inside a block and as independent as possible among blocks, which complies with the observation in [66, 67].

Table 3.2: Comparison of $\mathbb{E}[\max_b C_b]$ for three types of channels. CH_C denotes a channel with ideal frequency selectivity.

Channel type	CH_A	CH_B	CH_C
$\Psi_{\mathrm{SC}}(1,0,S_{\mathrm{RB}})$	1	$\frac{1}{S_{\mathrm{RB}}}$	1
$\frac{1}{\Psi_{\mathrm{RB}}(S_{\mathrm{RB}})}$	1	N_{RB}	N_{RB}
Frequency selectivity=$\frac{1}{\Psi_{\mathrm{SC}}(1,0,N_{\mathrm{SC}})}$	1	N_{SC}	N_{RB}
$\mathcal{E} = \sqrt{\Psi_{\mathrm{SC}}(1,0,S_{\mathrm{RB}}) \ln \frac{1}{\Psi_{\mathrm{RB}}(S_{\mathrm{RB}})}}$	0	$\sqrt{\frac{\ln N_{\mathrm{RB}}}{S_{\mathrm{RB}}}}$	$\sqrt{\ln N_{\mathrm{RB}}}$

[1] CH_A denotes a flat channel. CH_B denotes a channel with independent subcarriers. CH_C denotes a channel which is flat within a block and mutually independent between blocks.

[2] $\Psi_{\mathrm{SC}}(1,0,S_{\mathrm{RB}})$ determines $\mathrm{var}[C_b]$ in (B.8) and $\frac{1}{\Psi_{\mathrm{RB}}(S_{\mathrm{RB}})}$ represents the effective number of blocks.

[3] $\frac{1}{\Psi_{\mathrm{SC}}(1,0,N_{\mathrm{SC}})}$ can be computed from (3.20) and represents frequency selectivity.

[4] $\sqrt{\Psi_{\mathrm{SC}}(1,0,S_{\mathrm{RB}}) \ln \frac{1}{\Psi_{\mathrm{RB}}(S_{\mathrm{RB}})}}$ is from (3.24) and related to $\mathbb{E}[\max_b C_b]$.

In an open loop diversity system without feedback, the more frequency selective channel with low correlation between subcarriers is preferred to improve outage property

[56] or the BER [59]. However, we note from the above that there exists optimal frequency selectivity, *i.e.,* an optimal correlation in the frequency domain, that maximizes the maximum of C_b for a scheduling system.

Although we cannot reduce frequency selectivity for a given channel, we can increase frequency selectivity using a cyclic delay diversity technique. In Section 3.4, we propose a technique regarding how much selectivity should be added to maximize $\mathbb{E}[\max_b C_b]$ in a channel with low selectivity.

3.4 Optimal Addition of Frequency Selectivity Using CDD

In the previous section, we noted in (3.23) and (3.24) that there exists optimal frequency selectivity in maximizing $\mathbb{E}[\max_b C_b]$. The question we consider in this section is how much more channel selectivity should be added to maximize $\mathbb{E}[\max_b C_b]$ when we are given a limited fluctuating channel. One method to increase the number of paths in a channel is to use multiple transmit antennas. By sending the same signal in different antennas at the different time, we have an equivalent channel with more paths. For example, suppose that we have two transmit antennas each with flat fading and equal power. If we add a delay by one symbol time at the second transmit antenna, the equivalent channel at a receiver has two equal paths separated by one symbol time. This sort of delay diversity was first proposed in the single carrier system [58] and later for OFDM system in the name of cyclic delay diversity (CDD) [43]. Since cyclic delay in CDD determines frequency selectivity of the equivalent channel, we focus on how large cyclic delay we need to choose to maximize $\mathbb{E}[\max_b C_b]$.

Let N_{T} denote the number of transmit antennas in Fig. 3.3. Let D_i denote a cyclic delay in Tx antenna-i and let $\underline{\mathbf{D}} = [D_1, \cdots, D_{N_{\mathrm{T}}}]^T$. We note that D_i has an integer value within $[0, N_{\mathrm{SC}} - 1]$. We follow the same notation in (3.1) except for adding an index i to denote the transmit antenna. Then, the discrete time channel equation is given by

$$h^{\mathrm{cdd}}(t) = \sum_{i=1}^{N_{\mathrm{T}}} \sum_{m=1}^{L_i} \frac{\alpha_{i,m} h_{i,m}}{\sqrt{N_{\mathrm{T}}}} \, \delta\left(t - \frac{(m + D_i - 1)_{N_{\mathrm{SC}}} T}{N_{\mathrm{SC}}}\right) \tag{3.25}$$

where $(\cdot)_{N_{\mathrm{SC}}}$ denotes modulo-N_{SC} operation. Without loss of generality, we assume that D_1 is zero as in [68]. We assume that $h_{i,m}$ is *i.i.d.* in i and m.

Noting that $H_{i,n}$ denotes a frequency response at subcarrier-n in Tx antenna-i,

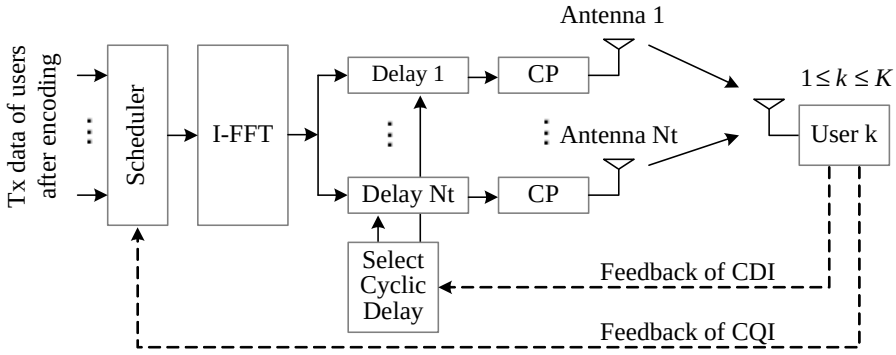

Figure 3.3: System block diagram of cyclic delay diversity (CDD). In addition to CQI, channel distribution information is also sent back to a transmitter.

we have the frequency response of CDD at subcarrier-n from (3.25) as

$$H_n^{\text{cdd}} = \sum_{i=1}^{N_{\text{T}}} \frac{H_{i,n}}{\sqrt{N_{\text{T}}}} e^{-j\frac{2\pi}{N_{\text{SC}}} D_i n}. \tag{3.26}$$

Since H_n^{cdd} is linear combination of independent $H_{i,n}$'s following $\mathcal{CN}(0,1)$ in Section 3.2, we can find that H_n^{cdd} follows $\mathcal{CN}(0,1)$ as well.

3.4.1 Determination of Cyclic Delay from Approximation of $\mathbb{E}[\max_b C_b]$

Let $\rho_{\text{SC}}^{\text{cdd}}$ and $\rho_{\text{RB}}^{\text{cdd}}$ denote the correlation coefficient for CDD of the SNR as in (3.7) and of C_b as in (3.15) respectively. Let $\Psi_{\text{SC}}^{\text{cdd}}$ and $\Psi_{\text{RB}}^{\text{cdd}}$ denote sum of $\rho_{\text{SC}}^{\text{cdd}}$ as in (3.10) and $\rho_{\text{RB}}^{\text{cdd}}$ as in (3.17) respectively. We can see that these values will be changed when we change cyclic delay because the channel delay profile (PDP) is changed from (3.1) into (3.25). For a given channel, these values will be a function of $\underline{\mathbf{D}}$, which will be shown later. Let $\underline{\mathbf{D}}_{\text{PerUser}}^*$ denote optimal cyclic delay that maximizes $\mathbb{E}[\max_b C_b]$ of an arbitrary user and $\underline{\mathbf{D}}_{\text{SumRate}}^*$ optimal cyclic delay that maximizes the sum rate. Then problem we focus is to find $\underline{\mathbf{D}}_{\text{PerUser}}^*$ and to compare it to $\underline{\mathbf{D}}_{\text{SumRate}}^*$. Further, we look at how much gain in the sum rate is achieved by this addition of frequency selectivity (*i.e.*, $\underline{\mathbf{D}}_{\text{PerUser}}^*$ or $\underline{\mathbf{D}}_{\text{SumRate}}^*$).

Using the approximations for $\mathbb{E}[\max_b C_b]$ in (3.23) and (3.24), we can find $\underline{\mathbf{D}}_{\text{PerUser}}^*$ in two ways as following.

$$\underline{\mathbf{D}}_{\text{PerUser}}^* = \arg\max_{\underline{\mathbf{D}}} \left[E_1 + \frac{\left(\frac{1}{\Psi_{\text{RB}}^{\text{cdd}}(S_{\text{RB}})} - 1\right)\sqrt{\Psi_{\text{SC}}^{\text{cdd}}(1,0,S_{\text{RB}})}}{\sqrt{\frac{2}{\Psi_{\text{RB}}^{\text{cdd}}(S_{\text{RB}})} - 1}} \sqrt{V_1} \right]. \tag{3.27}$$

$$\underline{\mathbf{D}}^{*}_{\text{PerUser}} = \arg\max_{\underline{\mathbf{D}}} \left[E_1 + \sqrt{\Psi^{\text{cdd}}_{\text{SC}}(1,0,S_{\text{RB}}) \ln \frac{1}{\Psi^{\text{cdd}}_{\text{RB}}(S_{\text{RB}})}} \sqrt{2V_1} \right]. \tag{3.28}$$

We note that we can omit E_1 and V_1 in both equations because the distribution of H^{cdd}_n is $\mathcal{CN}(0,1)$ and its statistics are not affected by $\underline{\mathbf{D}}$.

Derivation of Statistics of CDD

Using the bilinear property of covariance [69], we have from (3.26) as

$$\text{cov}(H^{\text{cdd}}_{n_1}, H^{\text{cdd}}_{n_2}) = \sum_{i=1}^{N_{\text{T}}} \frac{\text{cov}(H_{i,n_1}, H_{i,n_2})}{N_{\text{T}}} \, e^{-j\frac{2\pi}{N_{\text{SC}}} D_i (n_2 - n_1)}. \tag{3.29}$$

where $\text{cov}(H_{i,n_1}, H_{i,n_2})$ denotes covariance of SISO channel at Tx antenna-i in (3.9). Note that covariance depends on $\underline{\mathbf{D}}$ as well as Δ_n (*i.e.,* $n_2 - n_1$). Using this and following the same procedure in Appendix B.1 and Appendix B.2, we can compute for CDD the correlation coefficient of the SNR ($\rho^{\text{cdd}}_{\text{SC}}$) and of C_b ($\rho^{\text{cdd}}_{\text{RB}}$) and sum of those respectively ($\Psi^{\text{cdd}}_{\text{SC}}$, $\Psi^{\text{cdd}}_{\text{RB}}$). Although we can compute all these for the general PDP ($\alpha_{i,m}$), we assume for simplicity that PDP in each antenna is the same, *i.e.,* $\alpha_{i,m} = \alpha_{j,m}$ for $i \neq j$. However, this assumption is very feasible because Tx antennas are not separated so much. When we let $\text{cov}(H_{n_1}, H_{n_2})$ denote the covariance of SISO, the covariance in (3.29) reduces to

$$\text{cov}(H^{\text{cdd}}_{n_1}, H^{\text{cdd}}_{n_2}) = \text{cov}(H_{n_1}, H_{n_2}) \sum_{i=1}^{N_{\text{T}}} \frac{e^{-j\frac{2\pi}{N_{\text{SC}}} D_i (n_2 - n_1)}}{N_{\text{T}}}. \tag{3.30}$$

Noting that H^{cdd}_n follows the same distribution as that of H_n and that $\gamma^{\text{cdd}}_n = P|H^{\text{cdd}}_n|^2/\sigma^2_w$, we can easily have for the correlation coefficient between $\gamma^{\text{cdd}}_{n_1}$ and $\gamma^{\text{cdd}}_{n_2}$ from (3.8) and (3.30) as

$$\rho^{\text{cdd}}_{\text{SC}}(|\Delta_n|) = \rho_{\text{SC}}(|\Delta_n|) \left| \frac{\sum_{i=1}^{N_{\text{T}}} e^{-j\frac{2\pi}{N_{\text{SC}}} D_i (\Delta_n)}}{N_{\text{T}}} \right|^2. \tag{3.31}$$

This shows that the correlation coefficient of CDD is the correlation coefficient of SISO ($\rho_{\text{SC}}(|\Delta_n|)$) multiplied by a weight function. This weight function consists of sinusoidal functions each with period $\frac{N_{\text{SC}}}{D_i}$, while ρ_{SC} of SISO has a period of N_{SC}. Thus, $\rho^{\text{cdd}}_{\text{SC}}$ is periodic with a period N_{SC}. We can easily verify that the magnitude of the weight function is less than or equal to 1. We find for every Δ_n that $\rho^{\text{cdd}}_{\text{SC}}$ has a value between zero and ρ_{SC} depending on the sinusoidal weight with a shorter period, which indicates $\rho^{\text{cdd}}_{\text{SC}}$ is more fluctuating than ρ_{SC} with respect to Δ_n. That is, a channel of CDD is more fluctuating than that of SISO.

Using $\rho_{\mathrm{SC}}^{\mathrm{cdd}}$ in (3.31), we can compute $\Psi_{\mathrm{SC}}^{\mathrm{cdd}}$ from (3.10). Once we compute $\Psi_{\mathrm{SC}}^{\mathrm{cdd}}(r, |\Delta_b|, S_{\mathrm{RB}})$, we can compute $\rho_{\mathrm{RB}}^{\mathrm{cdd}}(|\Delta_b|)$ from (3.15) and $\Psi_{\mathrm{RB}}^{\mathrm{cdd}}(S_{\mathrm{RB}})$ from (3.17). From these and (3.27) and (3.28), we can find $\underline{\mathbf{D}}_{\mathrm{PerUser}}^{*}$ that maximizes $\mathbb{E}[\max_b C_b]$ by exhaustive search.

Role of Cyclic Delay on Frequency Selectivity

We mentioned that $\frac{1}{\Psi_{\mathrm{SC}}(1,0,N_{\mathrm{SC}})}$ represents frequency selectivity in Section 3.3.1 and also the effective number of paths in a channel or independent subcarriers in Section 3.3.1. For the better understanding about the role of cyclic delay (D_i) in $\frac{1}{\Psi_{\mathrm{SC}}^{\mathrm{cdd}}(1,0,N_{\mathrm{SC}})}$, let us consider a simple example. Suppose that we have two transmit antennas ($N_{\mathrm{T}} = 2$) and that the channel in each antenna has L-path uniform PDP, *i.e.,* $\alpha_{1,m} = \alpha_{2,m} = \sqrt{1/L}$, for $1 \le m \le L$. Cyclic delay is denoted by $\underline{\mathbf{D}} = [0, D]^T$ (*i.e.,* $D_2 = D$). We can easily verify in (3.14) that the effective number of paths is $\frac{1}{\Psi_{\mathrm{SC}}(1,0,N_{\mathrm{SC}})} = L$ for each SISO channel. Suppose in (3.25) that path-m in a channel of Tx antenna-1 is overlapped with path-$(m-D)$ in a channel of Tx antenna-2. Then, the average gain of CDD in path-m is $\alpha_m^{\mathrm{cdd}} = \sqrt{(\alpha_{1,m}^2 + \alpha_{2,m-D}^2)/2}$ since two channels are independent.

When $D < L$, two PDPs are overlapped for $D+1 \le m \le L$, but they are not in other range of m. Following the way mentioned above, we have PDP of CDD as

$$\alpha_m^{\mathrm{cdd}} = \begin{cases} \frac{1}{\sqrt{2L}}, & m \in [1, D] \text{ or } m \in [L+1, L+D] \\ \frac{1}{\sqrt{L}}, & m \in [D+1, L] \end{cases} . \tag{3.32}$$

When $D >= L$, two PDPs are not overlapped, and $\alpha_m^{\mathrm{cdd}} = \sqrt{1/2L}$ for $m \in [1, L]$ and $m \in [D+1, D+L]$. Then, the effective number of paths of CDD is given from (3.14) by

$$\frac{1}{\Psi_{\mathrm{SC}}^{\mathrm{cdd}}(1,0,N_{\mathrm{SC}})} = \begin{cases} \frac{2L^2}{2L-D}, & D < L \\ 2L, & D \ge L \end{cases} . \tag{3.33}$$

From (3.33), we note that $\frac{1}{\Psi_{\mathrm{SC}}^{\mathrm{cdd}}(1,0,N_{\mathrm{SC}})}$ increases with D for $D < L$, which indicates that the effective number of paths increases. This agrees well with the fact that the number of paths in CDD channel increases with D for $D < L$. However, $\frac{1}{\Psi_{\mathrm{SC}}^{\mathrm{cdd}}(1,0,N_{\mathrm{SC}})}$ does not increase any more for $D \ge L$. This also agrees well since the number of paths in CDD channel is always $2L$ in this range of D. We can verify this situation even in more general case of a channel with not necessarily uniform PDP. Suppose just that

$\alpha_{1,m} = \alpha_{2,m} = \alpha_m$. Following the same way mentioned above to calculate PDP of CDD channel, we have

$$\alpha_m^{\text{cdd}} = \begin{cases} \frac{\alpha_m}{\sqrt{2}}\,, & m \in [1, D] \text{ or } m \in [L+1, L+D] \\ \frac{\sqrt{\alpha_m^2 + \alpha_{m-D}^2}}{\sqrt{2}}\,, & m \in [D+1, L]. \end{cases} \tag{3.34}$$

Then, the effective number of paths of CDD is given from (3.14) by

$$\frac{1}{\Psi_{\text{SC}}^{\text{cdd}}(1, 0, N_{\text{SC}})} = \begin{cases} \frac{2}{\sum_{m=1}^{L} \alpha_m^4 + \sum_{m=D+1}^{L} \alpha_m^2 \alpha_{m-D}^2}\,, & D < L \\ \frac{2}{\sum_{m=1}^{L} \alpha_m^4}\,, & D \geq L. \end{cases} \tag{3.35}$$

For $D < L$, we note that the first sum in the denominator is not affected by D. We find that the number of product terms in the second sum of the denominator is $L - D$. Thus, an increase of D reduces the number of product terms, which leads to a decrease of the denominator and an increase of the effective number of paths. This indicates that cyclic delay (D) increases the effective number of paths, which leads to an increase of the effective number of subcarriers or frequency selectivity. We can also see that there is no more increase in $\frac{1}{\Psi_{\text{SC}}^{\text{cdd}}(1,0,N_{\text{SC}})}$ for $D \geq L$.

3.4.2 Determination of Cyclic Delay from τ_{rms}

In (3.28), we need to maximize $\sqrt{\Psi_{\text{SC}}^{\text{cdd}}(1, 0, S_{\text{RB}}) \ln \frac{1}{\Psi_{\text{RB}}^{\text{cdd}}(S_{\text{RB}})}}$ since E_1 and V_1 are constant with respect to $\underline{\mathbf{D}}$. Considering (3.20), we need to maximize $\sqrt{\Psi_{\text{SC}}^{\text{cdd}}(1, 0, S_{\text{RB}})} \times \sqrt{\ln \frac{\Psi_{\text{SC}}^{\text{cdd}}(1,0,S_{\text{RB}})}{\Psi_{\text{SC}}^{\text{cdd}}(1,0,N_{\text{SC}})}}$. In Section 3.3.2, we found that the channel should be as flat as possible inside a block and as independent as possible between blocks to maximize multiuser diversity. Coherence bandwidth is regarded as the bandwidth where correlation between any two frequency component is enough large or more specifically larger than or equal to a certain large threshold [70]. In this section, we take the coherence bandwidth as the criteria for the flatness inside a block. That is, we take that a channel is enough flat inside a block if block size is less than or equal to the coherence bandwidth. This also implies that it is enough for $\Psi_{\text{SC}}^{\text{cdd}}(1, 0, S_{\text{RB}})$ to be larger than or equal to a certain threshold. Under this assumption, we need to maximize $\frac{1}{\Psi_{\text{SC}}^{\text{cdd}}(1,0,N_{\text{SC}})}$ from the equation mentioned above.

In (3.33) and (3.35), we note that $\frac{1}{\Psi_{\text{SC}}^{\text{cdd}}(1,0,N_{\text{SC}})}$ does not increase when cyclic delay is larger than the number of paths. More generally in Fig. 3.4, we cannot obtain any

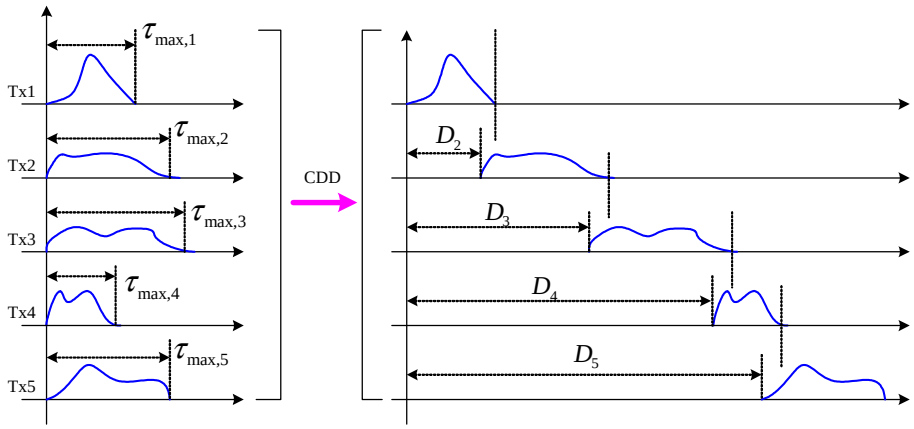

Figure 3.4: Example of power delay profile (PDP) in a cyclic delay diversity (CDD) channel. We note that PDP for Tx-i and Tx-$(i+1)$ does not overlap when $D_{i+1} > D_i + \tau_{\max,i}$, so that frequency selectivity does not increase any more.

more gain in $\frac{1}{\Psi_{\mathrm{SC}}^{\mathrm{cdd}}(1,0,N_{\mathrm{SC}})}$ when any two PDPs are not overlapped any more. Therefore, we need an additional constraint that PDP for Tx antenna-i with cyclic delay D_i should be overlapped with PDP for Tx antenna-$(i+1)$ with cyclic delay D_{i+1} as in Fig. 3.4. From the above, the problem we focus on is

$$\max_{\underline{\mathbf{D}}} \frac{1}{\Psi_{\mathrm{SC}}^{\mathrm{cdd}}(1,0,N_{\mathrm{SC}})} \quad \text{s.t.} \quad \begin{cases} B_{\mathrm{C}}^{\mathrm{cdd}} \geq S_{\mathrm{RB}} \\ D_{i+1} \leq D_i + \tau_{\max,i}, (1 \leq i < N_{\mathrm{T}}), \end{cases} \tag{3.36}$$

where $\tau_{\max,i}$ denotes the maximum delay spread in Tx antenna-i. As in many applications of CDD [68,71], we consider the case that $D_i = (i-1)D$. Then, we find that $\frac{1}{\Psi_{\mathrm{SC}}^{\mathrm{cdd}}(1,0,N_{\mathrm{SC}})}$ increases with D in (3.33) and (3.35). Since frequency selectivity increases with D, the coherence bandwidth decreases with D. Let $D_{\mathrm{B_c}}^*$ denote a maximum cyclic delay to meet $B_{\mathrm{C}}^{\mathrm{cdd}} \geq S_{\mathrm{RB}}$. Let $D_{\max}^* = \min_{1 \leq i < N_{\mathrm{T}}} \tau_{\max,i}$. Then, we note from (3.36) that cyclic delay which maximizes $\mathbb{E}[\max_b C_b]$ is the maximum of D while meeting two constraints of $D \leq D_{\mathrm{B_c}}^*$ and $D \leq D_{\max}^*$. That is, we can reduce (3.36) to

$$D_{\mathrm{PerUser}}^* = \min\{D_{\mathrm{B_c}}^*, D_{\max}^*\}. \tag{3.37}$$

Coherence Bandwidth of CDD Channel

A root mean square (RMS) delay spread following the notations in (3.1) is defined as [72]

$$\tau_{\mathrm{rms}} = \sqrt{\sum_{m=1}^{L}(m-1)^2\alpha_m^2 - \left(\sum_{m=1}^{L}(m-1)\alpha_m^2\right)^2}. \tag{3.38}$$

This is widely used in characterizing frequency selectivity of a channel [70,72,73]. When frequency selectivity increases (for example, the number of paths increases in a channel), τ_{rms} increases in (3.38).

Noting that the sum of a power delay profile (PDP) is normalized to 1 in (3.1), we can regard a delay spread (or excess delay) τ in Tx antenna-i as a random variable with a probability density function (PDF) of $f_i(\tau) = \sum_{m=1}^{L_i}\alpha_{i,m}^2\delta(\tau - m + 1)$. Let $\mu_i = \mathbb{E}[\tau]$ and $\tau_{\mathrm{rms},i} = \sqrt{\mathrm{var}[\tau]}$ denote the average and RMS delay spread in Tx antenna-i. We note that this $\tau_{\mathrm{rms},i}$ exactly matches with (3.38).

We mentioned in Section 3.4.1 that PDP in CDD channel is the average of PDP in each Tx antenna channel delayed by a cyclic delay. This is noted in Fig. 3.4 as well. Considering this property, we have a PDF for τ of CDD channel using its PDP as

$$f_{\mathrm{cdd}}(\tau) = \frac{1}{N_{\mathrm{T}}}\sum_{i=1}^{N_{\mathrm{T}}} f_i(\tau - D_i). \tag{3.39}$$

Then we can easily have the average delay spread as

$$\mu_{\mathrm{cdd}} = \int_0^\infty \tau f_{\mathrm{cdd}}(\tau)\, d\tau = \frac{1}{N_{\mathrm{T}}}\sum_{i=1}^{N_{\mathrm{T}}}(\mu_i + D_i). \tag{3.40}$$

Noting that $\mathrm{var}[\tau] = \mathbb{E}[\tau^2] - (\mathbb{E}[\tau])^2$, we also have for the RMS delay spread as

$$\tau_{\mathrm{rms}}^{\mathrm{cdd}} = \sqrt{\sum_{i=1}^{N_{\mathrm{T}}}\frac{{\tau_{\mathrm{rms},i}}^2 + (\mu_i + D_i)^2}{N_{\mathrm{T}}} - \left(\sum_{i=1}^{N_{\mathrm{T}}}\frac{\mu_i + D_i}{N_{\mathrm{T}}}\right)^2}. \tag{3.41}$$

When $D_i = (i-1)D$ as in [68,71], we can reduce (3.41) to

$$\tau_{\mathrm{rms}}^{\mathrm{cdd}} = \sqrt{aD^2 + bD + c + {\overline{\tau_{\mathrm{rms}}}}^2}, \tag{3.42}$$

where $\overline{\tau_{\mathrm{rms}}} = \sqrt{\sum_{i=1}^{N_{\mathrm{T}}}\tau_{\mathrm{rms},i}^2/N_{\mathrm{T}}}$ and other constants are defined as

$a \triangleq \frac{1}{12}({N_{\mathrm{T}}}^2 - 1)$	$b \triangleq 2\mu_{\mathrm{w}} - \mu^{(1)}(N_{\mathrm{T}} + 1)$	$c \triangleq \mu^{(2)} - (\mu^{(1)})^2$
$\mu^{(1)} \triangleq \frac{1}{N_{\mathrm{T}}}\sum_{i=1}^{N_{\mathrm{T}}}\mu_i$	$\mu_{\mathrm{w}} \triangleq \frac{1}{N_{\mathrm{T}}}\sum_{i=1}^{N_{\mathrm{T}}} i\mu_i$	$\mu^{(2)} \triangleq \frac{1}{N_{\mathrm{T}}}\sum_{i=1}^{N_{\mathrm{T}}}\mu_i^2$

. (3.43)

Since the channel coherence bandwidth can be represented as the inverse of the RMS delay spread [70, 72, 73], the coherence bandwidth of CDD channel is given by

$$B_{\mathrm{C}}^{\mathrm{cdd}} \simeq \frac{1}{K\tau_{\mathrm{rms}}^{\mathrm{cdd}}} = \frac{1}{K\sqrt{aD^2+bD+c+\overline{\tau_{\mathrm{rms}}}^{\,2}}} \tag{3.44}$$

where K is a constant to determine the coherence bandwidth, which is related to the minimum correlation coefficient of the SNR between two frequency components within the coherence bandwidth.

Relation between the Maximum Delay Spread and the RMS Delay Spread

For the delay spread τ in the channel of Tx antenna i with mean μ_i and variance $\tau_{\mathrm{rms},i}^2$, we have from the Chebyshev inequality [49]

$$\int_{|\tau-\mu_i|\le\epsilon} f_i(\tau)d\tau = Pr\{|\tau-\mu_i|\le\epsilon\} \ge 1-\frac{\tau_{\mathrm{rms},i}^2}{\epsilon^2} \triangleq \kappa. \tag{3.45}$$

This inequality indicates that the ratio of the total received power to the transmitted power is equal to or greater than κ when $|\tau-\mu_i|\le\epsilon$, *i.e.*, $\mu_i-\epsilon\le\tau\le\mu_i+\epsilon$. For example, $\kappa=0.9$ means that the received power is over 90% of the transmitted power in that range of τ. Then, we have from (3.45)

$$\epsilon = \frac{\tau_{\mathrm{rms},i}}{\sqrt{1-\kappa}}. \tag{3.46}$$

If we let the maximum delay spread $\tau_{\mathrm{max},i}$ be the length of the delay spread where the power ratio is equal to or larger than κ and we let $\tau_{\mathrm{max},i}$ be an integer for the later use for cyclic delay, $\tau_{\mathrm{max},i}$ is given by

$$\tau_{\mathrm{max},i} = [\mu_i+\epsilon]-[\mu_i-\epsilon]+1, \tag{3.47}$$

where $[x]$ indicates the maximum integer that is not greater than x. Since $\tau_{\mathrm{max},i} < 2\epsilon+2$ in (3.47) and it is an integer, we have from (3.46)

$$\tau_{\mathrm{max},i} = \lceil 2\epsilon\rceil + 1 = \left\lceil \frac{2\tau_{\mathrm{rms},i}}{\sqrt{1-\kappa}} \right\rceil + 1. \tag{3.48}$$

Determine $D_{\mathbf{PerUser}}^*$

From (3.44), the maximum cyclic delay $D_{\mathrm{B_c}}^*$ in (3.37) to meet $B_{\mathrm{C}}^{\mathrm{cdd}} \ge S_{\mathrm{RB}}$ is given by

$$D_{\mathrm{B_c}}^* = \left\lfloor \frac{1}{\sqrt{a}} \sqrt{\left(\frac{1}{K^2 S_{\mathrm{RB}}{}^2} - \overline{\tau_{\mathrm{rms}}}^2 + \frac{b^2-4ac}{4a}\right)_+} - \frac{b}{2a} \right\rfloor, \tag{3.49}$$

where $(x)_+$ denotes $\max(0, x)$. From (3.48), $D^*_{\max}$ in (3.37) is given by

$$D^*_{\max} = \min_{1 \le i < N_{\mathrm{T}}} \left\lceil \frac{2\tau_{\mathrm{rms},i}}{\sqrt{1-\kappa}} \right\rceil + 1. \tag{3.50}$$

Then, we have the per-user optimal cyclic delay D^*_{PerUser} in (3.37) as the minimum of $D^*_{\mathrm{B_c}}$ in (3.49) and $D^*_{\max}$ from (3.50).

To have an idea about the relation between D^*_{PerUser} and the RMS delay spread and block size S_{RB}, let us consider a simple and practical case. Suppose that channels in all Tx antennas have the same average delay spread and the same RMS delay spread, *i.e.*, $\tau_{\mathrm{rms},i} = \tau_{\mathrm{rms},j} = \tau_{\mathrm{rms}}$ and $\mu_i = \mu_j$ $(1 \le i, j \le N_{\mathrm{T}})$. We note that we do not put any other constraint on PDP's of channels. After some manipulation, we have for per-user optimal cyclic delay as

$$D^*_{\mathrm{PerUser}} = \min \left\{ \sqrt{\frac{12}{{N_{\mathrm{T}}}^2 - 1} \left(\frac{1}{K^2 {S_{\mathrm{RB}}}^2} - \tau^2_{\mathrm{rms}} \right)_+}, \left\lceil \frac{2\tau_{\mathrm{rms}}}{\sqrt{1-\kappa}} \right\rceil + 1 \right\} \tag{3.51}$$

We note in (3.51) that D^*_{PerUser} increases with τ_{rms} for the small RMS delay spread because the second term is dominant. When τ_{rms} is large, the first term is dominant and D^*_{PerUser} decreases with τ_{rms}. For example, in flat fading channel, $D^*_{\mathrm{PerUser}} = 1$ because $\tau_{\mathrm{rms}} = 0$, which agrees with the idea that there is no more gain in effective diversity $(\frac{1}{\Psi^{\mathrm{cdd}}_{\mathrm{SC}}(1,0,N_{\mathrm{SC}})})$ for larger cyclic delay than 1. We also note that D^*_{PerUser} should become smaller as S_{RB} grows larger. This agrees well with the idea that a large block size requires a large coherence bandwidth and thus small cyclic delay.

When frequency selectivity in a given channel is already large enough, τ^2_{rms} in (3.51) makes the first term zero, and D^*_{PerUser} reduces to zero. This indicates that CDD does not give any benefit for $\mathbb{E}[\max_b C_b]$ in this channel. From this, we note that there may exist an optimal threshold of τ_{rms} whereby we decide whether to employ CDD or not to enhance multiuser diversity, which is left as a future work. We can also say that this threshold decreases with S_{RB}.

3.5 Numerical Results

To obtain numerical results, we consider $N_{\mathrm{SC}} = 1024$ for the FFT size and exponential PDP for each channel of Tx antenna as following.

$$\alpha_m = \frac{e^{-\frac{m}{\tau_o}}}{\sqrt{\sum_{m=1}^{L} e^{-\frac{2m}{\tau_o}}}}. \tag{3.52}$$

Various RMS delay spreads are obtained by changing τ_o in α_m. We consider that the number of paths L is less than or equal to 64 depending on the RMS delay spread. For each obtained channel, we compute all functions in Section 3.3.1 for numerical evaluation of maximum of the block average throughput ($\mathbb{E}[\max_b C_b]$). For comparison purpose, we show Monte-Carlo simulation results for maximum of the block average throughput ($\mathbb{E}[\max_b C_b]$) and the sum rate (R_{SUM}) using proportional fair scheduling described in Section 3.2.1. Regarding CDD, we use $N_{\text{T}} = 2$ to better characterize the role of cyclic delay.

3.5.1 Frequency Selectivity, Intra-block Sum Correlation and the Effective Number of Blocks

When τ_o in (3.52) increases, both the RMS delay spread and the number of valid paths increase. Thus, frequency selectivity measure $\frac{1}{\Psi_{\text{SC}}(1,0,N_{\text{SC}})}$, also known as the effective number of paths, increases with the RMS delay spread in Fig. 3.5(a). This also explains an increase of the effective number of blocks[5] $\frac{1}{\Psi_{\text{RB}}(S_{\text{RB}})}$ for each block size in Fig. 3.5(a). Meanwhile, correlation between subcarriers decreases and thus the intra-block sum correlation decreases with the RMS delay spread in Fig. 3.5(b). Since the effective number of blocks increases but the intra-block sum correlation decreases with the RMS delay spread in this figure, we can verify the trade-off between them in (3.23) and (3.24).

As discussed in Section 3.4, frequency selectivity increases with cyclic delay in CDD. We can verify this in Fig. 3.6(a). In a different way from Fig. 3.5, frequency selectivity saturates to two times of the value for SISO (*i.e.,* $D = 0$). This confirms the discussion in Section 3.4.1 that the number of paths does not increase when cyclic delay is larger than the number of paths in a given channel. As cyclic delay increases, the sinusoidal components in (3.31) cause more local peaks in correlation because the period $\frac{N_{\text{SC}}}{D}$ decreases. This makes block correlation larger and the effective number of blocks does not increase monotonically with cyclic delay in Fig. 3.6(a). Meanwhile, we note that the intra-block sum correlation always decreases with cyclic delay in Fig. 3.6(b). We can find the trade-off between $\frac{1}{\Psi^{\text{cdd}}_{\text{RB}}(S_{\text{RB}})}$ and $\Psi^{\text{cdd}}_{\text{SC}}(1,0,S_{\text{RB}})$ with respect to cyclic delay. However, for the larger cyclic delay than that which gives the peak of $\frac{1}{\Psi_{\text{RB}}(S_{\text{RB}})}$, both of effective number of blocks and the intra-block sum correlation decrease. Thus,

[5]We note that the effective number of blocks is the inverse of inter-block sum correlation as discussed in Section 3.3.2.

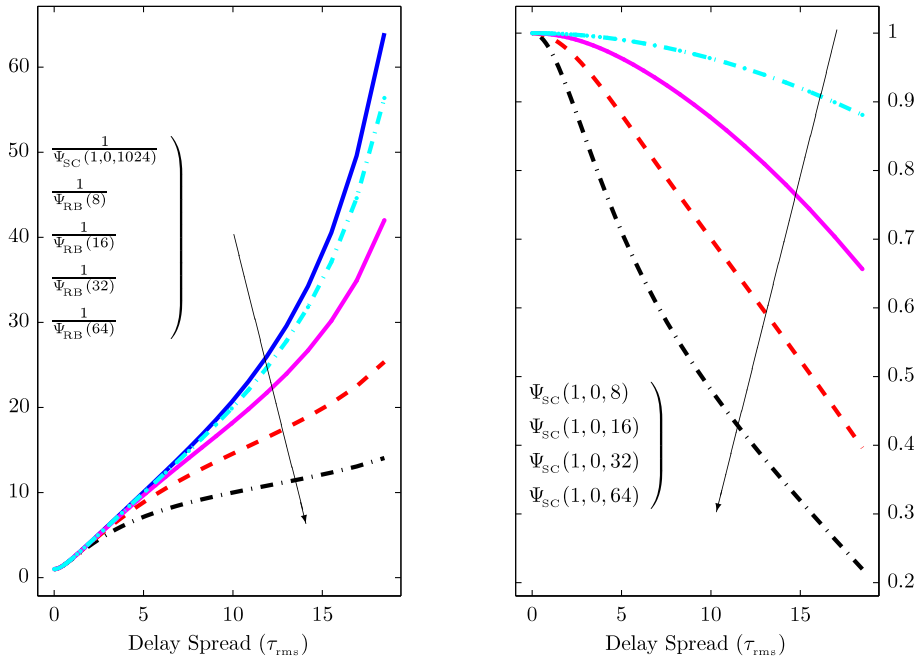

Figure 3.5: Effect of frequency selectivity (τ_{rms}) on the effective number of subcarriers ($\frac{1}{\Psi_{\text{SC}}(1,0,N_{\text{SC}})}$), the effective number of blocks ($\frac{1}{\Psi_{\text{RB}}(S_{\text{RB}})}$), and the intra-block sum correlation ($\Psi_{\text{SC}}(1,0,S_{\text{RB}})$).

we don't have to consider these cyclic delays for evaluation of (3.27) and (3.28), which much saves the load of exhaustive search.

3.5.2 Optimality of Frequency Selectivity on Multiuser Diversity and Optimal Addition of Frequency Selectivity

In Fig. 3.7, we first note that Gaussian approximation of $\mathbb{E}[\max_b C_b]$ in (3.24) better matches with the simulation than order statistic approximation in (3.23). Further, when we do not consider a round robin scheduling for the scheduling outage (*i.e.,* no user reports for a block), Gaussian approximation and the simulation result of $\mathbb{E}[\max_b C_b]$ are well matched with the simulation result of the sum rate. This can justify the Gaussian approximation of the block average throughput. We note that there exists optimal frequency selectivity that maximizes the sum rate. Since maximizing $\mathbb{E}[\max_b C_b]$ is related to the per-user optimality, we also note that per-user optimality is good for the approximation of the sum rate optimality. When we use a round-robin scheduling for blocks in scheduling outage, an arbitrary user is selected for those blocks. This causes the sum rate to decrease compared to other cases. However, optimal frequency selectivity

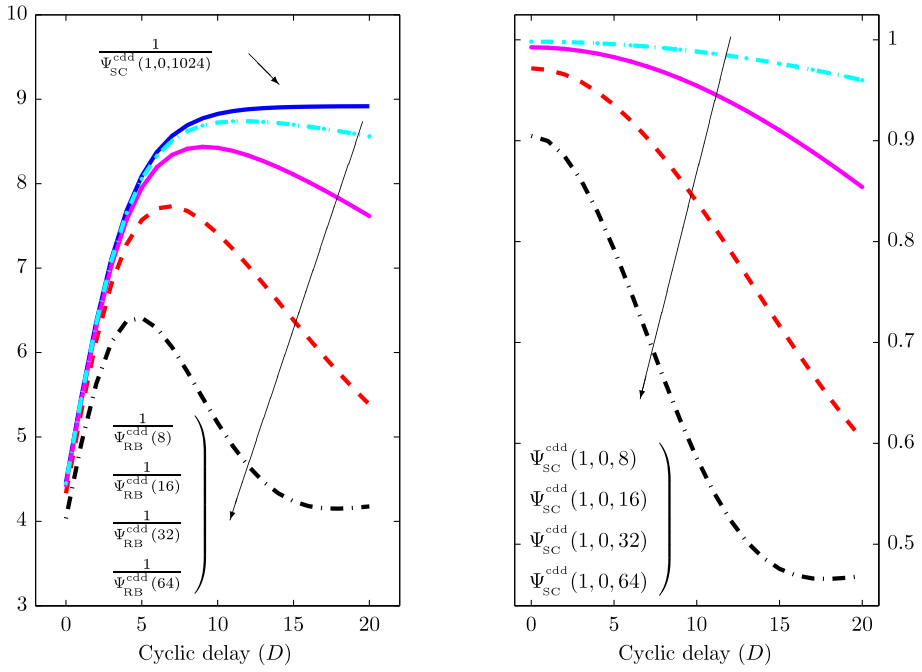

Figure 3.6: Effect of cyclic delay (D) on the effective number of subcarriers ($\frac{1}{\Psi_{\mathrm{SC}}(1,0,N_{\mathrm{SC}})}$), the effective number of blocks ($\frac{1}{\Psi_{\mathrm{RB}}(S_{\mathrm{RB}})}$), and the intra-block sum correlation ($\Psi_{\mathrm{SC}}(1,0,S_{\mathrm{RB}})$).

is not changed much. We also find that the sum rate in a limited fluctuating channel with small frequency selectivity is very small. This implies that addition of frequency selectivity would enhance the sum rate as in CDD.

Fig. 3.8 shows the sum rate change with cyclic delay when CDD is used to increase frequency selectivity. First, we find from simulation results that the sum rate gain by CDD to SISO (*i.e.,* $D = 0$) is remarkable and that there exists optimal cyclic delay in the sense of maximum sum rate. In the figure, we mark per-user optimal cyclic delays found by two approximations in (3.27) and (3.28) and the RMS delay spread in (3.51). Although per-user optimality is not perfectly matched with sum-rate optimality, the sum rate by per-user optimal cyclic delay is very close to that by sum-rate optimal one. This is also found in Fig. 3.9, which illustrates the sum rate of CDD with D^*_{PerUser} and D^*_{SumRate} and the sum rate of a SISO system. We note that D^*_{PerUser} achieves very close performance of D^*_{SumRate}. We find that the gain of CDD to SISO system is remarkable especially in the range of small frequency selectivity, but small in a channel with large frequency selectivity. This is because the achievable gain itself is small for a channel with frequency selectivity already close to optimal selectivity as shown in Fig. 3.7. This also

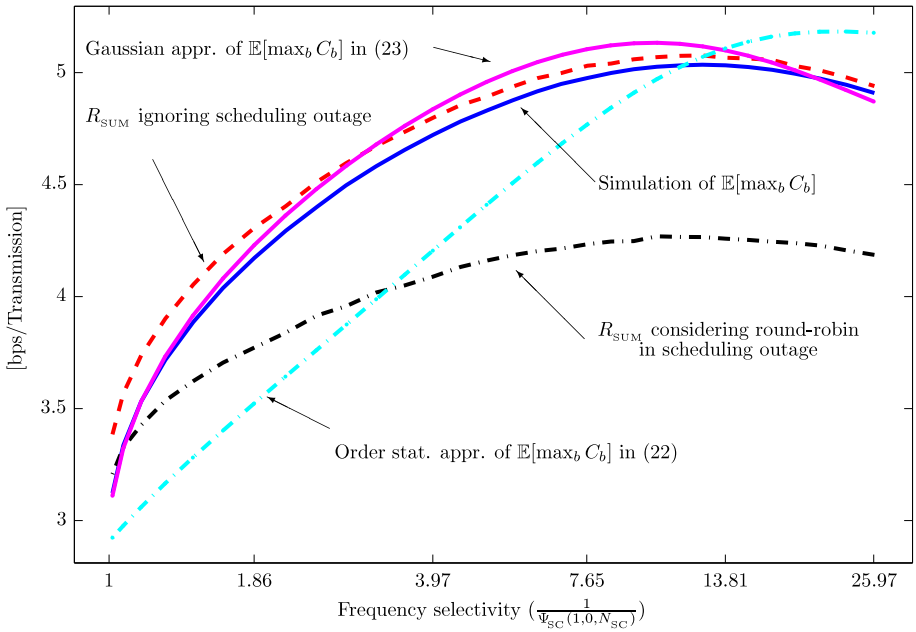

Figure 3.7: Effect of frequency selectivity ($\frac{1}{\Psi_{\text{SC}}(1,0,N_{\text{SC}})}$) on multiuser diversity (*i.e.*, maximum of the block average throughput of an arbitrary user ($\mathbb{E}[\max_b C_b]$) and the sum rate (R_{SUM})). Two approximations for $\mathbb{E}[\max_b C_b]$ in (3.23) and (3.24) are compared as well. 'RR' denotes round robin scheduling. In the case of without RR, blocks are ignored when a scheduling outage happens. (N_{RB}=32 blocks, K=32 users)

shows the reason why all the schemes related random beamforming [5,11] are considered in a channel with slow fading at the time domain.

In Fig. 3.10, we compare the sum rate gain to SISO for our D^*_{PerUser} and arbitrarily fixed cyclic delay (D^{x}). We find that D^*_{PerUser} shows more stable and better performance than any fixed one in the whole range of block sizes. In particular, misuse of cyclic delay leads to the smaller sum rate than that of SISO. This implies that adaptive cyclic delay based on our technique is better. The case that fixed cyclic delay shows better performance in a specific S_{RB} is corresponding to the case that fixed one happens to coincide with D^*_{SumRate}.

3.5.3 Factors to Affect Optimal Frequency Selectivity

We saw in Fig. 3.5(b) that the intra-block sum correlation $\Psi_{\text{SC}}(1,0,S_{\text{RB}})$ in (3.12) decreases much in large block size for a small increase of frequency selectivity. However, the effective number of blocks $\frac{1}{\Psi_{\text{RB}}(S_{\text{RB}})}$ does not increase much in Fig. 3.5(a). Thus, optimal frequency selectivity or cyclic delay that maximizes the trade-off in (3.24)

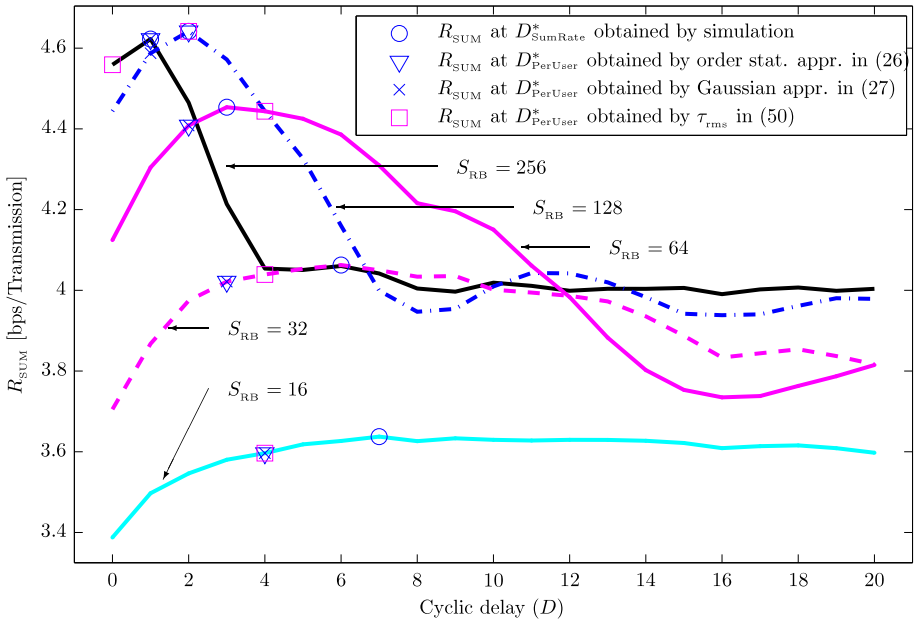

Figure 3.8: Effect of cyclic delay (D) on the sum rate. In each curve for the different block size, D^*_{SumRate} and D^*_{PerUser} are marked. ($\frac{1}{\Psi_{\mathrm{SC}}(1,0,N_{\mathrm{SC}})} = 1.6246$ of original channel, $K = 32$ users)

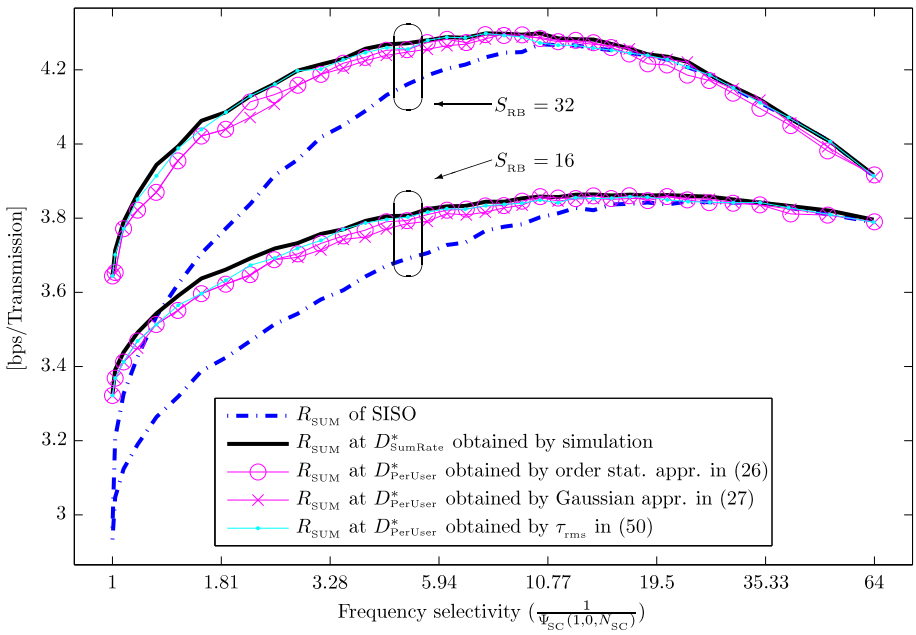

Figure 3.9: Sum rate comparison for SISO, CDD with per-user optimal cyclic delay D^*_{PerUser} and CDD with sum-rate optimal cyclic delay D^*_{SumRate} as a function of frequency selectivity ($\frac{1}{\Psi_{\mathrm{SC}}(1,0,N_{\mathrm{SC}})}$). Two approximations in (3.27) and (3.28) are used for D^*_{PerUser}. ($K = 32$ users)

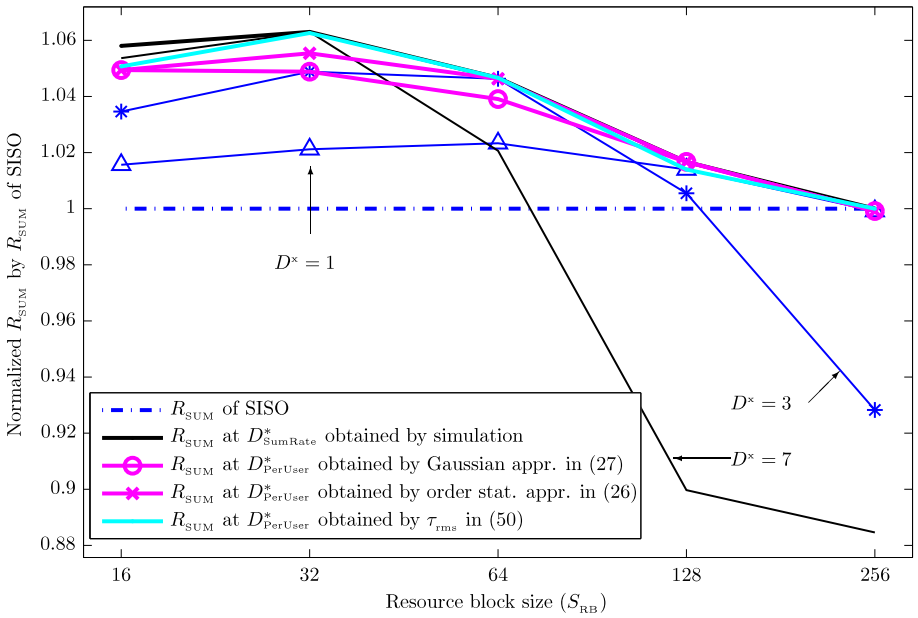

Figure 3.10: Sum rate gain of cyclic delay diversity compared to SISO by per-user optimal cyclic delay D^{*}_{PerUser} and sum-rate optimal cyclic delay D^{*}_{SumRate} as a function of block size (S_{RB}). Two approximations for D^{*}_{PerUser} in (3.27) and (3.28) and fixed cyclic delay scheme are compared as well. ($\frac{1}{\Psi_{\mathrm{SC}}(1,0,N_{\mathrm{SC}})} = 1.6246$ of original channel, $K = 32$ users)

and (3.28) decreases with the block size, both of which are illustrated in Fig. 3.11(a) and Fig. 3.11(b), respectively. We also find that per-user optimal frequency selectivity obtained by Gaussian approximation agrees well with that by simulation and with sum-rate optimal frequency selectivity except for $S_{\mathrm{RB}} = 256$ in Fig. 3.11(a). Although cyclic delay calculated by approximation is not well matched with sum-rate optimal one, we stress again that the sum rate is close to optimal value as in Fig. 3.9. When $S_{\mathrm{RB}} = 256$ and $K = 32$ in the figure, there are 4 blocks. Thus, about 8 users in the average sense contend for each block to be scheduled. Thus, variance of a block becomes a more important factor and thus the large intra-block sum correlation is preferred to improve the sum rate. This explains that frequency selectivity or cyclic delay for sum-rate optimality is smaller than that expected by the approximation in Fig. 3.11.

Frequency selectivity of a given channel is another factor to affect the optimal cyclic delay. In Fig. 3.12, we find that both of per-user optimal cyclic delay and sum-rate optimal cyclic delay increase with small frequency selectivity, but decrease with large frequency selectivity. This indicates that an increase of diversity (*i.e.,* effective number of blocks, $\frac{1}{\Psi_{\mathrm{RB}}(S_{\mathrm{RB}})}$) is dominant in a limited fluctuated channel. However, making a variance large by keeping $\Psi_{\mathrm{SC}}(1, 0, S_{\mathrm{RB}})$ large is more important in a channel with large selectivity. In a system employing a fixed cyclic delay without updating PDP, we note in Fig. 3.10 and Fig. 3.12 that large sum rate is achieved in rather small block size such as $S_{\mathrm{RB}} \leq 64$ when we use $D^{\mathrm{x}} = 3, 4$, or 5 suggested by D^{*}_{PerUser}.

3.6 Conclusion

In this chapter, we studied the effect of frequency selectivity on multiuser diversity. We focused on analyzing maximum of the block average throughput of an arbitrary user by considering two approximations for that. From these approximations, we found that there exists optimal frequency selectivity in the sense of maximizing multiuser diversity, and we verified this by a simulation as well. We showed that the optimal channel is flat within a block and mutually independent between blocks.

Motivated by the fact that cyclic delay diversity (CDD) increases a channel fluctuation, we considered to use CDD in a channel with small frequency selectivity to enhance the sum rate of a system. Based on the previous study of optimal frequency selectivity, we proposed two techniques to determine per-user optimal cyclic delay exploiting approximations we developed for multiuser diversity. We investigated the

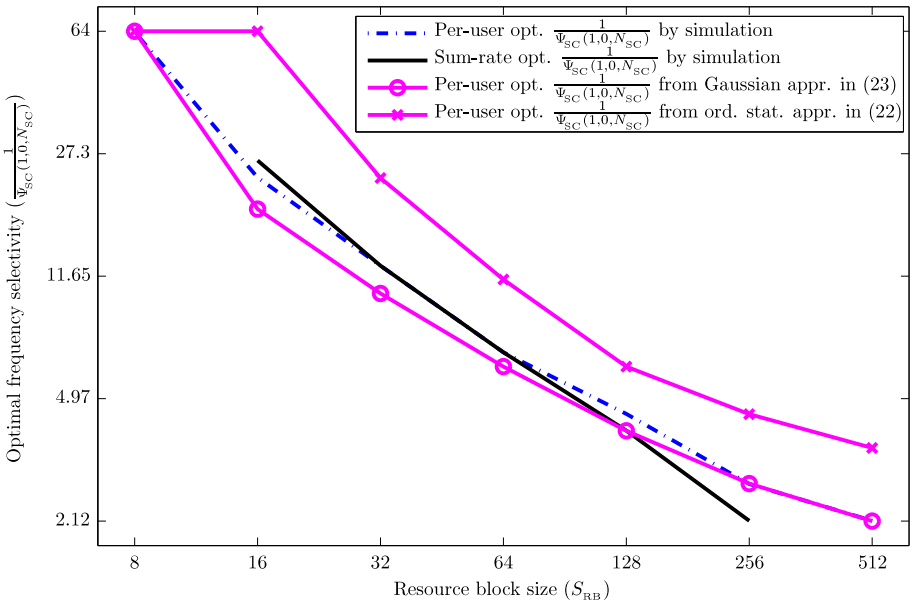

(a)

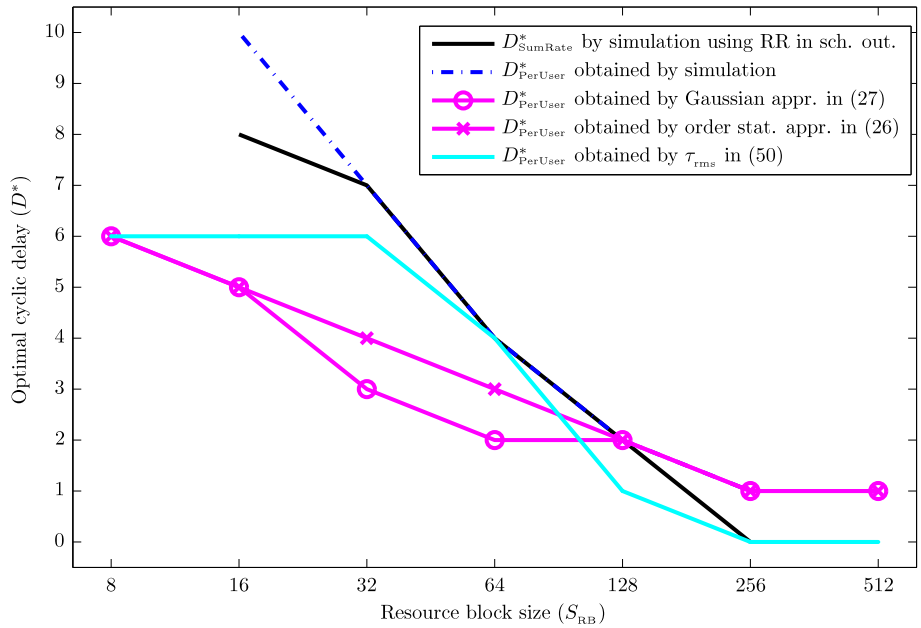

(b)

Figure 3.11: Effect of block size (S_{RB}) on optimal frequency selectivity ($\frac{1}{\Psi_{\mathrm{SC}}(1,0,N_{\mathrm{SC}})}$) (a) and on the optimal cyclic delay (b). Two approximations are compared to a simulation result. The simulated sum rate optimal one is compared as well. (K=32 users)

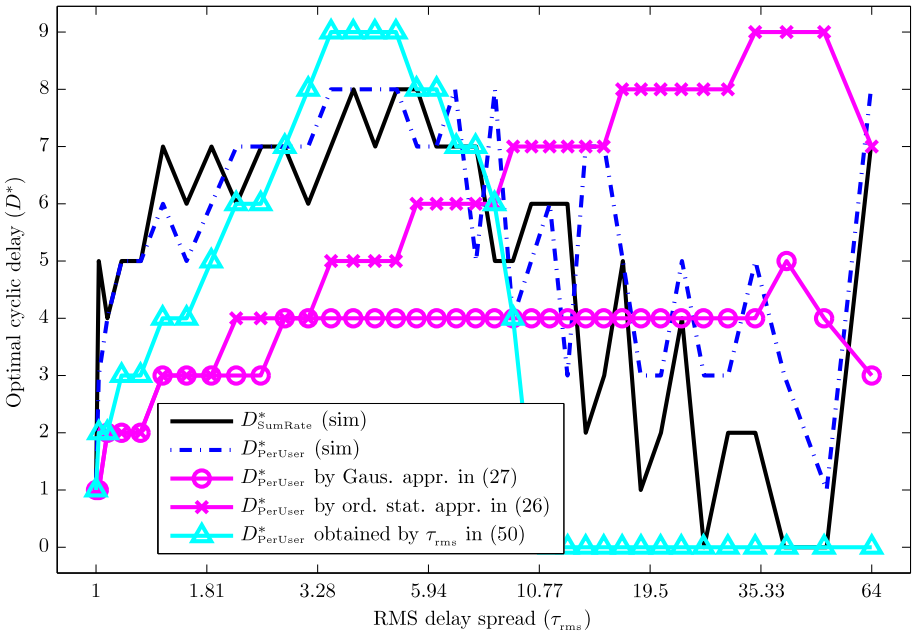

Figure 3.12: Comparison of per-user optimal cyclic delay (D^*_{PerUser}) and sum-rate optimal cyclic delay (D^*_{SumRate}) as a function of frequency selectivity (τ_{rms}). Two approximations for D^*_{PerUser} in (3.27) and (3.28) are compared as well. ($N_{\text{RB}} = 32$ blocks, $\frac{1}{\Psi_{\text{SC}}(1,0,N_{\text{SC}})} = 1.6246$ of original channel, $K = 32$ users)

role of cyclic delay to frequency selectivity as well. We showed by simulation that the proposed techniques achieve better performance than a conventional fixed cyclic delay scheme and that the throughput is very close to the optimal sum rate possible with CDD.

The material in this chapter is work which is in preparation for submission to the IEEE Transactions on Signal Processing under the title "*On the optimal frequency selectivity to maximize multiuser diversity in an OFDMA scheduling system*". Sections of this chapter appear in Asilomar Conference on Signals, Systems, and Computers 2010 under the title "*Determination of cyclic delay for CDD utilizing RMS delay spread in OFDMA multiuser scheduling systems*". Both of these works are co-authored with Professor Bhaskar D. Rao, Dr. James R. Zeidler, and Professor Min-Joong Rim. The dissertation author was the primary investigator and author of this paper.

Chapter 4

Interference Management in an Uplink Interference-limited Multi-cell Environment

4.1 Introduction

The capacity of the interference channel is not fully known even in the simplest two user interference channel. The best known result is about the approximate capacity region which is within one bit for all values of the channel parameters for the Gaussian interference channel [74]. Since the exact optimal scheme is not known, interference is usually managed depending on its magnitude compared to the signal strength: Treating as noise for weak interference, decoding and canceling for strong interference, and avoiding through orthogonalization or alignment for the comparable interference [75].

One of the most common systems with an interference channel is the multi-cell cellular network. Interference in the cellular network can be classified into intra-cell interference and inter-cell interference. Handling both types of interference is one of key challenges in the cellular network [33,34]. To minimize intra-cell interference, orthogonal user selection schemes utilizing such as zero-forcing beamforming were proposed in [76,77] and references therein. Various approaches have been suggested to tackle inter-cell interference. See, for example, [34] and references therein. From a signal processing point of view, interference suppression can be achieved by processing a signal at either the transmitter or the receiver, or at both ends [78–81]. Most of works are limited

to designing the spatial strategies *i.e.,* precoding vectors, to utilize the conventional diversity methods to handle the interference assuming that the active users have been already selected [78–81].

Another approach to mitigate inter-cell interference is to exploit multiuser diversity. In [5], inter-cell interference is effectively avoided in downlink multi-cell communication by the opportunistic nulling operation. The bottom line principle is to schedule a user at any time whose received signal to interference and noise ratio (SINR) is the largest, which also leads to multiuser diversity. However, in uplink multi-cell communication, the SINR at a base station depends on the selected users in other cells, which is generally not known to the base station. Due to this coupled nature, optimal user selection could be achieved if there exists a central unit which gathers the channel information from all the users in all the cells, or if full cooperation is possible among the involved base stations [82]. Unfortunately, this may not be feasible in a practical cellular network because it would be highly complex especially due to the required back-haul operation between base stations and exhaustive search for the best set of users. Therefore, a practical user scheduling method is needed while handling inter-cell interference.

In a communication system, a receive beamforming (BF) vector at a receiver affects only that receiver. However, a transmit BF vector at a transmitter affects all the receivers in a network. Thus, great care should be taken in designing a transmit BF vector. This explains why the problem of designing a transmit BF vector is more difficult than designing a receive BF vector. To avoid this challenge in designing a transmit BF vector, network duality was used to convert the problem into designing a receive BF vector [36]. Network duality states that there exists a dual network which achieves the same SINR with the same set of transmit and receive BF vectors [36]. Network duality was first implied in [35] as the virtual uplink concept and was generalized in [36]. In [35], the virtual uplink is constructed by considering the reciprocal of the downlink channels and changing the role of transmit and receive BF vectors. It was shown in [35] that the same SINR performance can be achieved in the downlink and its corresponding virtual uplink. This concept of network duality is utilized to find transmit BF vectors in a primal network by finding receive BF vectors in a dual network [36].

In the first part of this chapter, we consider joint user scheduling and beamforming to exploit multiuser diversity as well as develop signal processing methods to handle

inter-cell interference in the uplink. Users are required to compute a transmit beamforming vector and to feedback a metric which will be used as a user-scheduling metric at the base station (BS). For this purpose, we propose three schemes to enhance the sum rate of the system. First, we utilize a metric of the signal to generated interference and noise ratio (SGINR) [37], which is also known as the signal to leakage and noise ratio [38, 39]. Second, we propose a metric of the signal to interference and noise ratio in a dual network (DSINR). In both cases, a beamforming vector and a feedback metric are determined to maximize SGINR or DSINR. In BS, users are selected in a manner that the beamforming effect is maximized. The benefit of this procedure is that the calculation of the beamforming vector and user-scheduling metric is performed at each user based on its local channel state information (CSI) in a decoupled manner [37–39]. In addition, when multiple users are selected, intra-cell interference among the selected users in each cell should be reduced [76, 77]. For this purpose, we also propose a two-step user-selection procedure to improve the orthogonality of selected users, which leads to minimizing intra-cell interference.

Recently, interference alignment (IA) was proposed as a degree of freedom (DOF) optimal scheme [75]. The basic idea is to restrict all the undesired interference from other communication links into a pre-determined subspace which is independent of the desired signal subspace. However, the scheme demands that each transmitter should have the global knowledge of channel state information of other communication links and huge dimension of time, frequency or spatial expansions. To incorporate the conventional IA scheme in the uplink cellular network , the opportunistic IA scheme was proposed, where multiuser diversity gain is exploited to overcome the drawback of the conventional IA scheme mentioned above [40]. However, this scheme does not work well as the number of interfering base stations increases.

In the second part of this chapter, we consider the opportunistic IA scheme in an interference-limited uplink cellular network as an alternative approach to suppress inter-cell interference. We propose a method to enhance the sum rate by maximizing the DSINR developed for joint scheduling and beamforming. We show that the proposed methods greatly improve the sum rate compared to the conventional opportunistic scheme.

In summary, the main contribution of the chapter is to propose three schemes for joint scheduling and beamforming, and to propose one scheme for the opportunistic

IA scheme to enhance the sum rate in an uplink cellular network.

This chapter is organized as follows. In Section 4.2, we develop the sum rate of the system and propose schemes to enhance the sum rate of the system by considering joint scheduling and transmit beamforming. In Section 4.3, we develop a scheme to enhance the sum rate by maximizing DSINR for the opportunistic interference alignment scheme. We conclude in Section 4.4.

4.2 Joint User Scheduling and Beamforming

In this section, we develop a joint scheduling and transmit beamforming scheme to enhance the sum rate of the system. We first describe the system model and derive the sum rate of the system when joint decoding for the selected users is assumed at each BS. We also compute the sum rate when the MMSE receiver is utilized for the message detection of the selected users. Then, we describe the conventional user selection schemes to maximize the in-cell SNR and to minimize the generated interference (GIN) to other cells. We then propose three new schemes maximizing SGINR or DSINR to enhance the sum rate. This section is organized as follows. In Section 4.2.1, we describe the system model. In Section 4.2.2, we develop the sum rate of the system. In Section 4.2.3, we explain the conventional user selection schemes. In Section 4.2.4, we propose schemes to enhance the sum rate of the system. In Section 4.2.5, we compare the proposed beamforming strategy with the conventional ones. In Section 4.2.6, we show numerical results and compare the sum rate of the proposed schemes with the conventional one.

4.2.1 System Model

We consider an uplink time division duplex (TDD) cellular system with N_{BS} cells as in Fig. 4.1. Each cell has one base station (BS) and N_{US} users. Each base station is equipped with N_{R} receive antennas and each user has N_{T} transmit antennas. A channel from user-j in cell-i to BS-k is denoted as $H_{ij}^{(k)}$ which is an $N_{\mathrm{R}} \times N_{\mathrm{T}}$ matrix. We assume that the channels are reciprocal between the uplink and the downlink. Each entry of the channel matrix is assumed to follow a complex Gaussian distribution $\mathcal{CN}(0,1)$,[1] and all the entries are assumed to be mutually independent of one another. At each scheduling instant, user selection and data transmission consist of four stages; (i) feedback of one

[1] $\mathcal{CN}(\mu,\sigma^2)$ denotes a circularly symmetric complex Gaussian distribution with mean μ and variance σ^2.

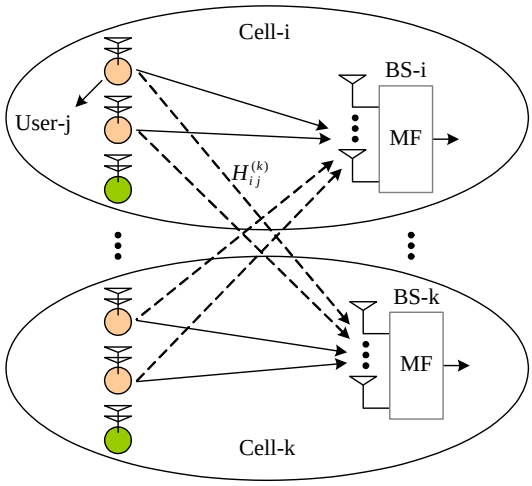

Figure 4.1: System block diagram for an uplink cellular system. Transmit beamforming vectors are utilized for selected users.

analog value from each user, (ii) selection of N_{ST} users at each BS, (iii) uplink signal transmission of the selected users employing transmit beamforming, and (iv) signal detection at each BS.

Specifically, in the first stage, user-j in cell-i measures the downlink channel coefficients from all the BSs, *i.e.,* $H_{ij}^{(k)}$ for $1 \leq k \leq N_{\mathrm{BS}}$. The user computes the covariance matrix K_{ij} based on the measured channel coefficients and finds the appropriate eigenvalue L_{ij} from K_{ij}. Both K_{ij} and L_{ij} depend on the signal processing strategy. Then, the user feeds back the eigenvalue to its own BS. Details of feedback information will be elaborated in Section 4.2.3 and Section 4.2.4. In the second stage, BS-i selects N_{ST} users, each of whom is denoted as $\pi_i(\ell)$ for $1 \leq \ell \leq N_{\mathrm{ST}}$. A set of the selected users at BS-i is denoted as Π_i. The scheduling policy for user selection will be given in Section 4.2.3 and Section 4.2.4. Suppose in the second stage that user-j is selected in cell-i. In the third stage, the selected user computes the beamforming vector $\mathbf{w}_{ij}$, which is used to transmit data x_{ij}. In the fourth stage, BS-i employs a minimum mean square estimation (MMSE) receiver to retrieve each message of the selected users treating others as noise. However, for the comparison, we also consider the capacity with joint decoding for the selected users at each base station as the upper-bound, which is equivalent to the capacity of the space division multiple access (SDMA) and can be achieved by successive interference cancelation (SIC) combined with MMSE detection [64, Ch.8].

Let ρ_{ij} denote the signal to noise ratio (SNR) of user-j at BS-i. Let $\eta_{ij}^{(k)}$ denote

the interference to noise ratio (INR) of user-j in cell-i to BS-k. Then, the received signal at BS-i satisfies the equation

$$\mathbf{y}_i = \sum_{j\in\,\Pi_i} \sqrt{\rho_{ij}}\; H_{ij}^{(i)}\mathbf{w}_{ij}\, x_{ij} + \sum_{k=1,k\neq i}^{N_{\mathrm{BS}}} \sum_{j\in\,\Pi_k} \sqrt{\eta_{kj}^{(i)}} H_{kj}^{(i)}\mathbf{w}_{kj}\, x_{kj} + \mathbf{z}_i \tag{4.1}$$

where $\mathbf{z}_i$ denotes the additive white Gaussian noise (AWGN) vector at BS-i which follows $\mathcal{CN}(\mathbf{0}, \mathbf{I}_{N_{\mathrm{R}}})$. Here, $\mathbf{I}_{N_{\mathrm{R}}}$ denotes the $N_{\mathrm{R}} \times N_{\mathrm{R}}$ identity matrix. For MMSE detection of user-$\pi(\ell)$ at BS-i, $\mathbf{y}_i$ can be rewritten as

$$\begin{aligned}\mathbf{y}_i = \sqrt{\rho_{i\pi_i(\ell)}}\; H_{i\pi_i(\ell)}^{(i)}\mathbf{w}_{i\pi_i(\ell)} x_{i\pi_i(\ell)} &+ \sum_{j\in\,\Pi_i, j\neq\pi_i(\ell)} \sqrt{\rho_{ij}}\; H_{ij}^{(i)}\mathbf{w}_{ij}\, x_{ij} \\ &+ \sum_{k=1,k\neq i}^{N_{\mathrm{BS}}} \sum_{j\in\,\Pi_k} \sqrt{\eta_{kj}^{(i)}} H_{kj}^{(i)}\mathbf{w}_{kj}\, x_{kj} + \mathbf{z}_i. \end{aligned} \tag{4.2}$$

Then, the message is retrieved by the MMSE detection as [64, Ch.8]

$$\hat{x}_{i\pi_i(\ell)} = (H_{i\pi_i(\ell)}^{(i)}\mathbf{w}_{i\pi_i(\ell)})^{\mathrm{H}} (Q_{\mathrm{INT},i\pi(\ell)} + \mathbf{I}_{N_{\mathrm{R}}})^{-1}\mathbf{y}_i, \tag{4.3}$$

where $Q_{\mathrm{INT},i\pi_i(\ell)}$ denotes the covariance matrix of the interference to user-$\pi_i(\ell)$ at BS-i in (4.2) as

$$Q_{\mathrm{INT},i\pi_i(\ell)} = \sum_{j\in\,\Pi_i, j\neq\pi_i(\ell)} \rho_{ij}\; (H_{ij}^{(i)}\mathbf{w}_{ij})(H_{ij}^{(i)}\mathbf{w}_{ij})^{\mathrm{H}} + \sum_{k=1,k\neq i}^{N_{\mathrm{BS}}} \sum_{j\in\,\Pi_k} \eta_{kj}^{(i)} (H_{kj}^{(i)}\mathbf{w}_{kj})(H_{kj}^{(i)}\mathbf{w}_{kj})^{\mathrm{H}}. \tag{4.4}$$

4.2.2 Sum rate of the system

When we assume joint decoding for the selected users by treating inter-cell interference as noise at each base station, the system is considered as SDMA. Then, the first summation in (4.1) can be regarded as the signal and the second summation can be regarded as the interference term. By exploiting the capacity calculation in the presence of the co-channel interference [83], we show in Appendix C.1 that the sum rate is given by

$$R_{\mathrm{SUM}}(\mathrm{SDMA}) \;= \frac{1}{N_{\mathrm{BS}}} \sum_{i=1}^{N_{\mathrm{BS}}} \mathbb{E}\left[\log_2 \det(\mathbf{I}_{N_{\mathrm{R}}} + Q_{\mathrm{SIG},i}(\mathbf{I}_{N_{\mathrm{R}}} + Q_{\mathrm{INT},i})^{-1})\right] \tag{4.5}$$

where $Q_{\mathrm{SIG},i}$ denotes the covariance matrix of the signal at BS-i as

$$Q_{\mathrm{SIG},i} = \sum_{j\in\,\Pi_i} \rho_{ij}\; (H_{ij}^{(i)}\mathbf{w}_{ij})(H_{ij}^{(i)}\mathbf{w}_{ij})^{\mathrm{H}} \tag{4.6}$$

and $Q_{\mathrm{INT},i}$ denotes the covariance matrix of the interference at BS-i as

$$Q_{\mathrm{INT},i} = \sum_{k=1,k\neq i}^{N_{\mathrm{BS}}} \sum_{j\in\,\Pi_k} \eta_{kj}^{(i)} (H_{kj}^{(i)} \mathbf{w}_{kj})(H_{kj}^{(i)} \mathbf{w}_{kj})^{\mathrm{H}}. \tag{4.7}$$

On the other hand, for the retrieved message by the MMSE detection in (4.3), in a similar way to Appendix C.1 for (4.5), the sum rate for the MMSE is given by

$$R_{\mathrm{SUM}}(\mathrm{MMSE}) = \frac{1}{N_{\mathrm{BS}}} \sum_{i=1}^{N_{\mathrm{BS}}} \sum_{\ell=1}^{N_{\mathrm{ST}}} \mathbb{E}\left[\log_2 \det(\mathbf{I}_{N_{\mathrm{R}}} + Q_{\mathrm{SIG},i\pi_i(\ell)}(\mathbf{I}_{N_{\mathrm{R}}} + Q_{\mathrm{INT},i\pi_i(\ell)})^{-1})\right] \tag{4.8}$$

where $Q_{\mathrm{SIG},i\pi_i(\ell)}$ denotes the covariance matrix of the signal of user-$\pi_i(\ell)$ at BS-i as

$$Q_{\mathrm{SIG},i\pi_i(\ell)} = \rho_{i\pi_i(\ell)} H_{i\pi_i(\ell)}^{(i)} \mathbf{w}_{i\pi_i(\ell)} (H_{i\pi_i(\ell)}^{(i)} \mathbf{w}_{i\pi_i(\ell)})^{\mathrm{H}} \tag{4.9}$$

and $Q_{\mathrm{INT},i\pi_i(\ell)}$ is in (4.4).

4.2.3 Conventional schemes

Maximizing the in-cell SNR (Max-SNR)

Since users have multiple transmit antennas, one simple strategy for joint scheduling and beamforming is to maximize the in-cell SNR. Each user first computes the covariance matrix of the channel to its own cell. For user-j in cell-i, the covariance matrix is given by

$$K_{\mathrm{SNR},ij} = H_{ij}^{(i)\mathrm{H}} H_{ij}^{(i)} \overset{(a)}{=} V_{ij} \Lambda_{ij} V_{ij}^{\mathrm{H}}, \tag{4.10}$$

where (a) follows from the eigenvalue decomposition. Then, each user finds the maximum eigenvalue and reports it to its own cell. Since the diagonal entries of Λ_{ij} are the eigenvalues of $K_{\mathrm{SNR},ij}$, feedback information for user-j in cell-i is

$$L_{ij} = \max_{1\leq \ell \leq N_{\mathrm{T}}} <\Lambda_{ij}>_{\ell\ell}, \tag{4.11}$$

where $<\cdot>_{\ell\ell}$ denotes the ℓ^{th} diagonal entry of a matrix. Based on this feedback information, each base station selects users who have one of the *largest-*N_{ST} L_{ij}'s out of N_{US} values as follows:

$$\pi_i(\ell) = j, \quad s.t. \;\; L_{ij} = L_{i[\ell]},\; N_{\mathrm{US}} - N_{\mathrm{ST}} + 1 \leq \ell \leq N_{\mathrm{US}}, \tag{4.12}$$

where $L_{i[\ell]}$ denotes the order statistics of L_{ij} in j such that $L_{i[1]} \leq \cdots \leq L_{i[N_{\mathrm{US}}]}$. For the transmit beamforming, the selected users find their beamforming vector from V_{ij} in

(4.10) corresponding to the *largest* eigenvalue, *i.e.,* L_{ij} as follows: when $L_{ij} = <\Lambda_{ij}>_{\ell\ell}$,

$$\mathbf{w}_{ij} = <V_{ij}>_{:\ell} \;\; s.t. \; \|\mathbf{w}_{ij}\|^2 = 1 \; , \tag{4.13}$$

where $<\cdot>_{:\ell}$ denotes the ℓ^{th} column vector of a matrix.

Minimizing the GIN to other cells (Min-GIN)

The strategy is to minimize the generated interference (GIN) from users to other BSs. For this purpose, the beamforming vectors and user scheduling are directed to the smallest eigenvalue of the covariance matrix of the GIN. Specifically, each user first computes the covariance matrix of GIN. For user-j in cell-i, the covariance matrix is given by

$$K_{\text{GIN},ij} = \sum_{k=1,k\neq i}^{N_{\text{BS}}} \eta_{ij}^{(k)} H_{ij}^{(k)^{\text{H}}} H_{ij}^{(k)} \overset{(a)}{=} V_{ij}\Lambda_{ij}V_{ij}^{\text{H}}, \tag{4.14}$$

where (a) follows from the eigenvalue decomposition. Then, each user finds the minimum eigenvalue and reports it to its own cell. Feedback information for user-j in cell-i is

$$L_{ij} = \min_{1\leq\ell\leq N_{\text{T}}} <\Lambda_{ij}>_{\ell\ell} \; . \tag{4.15}$$

Based on this feedback information, each base station selects users who have one of the *smallest-*N_{ST} L_{ij}'s out of N_{US} values as follows:

$$\pi_i(\ell) = j, \quad s.t. \;\; L_{ij} = L_{i[\ell]}, \; 1 \leq \ell \leq N_{\text{ST}}. \tag{4.16}$$

For the transmit beamforming, the selected users find their beamforming vector from V_{ij} in (4.14) corresponding to the *smallest* eigenvalue, *i.e.,* L_{ij} as follows: when $L_{ij} = <\Lambda_{ij}>_{\ell\ell}$,

$$\mathbf{w}_{ij} = <V_{ij}>_{:\ell} \;\; s.t. \; \|\mathbf{w}_{ij}\|^2 = 1 \; . \tag{4.17}$$

4.2.4 Proposed schemes

In this subsection, we propose new schemes of joint scheduling and beamforming based on maximizing SGINR or DSINR in each user. We also propose a two-step user-selection procedure for the better orthogonality among selected users, which leads to minimizing intra-cell interference.

Maximizing the signal to generated interference and noise ratio (Max-SGINR)

The strategy is to maximize the in-cell SNR from users and minimize the generated interference to other BSs. For this purpose, the beamforming vectors and user scheduling are directed to the largest eigenvalue of the covariance matrix of the SGINR. Specifically, each user first computes the covariance matrix of SGINR. For user-j in cell-i, the covariance matrix is given by [37]

$$K_{\mathrm{SGINR},ij} = \left(\mathbf{I}_{N_{\mathrm{T}}} + \sum_{k=1,k\neq i}^{N_{\mathrm{BS}}} \eta_{ij}^{(k)} H_{ij}^{(k)^{\mathrm{H}}} H_{ij}^{(k)} \right)^{-1} \rho_{ij} H_{ij}^{(i)^{\mathrm{H}}} H_{ij}^{(i)} \overset{(a)}{=} V_{ij} \Lambda_{ij} V_{ij}^{\mathrm{H}}, \tag{4.18}$$

where (a) follows from the eigenvalue decomposition. Then, each user finds the maximum eigenvalue and reports it to its own cell. Feedback information for user-j in cell-i is

$$L_{ij} = \max_{1\leq \ell \leq N_{\mathrm{T}}} <\Lambda_{ij}>_{\ell\ell} . \tag{4.19}$$

Based on this feedback information, each base station selects users who have one of the *largest-*N_{ST} L_{ij}'s out of N_{US} values as follows:

$$\pi_i(\ell) = j, \quad s.t. \;\; L_{ij} = L_{i[\ell]},\; N_{\mathrm{US}} - N_{\mathrm{ST}} + 1 \leq \ell \leq N_{\mathrm{US}}. \tag{4.20}$$

For the transmit beamforming, the selected users find their beamforming vector from V_{ij} in (4.18) corresponding to the *largest* eigenvalue, *i.e.,* L_{ij} as follows: when $L_{ij} = <\Lambda_{ij}>_{\ell\ell}$,

$$\mathbf{w}_{ij} = <V_{ij}>_{:\ell} \;\; s.t. \; \|\mathbf{w}_{ij}\|^2 = 1 . \tag{4.21}$$

Maximizing the signal to interference and noise ratio in the dual network (Max-DSINR)

Let us consider a multiple-input multiple-output (MIMO) network in Fig. 4.2(a), where $\mathbf{v}_{ij}$ and $\mathbf{w}_{ij}$ denote a receive beamforming vector and a transmit beamforming vector for user-j in cell-i, respectively. $\mathbf{v}_{kj}$ is a receive beamforming vector for user-j in cell-k. Transmit beamforming affects the SINR at all the receivers in the network by influencing the received interference signal. On the contrary, receive beamforming affects the SINR of the corresponding receiver only. For this reason, the dual network is utilized to solve the problem of designing transmit beamforming vectors, where the problem is converted into that of determining receive beamforming vectors [36]. A dual network

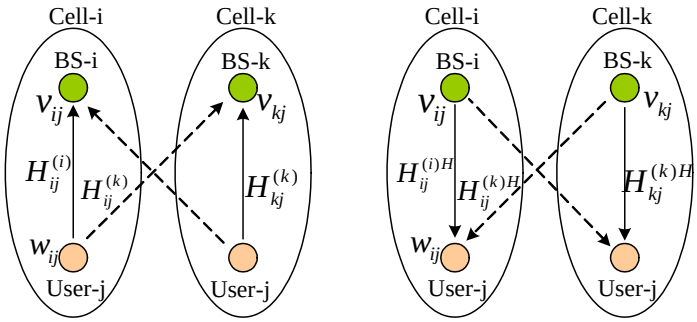

(a) Primal network (b) Dual network

Figure 4.2: Example of the primal network and dual network. The role of transmitter and receiver is switched.

to the primal network can be constructed as follows [36]: 1) reverse the directions of all links; 2) convert all channels into their conjugate transpose (*e.g.,* $H \rightarrow H^{\mathrm{H}}$); and 3) use transmit beamforming vectors as receive beamforming vectors, and the other way around. Fig. 4.2(b) shows an example of a dual network to the primal network in Fig. 4.2(a).

Let us consider the dual network in Fig. 4.2(b), where $\mathbf{v}_{ij}$ and $\mathbf{w}_{ij}$ denote a transmit beamforming vector and a receive beamforming vector for user-j in cell-i, respectively. The objective is to find the receive beamforming vector $\mathbf{w}_{ij}$ to maximize the DSINR, which will be eventually used as a transmit beamforming vector in the primal network when the user is selected. Since all the channels in the primal network are converted to their Hermitian in the dual network, the DSINR of user-j in cell-i is given by

$$\mathrm{DSINR}_{ij} = \frac{\rho_{ij} \, |\mathbf{w}_{ij}^{\mathrm{H}} H_{ij}^{(i)^{\mathrm{H}}} \mathbf{v}_{ij}|^2}{1 + \sum_{k=1, k \neq i}^{N_{\mathrm{BS}}} \eta_{ij}^{(k)} \mathbf{w}_{ij}^{\mathrm{H}} H_{ij}^{(k)^{\mathrm{H}}} \mathbf{v}_{kj} \mathbf{v}_{kj}^{\mathrm{H}} H_{ij}^{(k)} \mathbf{w}_{ij}}. \tag{4.22}$$

Regarding a transmit beamforming vector in the dual network, we assume that it is aligned to maximize the in-cell SNR. Specifically, $\mathbf{v}_{ij}$ is assumed to be the right singular vector of $H_{ij}^{(i)^{\mathrm{H}}}$ corresponding to the maximum singular value. Then, we have

$$H_{ij}^{(i)^{\mathrm{H}}} \mathbf{v}_{ij} = \sigma_{\max,ij} \mathbf{u}_{\max,ij}, \tag{4.23}$$

where $\sigma_{\max,ij}$ denotes the maximum singular value of $H_{ij}^{(i)^{\mathrm{H}}}$ and $\mathbf{u}_{\max,ij}$ denotes the corresponding left singular vector. In the same way, we assume that $\mathbf{v}_{kj}$ at BS-k is the right singular vector of $H_{kj}^{(k)^{\mathrm{H}}}$ corresponding to the maximum singular value. On the

contrary to the previous case, user-j in cell-i has no idea about $H_{kj}^{(k)^{\mathrm{H}}}$, *i.e.,* a channel from BS-k to user-j in cell-k. Thus, we assume that $\mathbf{v}_{kj}$ can be regarded as the complex Gaussian random vector and replace $\mathbf{v}_{kj}\mathbf{v}_{kj}^{\mathrm{H}}$ in (4.22) with $\mathbb{E}[\mathbf{v}_{kj}\mathbf{v}_{kj}^{\mathrm{H}}] = \frac{\mathbf{I}_{N_{\mathrm{R}}}}{N_{\mathrm{R}}}$. Then, DSINR_{ij} in (4.22) is rewritten as

$$\mathrm{DSINR}_{ij} = \frac{\rho_{ij}\ |\sigma_{\max,ij}|^2\ \mathbf{w}_{ij}^{\mathrm{H}}\mathbf{u}_{\max,ij}\mathbf{u}_{\max,ij}^{\mathrm{H}}\mathbf{w}_{ij}}{\mathbf{w}_{ij}^{\mathrm{H}}(\mathbf{I}_{N_{\mathrm{T}}} + \frac{1}{N_{\mathrm{R}}}\sum_{k=1,k\neq i}^{N_{\mathrm{BS}}}\eta_{ij}^{(k)}H_{ij}^{(k)^{\mathrm{H}}}H_{ij}^{(k)})\mathbf{w}_{ij}}. \tag{4.24}$$

The problem of finding the optimal receive beamforming vector to maximize DSINR_{ij} can be solved using the Rayleigh-Ritz theorem related to the generalized eigenvalue problem [84]. Several similar examples are also found in [37,39]. To formulate the problem more specifically, let us define $K_{\mathrm{DSINR},ij}$ as

$$K_{\mathrm{DSINR},ij} = \rho_{ij}\ |\sigma_{\max,ij}|^2\left(\mathbf{I}_{N_{\mathrm{T}}} + \sum_{k=1,k\neq i}^{N_{\mathrm{BS}}}\frac{\eta_{ij}^{(k)}H_{ij}^{(k)^{\mathrm{H}}}H_{ij}^{(k)}}{N_{\mathrm{R}}}\right)^{-1}\mathbf{u}_{\max,ij}\mathbf{u}_{\max,ij}^{\mathrm{H}} \overset{(a)}{=} V_{ij}\Lambda_{ij}V_{ij}^{\mathrm{H}}, \tag{4.25}$$

where (a) follows from the eigenvalue decomposition. Then, the problem of finding the optimal receive beamforming vector to maximize DSINR_{ij} in (4.24) can be written as [84]

$$\mathbf{w}_{ij}^{\mathrm{o}} = \arg\max_{\mathbf{w}_{ij}}\mathbf{w}_{ij}^{\mathrm{H}}K_{\mathrm{DSINR},ij}\mathbf{w}_{ij}, \tag{4.26}$$

and the solution corresponds to the eigenvector corresponding to the largest eigenvalue of $K_{\mathrm{DSINR},ij}$. Thus, feedback information for user-j in cell-i can be found as

$$L_{ij} = \max_{1\leq\ell\leq N_{\mathrm{T}}} <\Lambda_{ij}>_{\ell\ell}\ . \tag{4.27}$$

Based on this feedback information, each base station selects users who have one of the *largest-*N_{ST} L_{ij}'s out of N_{US} values as follows:

$$\pi_i(\ell) = j, \quad s.t.\ \ L_{ij} = L_{i[\ell]},\ N_{\mathrm{US}} - N_{\mathrm{ST}} + 1 \leq \ell \leq N_{\mathrm{US}}. \tag{4.28}$$

Finally, selected users utilize the receive beamforming vector found in the dual network, *i.e.,* $\mathbf{w}_{ij}^{\mathrm{o}}$ in (4.26), as their transmit beamforming vector in the primal network. We then note that once the transmit beamforming vectors have been determined in the primal network, a receive beamforming vector can always be optimized again, for example, through the MMSE detection.

Two step selection

When multiple users are served at a time by a base station, it is better in enhancing the sum rate to minimize intra-cell interference and select users whose channels are mutually orthogonal. To select more orthogonal users while handling inter-cell interference, we propose two-step selection of users wherein each base station selects more users in Step-1 than is needed and finds the set of users who are best orthogonal to one another. Specifically, in Step-1, BS-i selects $N_{\mathrm{SU},1}$ users based on (4.12), (4.16), (4.20), or (4.28) depending on the used scheme where $N_{\mathrm{ST}} \leq N_{\mathrm{SU},1} \leq N_{\mathrm{US}}$. In Step-2, similar to the semi-orthogonal user selection procedure in [77], BS-i sequentially finds users who have the largest component orthogonal to the subspace spanned by the channels of the selected users.

To explain the specific procedure of Step-2, let $U_{\mathrm{sel},\ell}$ denote a set of the selected users after ℓ^{th} iteration where $0 \leq \ell \leq N_{\mathrm{ST}}$. Let $U_{\mathrm{rem},\ell}$ denote a set of remaining candidate users for selection after ℓ^{th} iteration. We note that $U_{\mathrm{rem},0}$ denotes the set of the selected users as a consequence of Step-1. BS-i follows the procedure of Step-2 in Table 4.1. Then, we note that $U_{\mathrm{sel},N_{\mathrm{ST}}}$ will be the final set of the selected users.

4.2.5 Comparison of DSINR-type metric and SGINR-type metric

In this subsection, we compare the proposed DSINR-type metric in (4.25) with the SGINR-type metric in (4.18) and show the similarity and distinction between them.

When $N_{\mathrm{R}} = 1$ and $N_{\mathrm{T}} \geq 1$, the singular value decomposition of $H_{ij}^{(i)^{\mathrm{H}}}$ is given by

$$H_{ij}^{(i)^{\mathrm{H}}} = [\mathbf{u}_{1,ij}, \cdots, \mathbf{u}_{N_{\mathrm{T}},ij}][\sigma_{\max,ij}, 0, \cdots, 0]^{\mathrm{T}} v_{ij}^{*} = v_{ij}^{*}\sigma_{\max,ij}\mathbf{u}_{\max,ij}, \tag{4.33}$$

where $\mathbf{u}$, v, σ denote the left singular vectors, the right singular vector (the scalar value in this case), and the singular value, and $(\cdot)^{\mathrm{T}}$ denotes the matrix transpose operation. Since the rank of $H_{ij}^{(i)^{\mathrm{H}}}$ is 1, there exists only one non-zero singular value and thus $\mathbf{u}_{\max,ij} = \mathbf{u}_{1,ij}$ corresponding to $\sigma_{\max,ij}$. Thus, we have

$$H_{ij}^{(i)^{\mathrm{H}}} H_{ij}^{(i)} = |\sigma_{\max,ij}|^2 \, \mathbf{u}_{\max,ij}\mathbf{u}_{\max,ij}^{\mathrm{H}}, \tag{4.34}$$

since $|v_{ij}|^2 = 1$ from the singular vector property. From (4.34), we can see that (4.18) leads to (4.25), which indicates that the Max-SGINR scheme in Section 4.2.4 and the Max-DSINR scheme in Section 4.2.4 are equivalent when $N_{\mathrm{R}} = 1$. In the same way, we can show that (4.34) holds as well when $N_{\mathrm{T}} = 1$. However, when $N_{\mathrm{R}} \neq 1$, we note

Table 4.1: Specific procedure of Step-2 for the two-step user-selection. The final set of selected users will be $U_{\text{sel},N_{\text{ST}}}$.

When $\ell = 0$, BS-i sets $U_{\text{sel},0} = \phi$ and $U_{\text{rem},0} = \{1, \cdots, N_{\text{SU},1}\}$.
When $\ell = 1$, BS-i finds the best channel user out of $U_{\text{rem},0}$ as follows: $$\pi_i(1) = \arg \max_{j \in U_{\text{rem},0}} \|H_{ij}^{(i)} \mathbf{w}_{ij}^{(i)}\|^2. \quad (4.29)$$ Then, BS-i updates $U_{\text{sel},1} = \{\pi_i(1)\}$ and $U_{\text{rem},1} = U_{\text{rem},0} - \{\pi_i(1)\}$ and makes $\mathbf{g}_{i\pi_i(1)} = H_{i\pi_i(1)}^{(i)} \mathbf{w}_{i\pi_i(1)}^{(i)}$.
When $2 \leq \ell \leq N_{\text{ST}}$, BS-$i$ first computes the orthogonal components of the channel vectors of the remaining users as following: $$\mathbf{g}_j = H_{ij}^{(i)} \mathbf{w}_{ij}^{(i)} - \sum_{m=1}^{\ell-1} \frac{\mathbf{g}_{\pi_i(m)}^{\text{H}} H_{ij}^{(i)} \mathbf{w}_{ij}^{(i)}}{\|\mathbf{g}_{\pi_i(m)}\|^2} \mathbf{g}_{\pi_i(m)}, \quad j \in U_{\text{rem},\ell-1}. \quad (4.30)$$ Then, BS-i finds a user with the maximum orthogonal component as following: $$\pi_i(\ell) = \arg \max_{j \in U_{\text{rem},\ell-1}} \|\mathbf{g}_j\|^2 \quad (4.31)$$ BS-i updates $U_{\text{sel},\ell}$ and $U_{\text{rem},\ell}$ as following: $$U_{\text{sel},\ell} = U_{\text{sel},\ell-1} \cup \{\pi_i(\ell)\}, \quad U_{\text{rem},\ell} = U_{\text{rem},\ell-1} - \{\pi_i(\ell)\} \quad (4.32)$$

that the terms inside the inverse in (4.25) are different by the scale factor N_{R} as in (4.18), which makes the eigenvalue of a DSINR-type metric in (4.25) larger than that of a SGINR-type metric in (4.18) when $N_{\text{R}} > 1$. Although the larger eigenvalue does not directly lead to a larger sum rate, it usually helps to improve the sum rate, which will be shown in the numerical examples in Section 4.2.6. The similar relation between the DSINR-metric and the SGINR-metric is found when $N_{\text{R}} \neq 1$ and $N_{\text{T}} \neq 1$.

4.2.6 Numerical Results

In this section, we show the simulation results of the proposed schemes and compare with the conventional scheme.

Comparison between joint decoding and MMSE detection

In Fig. 4.3, we show the per-cell sum rate for both joint decoding and the MMSE detection when we use Max-DSINR-type joint scheduling and beamforming in

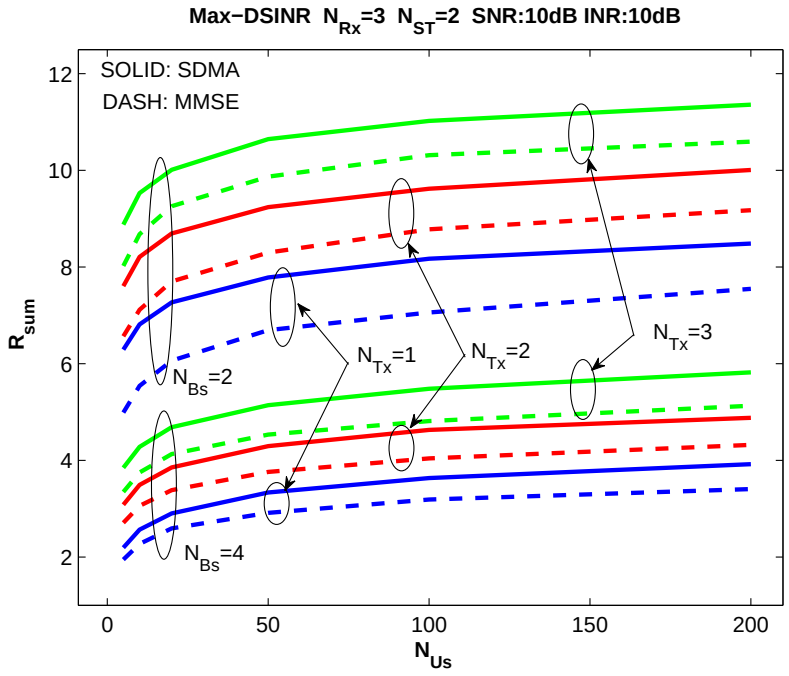

Figure 4.3: Sum rate comparison between joint decoding and MMSE detection for different N_{T}. ($N_{\mathrm{ST}} = 2$, $N_{\mathrm{R}} = 3$)

Section 4.2.4. Since joint decoding achieves the sum capacity in an interference-free environment such as space division multiple access (SDMA) [64], we can see that joint decoding outperforms the MMSE detection in an interference-limited environment. Note that the sum rate increases with the number of users, which follows from multiuser diversity. The sum rate also increases with the number of antennas with the help of beamforming gain to maximize DSINR in (4.24), while the per-cell sum rate decreases as the number of cells increase due to more co-channel interfering users.

Fig. 4.4 shows the effect of the number of selected users (N_{ST}) for the different number of the transmit antennas (N_{T}). When the number of selected users increases, the inter-user interference among the selected users in each cell can reduce the sum rate when the selected users are not orthogonal. This is more apparent for the MMSE detection in Fig. 4.4(a), where the sum rate for $N_{\mathrm{ST}} = 3$ is smaller than that for $N_{\mathrm{ST}} = 2$. However, this inter-user interference can be reduced by transmit beamforming as in Fig. 4.4(b), where the sum rate increases with N_{ST}. We note in Fig. 4.4(a) that multiuser diversity also reduces the inter-user interference in joint decoding since the sum rate increases with N_{ST} when the number of users is large, *e.g.*, $N_{\mathrm{US}} \geq 50$.

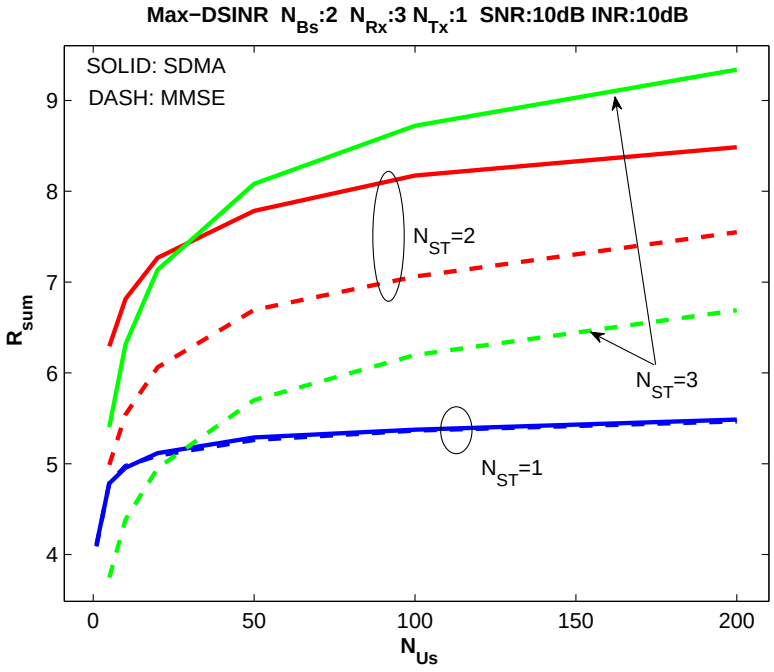

(a) $N_{\mathrm{T}} = 1$

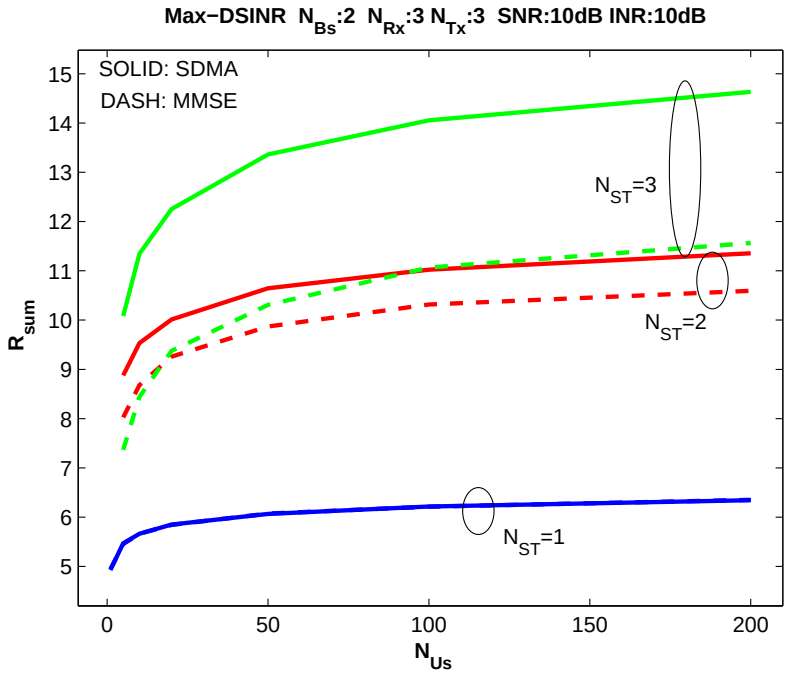

(b) $N_{\mathrm{T}} = 3$

Figure 4.4: Sum rate comparison between joint decoding and MMSE detection for the different number of selected users (N_{ST}). ($N_{\mathrm{BS}} = 2$, $N_{\mathrm{R}} = 3$)

Comparison between the schemes of joint beamforming and scheduling

In Fig. 4.5, we show the sum rate results of the proposed Max-SGINR-type scheme and Max-DSINR-type scheme in Section 4.2.4, and compare them with the Max-SNR-type scheme and the Min-GIN-type scheme in Section 4.2.3. In Fig. 4.5(a), both Max-SGINR-type and Max-DSINR-type beamforming schemes outperform the conventional Max-SNR-type and Min-GIN-type schemes when $N_{\mathrm{R}} = 3 < N_{\mathrm{ST}} \times N_{\mathrm{BS}} = 2 \times 2$. However, in Fig. 4.5(b) for $N_{\mathrm{R}} = 3 > N_{\mathrm{ST}} \times N_{\mathrm{BS}} = 1 \times 2$, the proposed schemes which consider generating interference to other cells yield smaller sum rates than the Max-SNR-type scheme. This implies that consideration of the generated interference is not needed when the number of total streams in a system (*i.e.*, $N_{\mathrm{ST}} \times N_{\mathrm{BS}}$) is smaller than the number of Rx antennas N_{R}. In this case, inter-cell interference can be better mitigated by only receiver beamforming directed to the signal. On the other hand, let us compare the sum rate of two schemes at their favorable N_{ST}, *i.e.,* the sum rate at $N_{\mathrm{ST}} = 2$ in Fig. 4.5(a) for the Max-SGINR-type or Max-DSINR scheme and the sum rate at $N_{\mathrm{ST}} = 1$ in Fig. 4.5(b) for the Max-SNR-type scheme. We can see that the Max-SGINR-type or Max-DSINR scheme outperforms the Max-SNR-type scheme.

In Fig. 4.6, we show the overall comparison of the sum rate between Max-DSINR-type and Max-SNR-type scheme for various combination of N_{BS} and N_{R} in the horizontal axis, and N_{T} and N_{ST} in the vertical axis. In both figures, we note that Max-DSINR-type scheme outperforms the conventional scheme in a large number of cases. Especially, Max-DSINR-type scheme shows the better sum rate in larger N_{BS} and N_{ST} *i.e.,* more other-cell interferers. We also note that Max-DSINR-type scheme works better with larger N_{T}, which implies that Max-DSINR-type beamforming works better with larger N_{T}.

In Fig. 4.7, we show the sum rate at the optimal number of selected users N_{ST}^{*}, where the sum rate is the largest when N_{BS}, N_{R} and N_{T} are given. Both figures are for $N_{\mathrm{US}} = 10$ and $N_{\mathrm{US}} = 200$ respectively. We first note that Max-DSINR-type scheme prevails in most instances for N_{ST}^{*} than in Fig. 4.6 where two schemes are compared for each N_{ST}. We also note that Max-DSINR-type scheme shows better performance with the larger number of users, which means that Max-DSINR-type scheme has greater benefit from multiuser diversity than Max-SNR-type scheme.

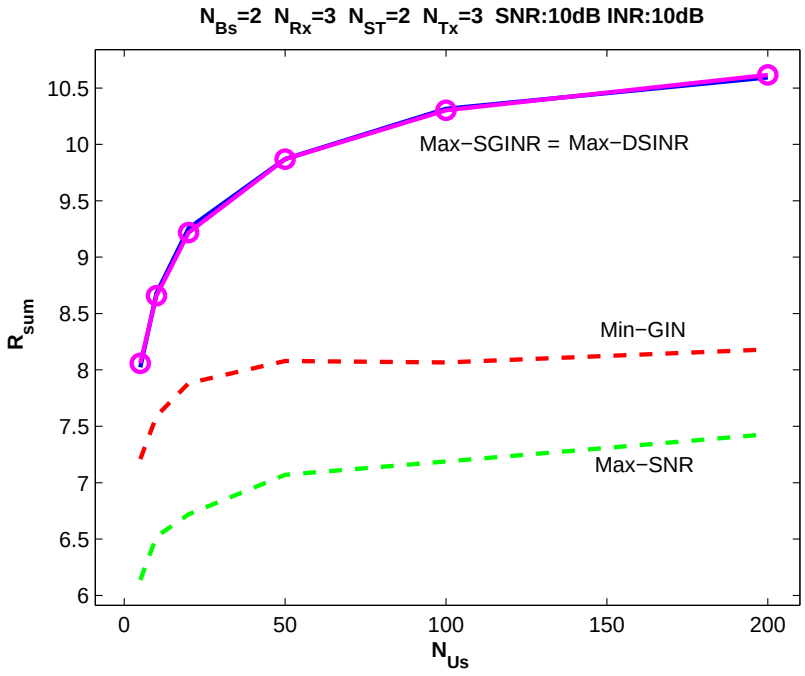

(a) $N_{\mathrm{R}} < N_{\mathrm{ST}} \times N_{\mathrm{BS}}$

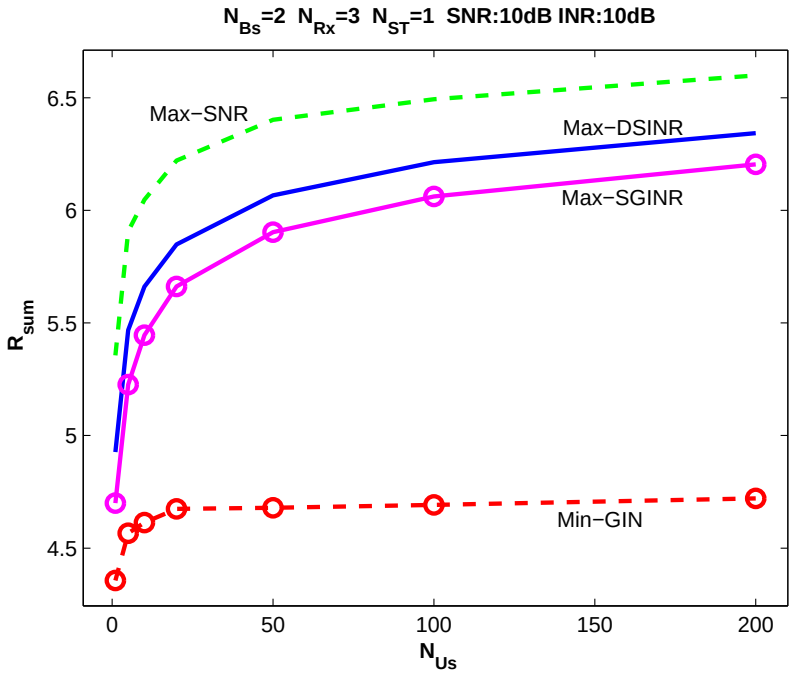

(b) $N_{\mathrm{R}} > N_{\mathrm{ST}} \times N_{\mathrm{BS}}$

Figure 4.5: Sum rate comparison of Max-SGINR-type, Max-DSINR-type, Min-GIN-type, and Max-SNR-type schemes for MMSE detection.

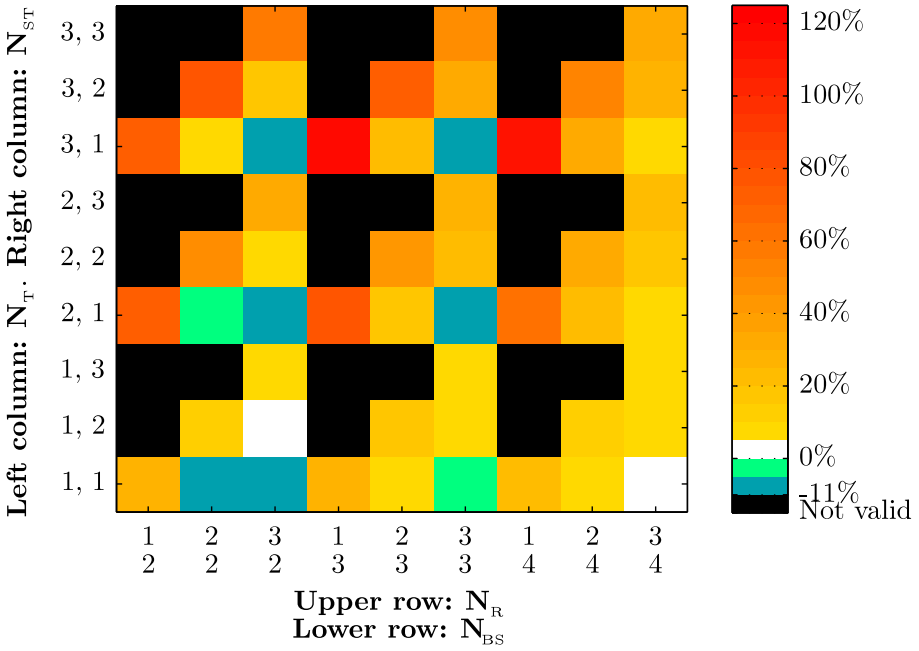

(a) Joint decoding

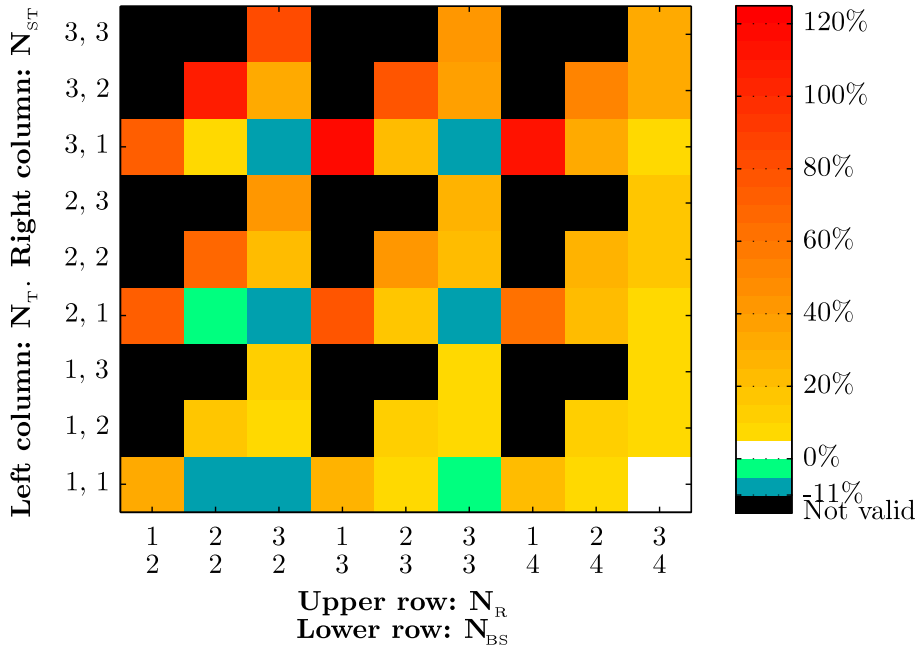

(b) MMSE detection

Figure 4.6: Overall sum rate comparison between Max-DSINR-type and Max-SNR-type scheme. Each grid shows the sum rate difference *i.e.*, $R_{\mathrm{SUM,SGINR}} - R_{\mathrm{SUM,SNR}}$ for given N_{BS}, N_{R}, N_{T} and N_{ST}. The black color indicates the invalid region because $N_{\mathrm{ST}} > N_{\mathrm{R}}$.

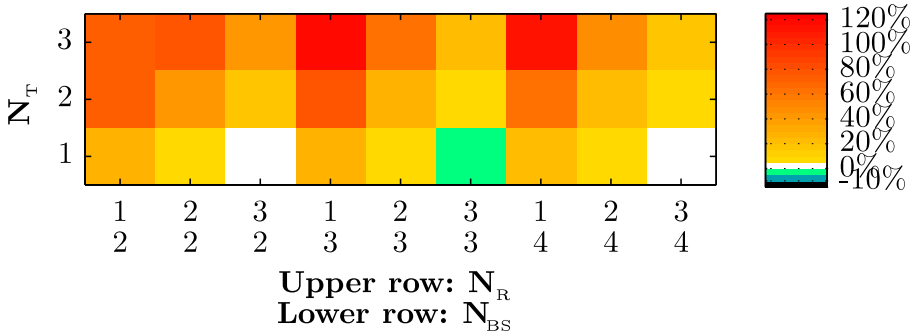

(a) $N_{US} = 10$

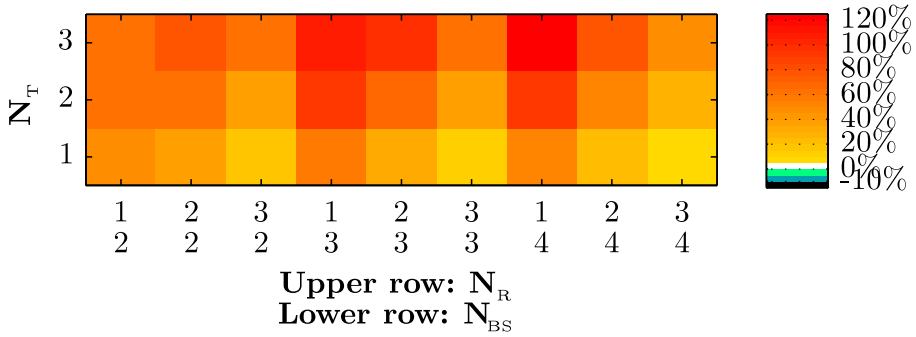

(b) $N_{US} = 200$

Figure 4.7: Overall sum rate comparison between Max-DSINR-type and Max-SNR-type scheme when the optimal number of users are selected. Each grid shows the sum rate difference *i.e.*, $R_{\mathrm{SUM,SGINR}} - R_{\mathrm{SUM,SNR}}$ for given N_{BS}, N_{R}, N_{T} and N_{ST}. The white, orange and reddish color indicate the region where the Max-DSINR-type scheme is preferred. (SNR = INR = 10dB)

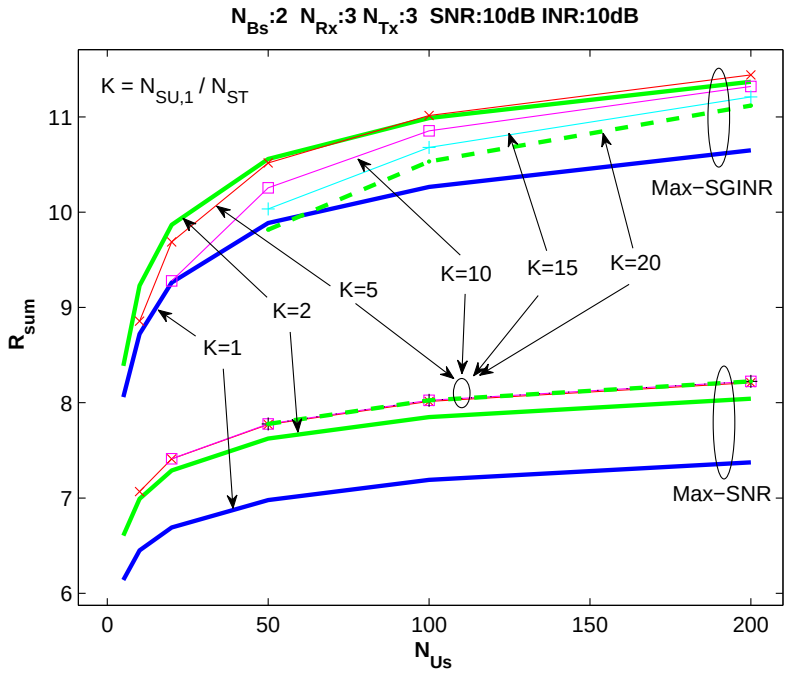

Figure 4.8: Sum rate of a two-step user-selection procedure in Table 4.1 for the Max-SNR-type scheme for the different $N_{\mathrm{SU},1}$ where $K = \frac{N_{\mathrm{SU},1}}{N_{\mathrm{ST}}}$. ($N_{\mathrm{BS}} = 2$, $N_{\mathrm{R}} = 3$, $N_{\mathrm{T}} = 3$ and $N_{\mathrm{ST}} = 2$)

Sum rate improvement by two-step selection

Fig. 4.8 shows the sum rate achieved by a two-step user-selection procedure in Table 4.1, where $K = \frac{N_{\mathrm{SU},1}}{N_{\mathrm{ST}}}$. The term K indicates the overselection factor, *i.e.,* K times more users are selected in Step-1, compared to the number of users which are finally selected in Step-2. We find that a two-step user-selection procedure improves the sum rate in both Max-SGINR-type and Max-SNR-type schemes. We note for the Max-SGINR-type scheme that the largest sum rate is achieved when $2 \leq K \leq 5$ and that the sum rate considerably decreases when $K \geq 15$. This means that we need moderately large number of users in Step-1, and that selection of too many users in Step-1 is likely to increase the interference to other cells in the end. For the Max-SNR-type scheme, we find that the sum rate increases with K, but saturated when $K \geq 5$. This implies that since Max-SNR-type scheme does not care for the interference to other cells, selection of more users in Step-1 directly leads to the larger sum rate due to the improved mutual orthogonality between selected users in Step-2.

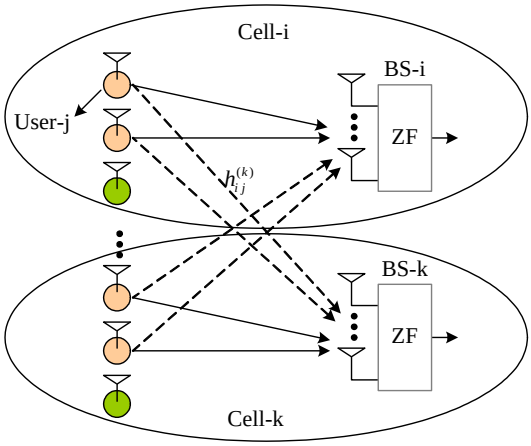

Figure 4.9: System block diagram for an uplink cellular system. The zero forcing operation is assumed at base stations.

4.3 Opportunistic Interference Alignment

In this section, we consider the opportunistic interference alignment (IA) scheme in an interference-limited uplink cellular network. We propose a method to enhance the sum rate by maximizing the SINR of each user in a dual network developed in Section 4.2. We try to find the optimal signal dimension at the base station. We show that the proposed methods greatly improve the sum rate compared to the conventional opportunistic scheme.

This section is organized as follows. In Section 4.3.1, we describe the system model. In Section 4.3.2, we develop the sum rate of the system. In Section 4.3.3, we explain the conventional user selection schemes. In Section 4.3.4, we propose schemes to enhance the sum rate of the system. In Section 4.3.5, we show numerical results and compare the sum rate of the proposed schemes with the conventional one.

4.3.1 System Model

We consider an uplink time division duplex (TDD) cellular system with N_{BS} cells as in Fig. 4.9. Each cell has one base station (BS) and N_{US} users. Each base station is equipped with N_{R} receive antennas and each user has a single transmit antenna. A channel from user-j in cell-i to BS-k is denoted as $\mathbf{h}_{ij}^{(k)}$. Each element of the channel is assumed to follow a complex Gaussian distribution $\mathcal{CN}(0,1)$.[2] Let $\mathcal{S}_i$ and $\mathcal{I}_i$ denote

[2] $\mathcal{CN}(\mu,\sigma^2)$ denotes a circularly symmetric complex Gaussian distribution with mean μ and variance σ^2.

the signal subspace and the interference subspace of BS-i where $1 \leq i \leq N_{\mathrm{BS}}$. We assume that $\mathcal{S}_i$ and $\mathcal{I}_i$ are orthogonal and that the dimension of each subspace is N_{SG} and N_{IN} respectively. Let $\mathbf{u}_{im}$ and $\mathbf{v}_{in}$ denote the orthonormal basis vectors for $\mathcal{S}_i$ and $\mathcal{I}_i$ respectively, where $1 \leq m \leq N_{\mathrm{SG}}$, $1 \leq n \leq N_{\mathrm{IN}}$, $1 \leq N_{\mathrm{SG}} \leq N_{\mathrm{R}}$ and $N_{\mathrm{SG}} + N_{\mathrm{IN}} = N_{\mathrm{R}}$.

User-j in cell-i measures all the downlink channels from each base station. We also assume that channels are reciprocal between the uplink and downlink. We assume that each user in the system is informed of $\mathbf{u}_{im}$ and $\mathbf{v}_{in}$ for all i, m, and n through the broadcast system message. User-j in cell-i computes the metric for the interference to BS-k, which is denoted as $L_{ij}^{(k)}$. Then users compute the total generated interference denoted as L_{ij}. In the conventional scheme [40], minimizing the interference to other cells was considered. To enhance the sum rate of the system, we propose two new schemes based on maximizing the signal to the generated interference and noise ratio (SGINR) or two-step user-selection, which will be discussed in Section 4.3.4.

Each user feeds back its own interference metric (L_{ij}) to the base station. Then, each base station selects the best N_{ST} users out of N_{US} users, depending on the type of the reported metric. Each base station has the selected users transmit their signal. The received signal at BS-i is given by

$$\mathbf{y}_i = \sum_{j=1}^{N_{\mathrm{ST}}} \mathbf{h}_{ij}^{(i)} x_{ij} + \sum_{k=1, k\neq i}^{N_{\mathrm{BS}}} \sum_{j=1}^{N_{\mathrm{ST}}} \mathbf{h}_{kj}^{(i)} x_{kj} + \mathbf{z}_i, \tag{4.35}$$

where x_{ij} denotes the transmitted message from user-j in cell-i, $\mathbf{z}_i$ denotes the additive white Gaussian noise vector $\mathcal{CN}(\mathbf{0}, \sigma_w^2 \mathbf{I}_{N_{\mathrm{R}} \times N_{\mathrm{R}}})$ at BS-i, and $\mathbf{I}$ denotes the identity matrix. To retrieve the messages of the desired users, each base station performs the zero-forcing (ZF) detection. The ZF matrix is constructed as

$$\mathbf{H}_i^{\dagger} = (\mathbf{H}_i^{\mathrm{H}} \mathbf{H}_i)^{-1} \mathbf{H}_i^{\mathrm{H}}, \quad \text{for} \quad \mathbf{H}_i = \left[\mathbf{h}_{i\pi_i(1)}^{(i)}, \cdots, \mathbf{h}_{i\pi_i(N_{\mathrm{ST}})}^{(i)}, \mathbf{v}_{i1}, \cdots, \mathbf{v}_{iN_{\mathrm{IN}}} \right], \tag{4.36}$$

where $\pi_i(1), \cdots, \pi_i(N_{\mathrm{ST}})$ denote the selected user index in cell-i. The messages for the desired users are retrieved by multiplying $\mathbf{H}_i^{\dagger}$ to the received signal and extracting the first N_{ST} elements in the resulting vector as follows:

$$[\hat{x}_{i\pi_i(1)}, \cdots, \hat{x}_{i\pi_i(N_{\mathrm{ST}})}] = \mathbf{D}\mathbf{H}_i^{\dagger}\mathbf{y}_i, \tag{4.37}$$

where $\mathbf{D}$ denotes $N_{\mathrm{ST}} \times N_{\mathrm{R}}$ matrix obtained by the first N_{ST} rows of $\mathbf{I}_{N_{\mathrm{R}} \times N_{\mathrm{R}}}$.

4.3.2 Sum rate of the system

The signal after ZF processing for the received signal in (4.35) is given by

$$\mathbf{H}_i^{\dagger}\mathbf{y}_i = \begin{bmatrix} x_{i1} \\ \vdots \\ x_{iN_{\mathrm{ST}}} \\ \mathbf{0}_{(N_{\mathrm{R}}-N_{\mathrm{ST}})\times 1} \end{bmatrix} + \mathbf{H}_i^{\dagger}\left(\sum_{k=1,k\neq i}^{N_{\mathrm{BS}}}\sum_{j=1}^{N_{\mathrm{ST}}}\mathbf{h}_{kj}^{(i)}x_{kj} + \mathbf{z}_i\right) \tag{4.38}$$

It is shown in Appendix C.2 that the instantaneous SINR for the selected user $\pi_i(\ell)$ in cell-i is given by

$$\mathrm{SINR}_{i\ell} = \frac{\mathrm{SNR}}{\left\langle \mathrm{SNR}\,\mathbf{H}_i^{\dagger}\sum_{k=1,k\neq i}^{N_{\mathrm{BS}}}\sum_{j=1}^{N_{\mathrm{ST}}}\mathbf{h}_{kj}^{(i)}\mathbf{h}_{kj}^{(i)\mathrm{H}}\mathbf{H}_i^{\dagger^{\mathrm{H}}} + (\mathbf{H}_i^{\mathrm{H}}\mathbf{H}_i)^{-1}\right\rangle_{\ell\ell}} \tag{4.39}$$

where $\mathrm{SNR} = \frac{P}{\sigma_w^2}$ for the transmit power P, and $<\cdot>_{\ell\ell}$ denotes the ℓ^{th} diagonal element of a matrix. Then, the sum rate per cell can be obtained by taking an average over all $\mathbf{h}$'s as

$$R_{\mathrm{SUM}} = \frac{1}{N_{\mathrm{BS}}}\sum_{i=1}^{N_{\mathrm{BS}}}\sum_{\ell=1}^{N_{\mathrm{ST}}}\mathbb{E}[\log_2(1+\mathrm{SINR}_{i\ell})]. \tag{4.40}$$

4.3.3 Conventional schemes

Conventional scheme to select the users with the large in-cell channel power (Max-SNR)

One simple scheme for user selection is that each base station select the users with the good channel within a cell. The metric for a user-j in cell-i is simply the magnitude of a channel to BS-i as follows:

$$L_{ij} = \left\|\mathbf{h}_{ij}^{(i)}\right\|^2. \tag{4.41}$$

Then, users feedback L_{ij} to their own base station and BS-i selects N_{ST} users $\pi_i(\ell), 1 \leq \ell \leq N_{\mathrm{ST}}$, who have one of the *largest-*N_{ST} L_{ij}'s out of N_{US} values as follows:

$$\pi_i(\ell) = j, \quad s.t. \;\; L_{ij} = L_{i[\ell]},\; N_{\mathrm{US}} - N_{\mathrm{ST}} + 1 \leq \ell \leq N_{\mathrm{US}}. \tag{4.42}$$

Conventional scheme to minimize the generated interference (Min-INR) [40]

To make interferences from other cells aligned in each cell in an opportunistic way, a scheme to minimize the generated interference was proposed in [40]. For a metric to measure the interference to BS-k from user-j in cell-i, the leakage is defined as

$$L_{ij}^{(k)} = \left\| \sum_{m=1}^{N_{\mathrm{SG}}} (\mathbf{u}_{km}^{\mathrm{H}} \mathbf{h}_{ij}^{(k)}) \mathbf{u}_{km} \right\|^2 = \sum_{m=1}^{N_{\mathrm{SG}}} \left| \mathbf{u}_{km}^{\mathrm{H}} \mathbf{h}_{ij}^{(k)} \right|^2. \tag{4.43}$$

We see that this metric is the 2-norm of the channel $\mathbf{h}_{ij}^{(k)}$ projected to the subspace $\mathcal{S}_k$. The total generated interference is given by

$$L_{ij} = \sum_{k=1, k\neq i}^{N_{\mathrm{BS}}} L_{ij}^{(k)}. \tag{4.44}$$

Then, users feedback L_{ij} to their own base station and BS-i selects N_{ST} users $\pi_i(\ell), 1 \leq \ell \leq N_{\mathrm{ST}}$, who have one of the *smallest-*N_{ST} L_{ij}'s out of N_{US} values as follows:

$$\pi_i(\ell) = j, \quad s.t. \;\; L_{ij} = L_{i[\ell]}, \; 1 \leq \ell \leq N_{\mathrm{ST}} \tag{4.45}$$

where $L_{i[\ell]}$ denotes the order statistics of L_{ij} in j such that $L_{i[1]} \leq \cdots \leq L_{i[N_{\mathrm{US}}]}$.

4.3.4 Proposed schemes

In this subsection, we propose a scheme to enhance the sum rate of the system.

Maximizing DSINR (Max-DSINR)

We note that the conventional scheme in Section 4.3.3 does not consider how good the channel of a selected user is to its own serving base station. To improve the sum rate, we propose that each base station should select users who have a large component projected to its own signal subspace in addition to generating small interferences to other cells. Considering the concept of the DSINR in Section 4.2.4, we use the following metric to simultaneously include projection of channels to the subspace of own cell and other cells.

$$L_{ij} = \frac{\mathrm{SNR} \sum_{m=1}^{N_{\mathrm{SG}}} |\mathbf{u}_{im}^{\mathrm{H}} \mathbf{h}_{ij}^{(i)}|^2}{1 + \mathrm{SNR} \sum_{k=1, k\neq i}^{N_{\mathrm{BS}}} \sum_{m=1}^{N_{\mathrm{SG}}} |\mathbf{u}_{km}^{\mathrm{H}} \mathbf{h}_{ij}^{(k)}|^2}. \tag{4.46}$$

We can see that the numerator reflects the projection of an in-cell channel to the signal subspace of its own base station, (*i.e.*,$\mathbf{h}_{ij}^{(i)} \rightarrow \mathcal{S}_i$) and the denominator reflects the

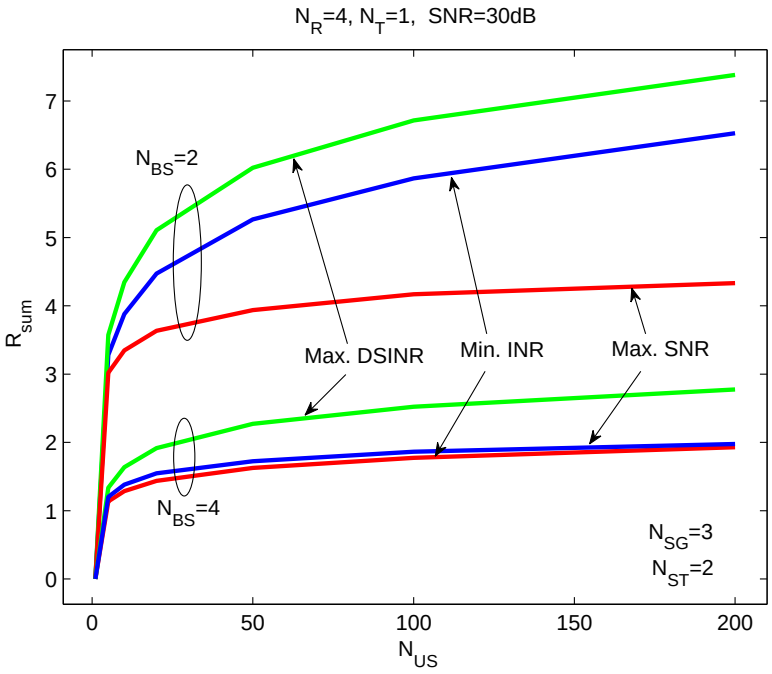

Figure 4.10: Sum rate comparison of the schemes to maximize DSINR in (4.47) or SNR in (4.42) or minimize the generated INR in (4.45). ($N_{\rm SG} = 3$ and $N_{\rm ST} = 2$)

projection of interfering channels to the signal subspace of other cells (*i.e.*,$\mathbf{h}_{ij}^{(k)} \rightarrow \mathcal{S}_k$). Then, BS-$i$ selects $N_{\rm ST}$ users $\pi_i(\ell), 1 \leq \ell \leq N_{\rm ST}$, who have one of the *largest*-$N_{\rm ST}$ L_{ij}'s out of $N_{\rm US}$ values as follows:

$$\pi_i(\ell) = j, \quad s.t. \quad L_{ij} = L_{i[\ell]}, \; N_{\rm US} - N_{\rm ST} + 1 \leq \ell \leq N_{\rm US}. \tag{4.47}$$

4.3.5 Numerical Results

Comparison between three schemes

Fig. 4.10 shows the sum rate comparison of the three schemes; a scheme to maximize DSINR in (4.47), a scheme to maximize SNR in (4.42) and a scheme to minimize the generated interference to noise ratio (INR) in (4.45). The sum rate is depicted as a function of the number of users ($N_{\rm US}$). We find that the Max-DSINR scheme is the best among three schemes with both $N_{\rm BS} = 2$ and $N_{\rm BS} = 4$. The Min-INR scheme achieves the larger sum rate than the Max-SNR scheme when $N_{\rm BS} = 2$, but has a slightly smaller sum rate when $N_{\rm BS} = 4$.

Sum rate by two-step selection

Fig. 4.11 and Fig. 4.12 show the sum rate achieved by two-step selection in Table 4.1, where $K = \frac{N_{\mathrm{SU},1}}{N_{\mathrm{ST}}}$ which is the overselection factor, *i.e.,* K times more users are selected in Step-1 compared to the number of users which are selected in Step-2. In Step-1, the Min-INR scheme is used in Fig. 4.11 and the Max-DSINR scheme is used in Fig. 4.12. We find in Fig. 4.11 that the largest sum rate is achieved when $2 \leq K \leq 5$ and that the sum rate considerably decreases when $K \geq 10$. This means that we need moderately large number of users in Step-1, but that selection of too many users in Step-1 is likely to increase the interference to other cells in the end. In Fig. 4.12(a), we find that the sum rate is large when $1 \leq K \leq 2$, but that the sum rate considerably decreases when $K \geq 5$. This means that the required number of users is smaller than that for the Min-INR scheme. This also indicates that the gain by a two-step user-selection procedure is smaller in the Max-DSINR scheme. However, when the number of the BSs increase, the required number of users in Step-1 increases as in Fig. 4.12(b). In Fig. 4.13, we compare the resulting sum rate of two-step selection for the Max-DSINR scheme and the Min-INR scheme. We can see that the Max-DSINR scheme still shows the better sum rate but the gap of the sum rate between two schemes is decreased compared to Fig. 4.10.

Effect of N_{ST} and N_{SG}

Fig. 4.14 shows the effect of N_{ST} when $N_{\mathrm{SG}} = 3$. When $N_{\mathrm{BS}} = 2$, $N_{\mathrm{ST}} = 2$ shows the largest sum rate. However, when $N_{\mathrm{BS}} = 4$, the case of $N_{\mathrm{ST}} = 1$ is slightly better than the case of $N_{\mathrm{ST}} = 2$. This indicates that the optimal number of the served users decreases as the amount of total interference increases.

4.4 Conclusion

In this chapter, we proposed several schemes to enhance the sum rate in an interference-limited uplink cellular network. In the first part of this chapter, we considered joint scheduling and beamforming to exploit multiuser diversity as well as signal processing methods to handle inter-cell interference. We proposed three schemes for that purpose. Specifically, one method for joint consideration is to maximize the signal to generated interference and noise ratio and another is to maximize the SINR

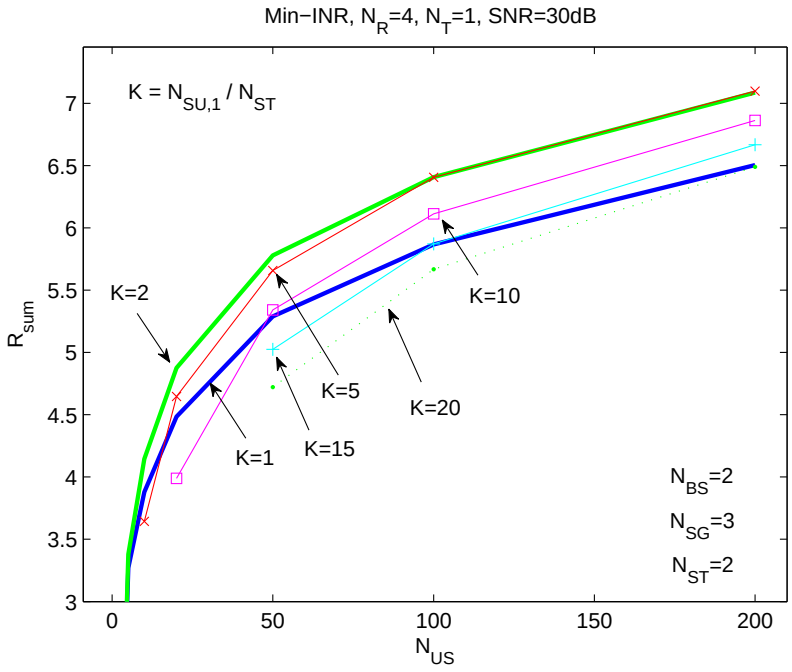

Figure 4.11: Sum rate of a two-step user-selection procedure in Table 4.1 for the scheme to minimize the generated INR in (4.42) for the different $N_{\mathrm{SU},1}$ where $K = \frac{N_{\mathrm{SU},1}}{N_{\mathrm{ST}}}$. ($N_{\mathrm{SG}} = 3$ and $N_{\mathrm{ST}} = 2$)

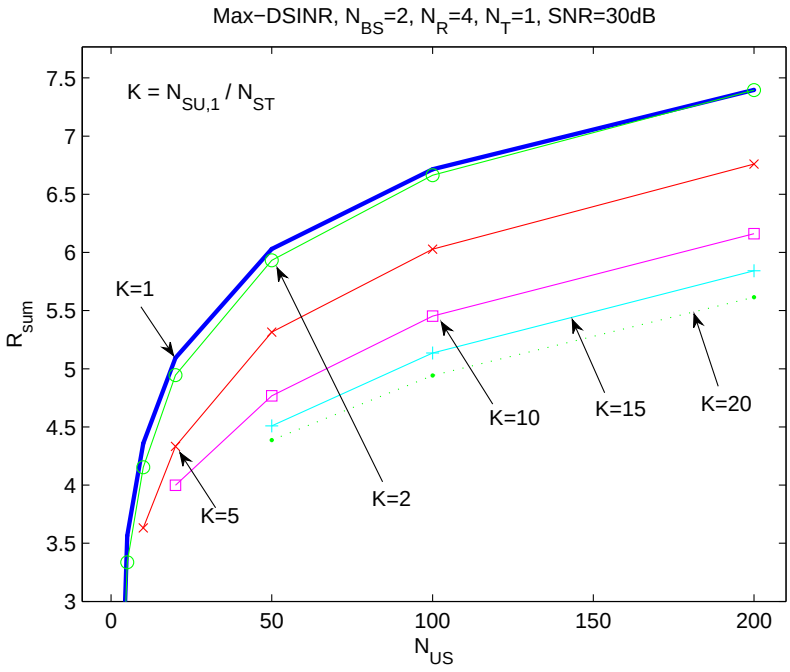

(a) $N_{\mathrm{BS}} = 2$

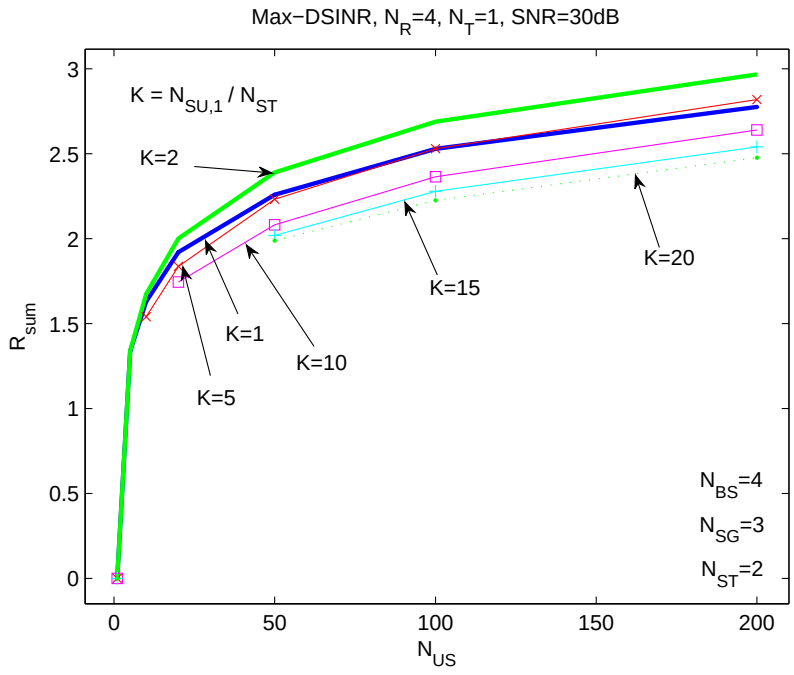

(b) $N_{\mathrm{BS}} = 4$

Figure 4.12: Sum rate of a two-step user-selection procedure in Table 4.1 for the scheme to maximize the DSINR in (4.47) for the different $N_{\mathrm{SU},1}$ where $K = \frac{N_{\mathrm{SU},1}}{N_{\mathrm{ST}}}$.

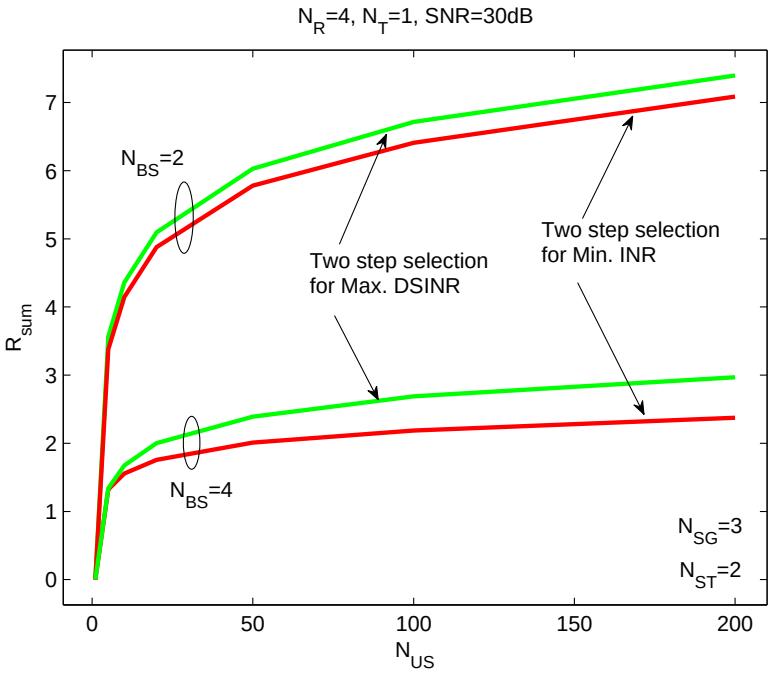

Figure 4.13: Sum rate comparison of the schemes utilizing two-step selection in Table 4.1 for the scheme to maximize the DSINR in (4.47) and the scheme to minimize the generated INR in (4.45) where $K = \frac{N_{\mathrm{SU},1}}{N_{\mathrm{ST}}}$. ($N_{\mathrm{SG}} = 3$ and $N_{\mathrm{ST}} = 2$)

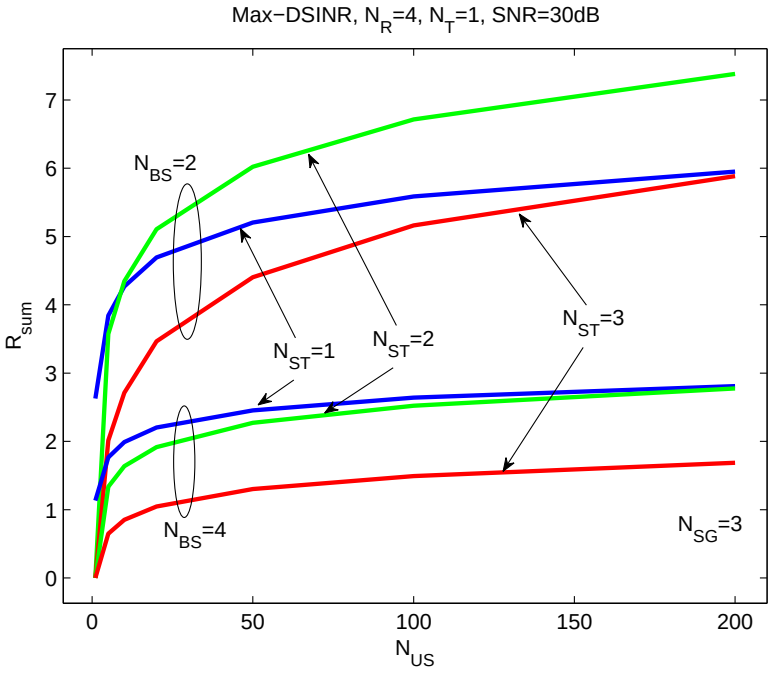

Figure 4.14: Sum rate for the different N_{ST} with fixed N_{SG}. (Max. DSINR scheme $N_{\mathrm{SG}} = 3$)

in a dual network. We also proposed a two-step user-selection procedure to improve the orthogonality of selected users and reduce intra-cell interference.. In the second part of this chapter, we considered an opportunistic interference alignment scheme as an alternative to reduce inter-cell interference. We proposed a method to maximize the DSINR to better align the interference. In both parts of this chapter, we compared the proposed schemes with the conventional schemes and showed that the proposed schemes outperform the conventional ones in most cases, and better exploited multiuser diversity in reducing inter-cell interference.

The material in this chapter is work which is in preparation for submission to the IEEE Transactions on Signal Processing under the title "*Joint User Scheduling and Beamforming in an Uplink Interference-Limited Multi-Cell System*". Sections of this chapter are submitted to Asilomar Conference on Signals, Systems, and Computers 2011 under the title "*Sum rate enhancement by maximizing DSINR in an opportunistic interference alignment scheme*". Both of these works are co-authored with Professor Bang-Chul Jung and Professor Bhaskar D. Rao. The dissertation author was the primary investigator and author of this paper.

Chapter 5

Contributions and Conclusions

This dissertation presented the study of the effect of joint scheduling and diversity in multiuser communication systems. The main contributions and possible future extensions are summarized in the following sections.

5.1 Sum Rate Analysis of a Reduced Feedback OFDMA System (Chapter 2)

In this chapter, we considered joint scheduling and diversity to enhance the benefits of multiuser diversity in a multiuser OFDMA scheduling system with reduced feedback.

The first contribution of this chapter is that the CDF of the SNR of a selected user is derived in closed-form expression. Since the result is a polynomial form of the CDF of an individual user's SNR, it is amenable to the further manipulation to derive system performance. The second is that we provided a unified framework to derive the performance of the system for various diversity techniques. Although we considered Rayleigh fading and transmit diversity techniques, it can be readily used for receive diversity techniques and other types of fading such as Nakagami fading. The third is that we provided the exact sum rate for the general value of N_{FB} for reduced feedback. The result includes both non-quantized and quantized CQI feedback and user-fair scheduling. The fourth is that we provided the approximation of the sum rate for partial feedback as a function of the sum rate of a system with full feedback. This result leads to the derivation of the required feedback N_{FB} whereby the system can achieve throughput

comparable to that obtained by a full feedback scheme.

The first possible extension is that we can consider strict short-term fairness, while we considered long-term fairness in this chapter. The second is that we can consider imperfect feedback caused by feedback delay, feedback error, or estimation error. The third is that we can consider different feedback schemes such as an average best-N_{FB} scheme.

5.2 Optimal Frequency Selectivity to Multiuser Diversity (Chapter 3)

In this chapter, we studied the effect of frequency selectivity on multiuser diversity in a multiuser OFDMA scheduling system for a frequency selective channel.

The first contribution of this chapter is that we derived correlation of subcarriers and blocks of subcarriers in closed-form when a channel shows frequency selectivity. The second is that we provided an accurate approximation of the maximum block average throughput and showed that it is closely related to the sum rate of the system. The third is that we showed that there exists a trade-off between multiuser diversity and frequency selectivity. Based on this, we showed that the optimal frequency selectivity to maximize multiuser diversity is flat inside a block and independent across blocks. The fourth is that we analyzed the role of cyclic delay with respect to frequency selectivity. Based on this, we proposed two techniques to determine per-user optimal cyclic delay to maximize multiuser diversity.

The possible extension is that we can approximate the maximum block average throughput for STBC utilizing the developed method. Comparing the sum rate of STBC and CDD, we can find the frequency selectivity region to determine the better diversity technique.

5.3 Interference Management in an Uplink Cellular Multi-cell Environment (Chapter 4)

In this chapter, we considered joint scheduling and beamforming to enhance the sum rate in a interference-limited uplink cellular network.

The first contribution of this chapter is that utilizing network duality, we

proposed a strategy for user selection and transmit beamforming design in an uplink cellular network to enhance the sum rate. The second is that for user selection and transmit beamforming, we proposed a metric of DSINR, that is, the SINR in a dual network. We showed that the proposed metric is equivalent to a what is called the SGINR metric in special antenna configurations. The third is that we proposed a two-step user-selection procedure to further enhance the sum rate by improving the orthogonality among selected users and reducing intra-cell interference. The fourth is that we applied network duality to the opportunistic interference alignment scheme and proposed a scheme to enhance the sum rate of the system.

The first possible extension is that we can consider reduced feedback in the system, such as a threshold-based feedback scheme. The second is to find better suboptimal solutions with low complexity since no optimal solution is known in an interference-limited uplink communication system and thus much remains to be done. In this dissertation, we assumed a TDD system. However, the sum rate can be investigated for a frequency division duplex (FDD) system, which is the third extension.

Appendix A

Sum Rate Analysis of a Reduced Feedback OFDMA System Employing Joint Scheduling and Diversity

A.1 Proof of Lemma 1

The $Z_{k,r}$'s are *i.i.d.* in r and thus $Y_{k,r}$'s in (2.4) are *i.i.d.* in r, which leads to the simplification in notation $F_{Y_k}(x) \triangleq F_{Y_{k,r}}(x) = \Pr\{Y_{k,r} \leq x\}$ and $F_{Z_k}(x) \triangleq F_{X_{k,r}}$. For additional simplicity in derivation, we first consider the case $\rho = 1$ in (2.4). Since $Y_{k,r}$ is selected among best-N_{FB} random variables, using Bayes' rule [49], we have

$$F_{Y_k}(x) = \sum_{m=N_{\text{RB}}-N_{\text{FB}}+1}^{N_{\text{RB}}} \Pr\{Y_{k,r} = Z_{k,(m)}\} \Pr\{Y_{k,r} \leq x | Y_{k,r} = Z_{k,(m)}\}.$$

We note that $\Pr\{Y_{k,r} \leq x | Y_{k,r} = Z_{k,(m)}\} = \Pr\{Z_{k,(m)} \leq x\} = I_{F_{Z_k}(x)}(m, N_{\text{RB}} - m + 1)$, where $I_x(\cdot,\cdot)$ denotes an incomplete Beta function [48, 2.1.5], and that $\Pr\{Y_{k,r} = Z_{k,(m)}\} = \Pr\{R_{k,r} = m\} = \frac{1}{N_{\text{FB}}}$. With a suitable change of variables followed by using a summation form of the incomplete Beta function [48, 2.1.3], we have

$$F_{Y_k}(x) = \frac{1}{N_{\text{FB}}} \sum_{m=1}^{N_{\text{FB}}} \sum_{\ell=N_{\text{RB}}-m+1}^{N_{\text{RB}}} \binom{N_{\text{RB}}}{\ell} \{F_{Z_k}(x)\}^{\ell} \{1 - F_{Z_k}(x)\}^{N_{\text{RB}}-\ell}. \tag{A.1}$$

We note in (A.1) that $F_{Y_k}(x)$ is a polynomial form of $F_{Z_k}(x)$. Finding a coefficient for each power of $F_{Z_k}(x)$, we can more directly represent $F_{Y_k}(x)$ in terms of a polynomial in $F_{Z_k}(x)$, a form suitable for the subsequent analysis. Thus, our purpose is to find the coefficients for those terms. Then we have

$$F_{Y_k}(x) \overset{(a)}{=} \sum_{\ell=0}^{N_{\mathrm{FB}}-1} \frac{N_{\mathrm{FB}}-\ell}{N_{\mathrm{FB}}} \binom{N_{\mathrm{RB}}}{\ell} \{F_{Z_k}(x)\}^{N_{\mathrm{RB}}-\ell} \{1-F_{Z_k}(x)\}^{\ell} \tag{A.2}$$

$$\overset{(b)}{=} \sum_{\ell=0}^{N_{\mathrm{FB}}-1} \sum_{r=0}^{\ell} \frac{N_{\mathrm{FB}}-\ell}{N_{\mathrm{FB}}} \binom{N_{\mathrm{RB}}}{\ell} \binom{\ell}{r} (-1)^r \{F_{Z_k}(x)\}^{N_{\mathrm{RB}}-\ell+r} \tag{A.3}$$

$$\overset{(c)}{=} \sum_{m=0}^{N_{\mathrm{FB}}-1} \sum_{\ell=m}^{N_{\mathrm{FB}}-1} \frac{N_{\mathrm{FB}}-\ell}{N_{\mathrm{FB}}} \binom{N_{\mathrm{RB}}}{\ell} \binom{\ell}{m} (-1)^{\ell-m} \{F_{Z_k}(x)\}^{N_{\mathrm{RB}}-m}, \tag{A.4}$$

where (a) follows from switching the order of m and ℓ in (A.1) and adjusting ℓ; (b) follows from applying the binomial theorem [49] to $\{1-F_{Z_k}(x)\}^{\ell}$ in (A.2); (c) follows from replacing $\ell - r$ with m in (A.3) and switching m and ℓ. Since the power of $F_{Z_k}(x)$ is independent of ℓ in (A.4), we can represent (A.4) as (2.5) with $e_1(N_{\mathrm{RB}}, N_{\mathrm{FB}}, m)$ given by (2.6) after considering a constant ρ.

A.2 Proof of Corollary 1

When $N_{\mathrm{FB}} = N_{\mathrm{RB}}$, (2.6) reduces to $e_1(N_{\mathrm{RB}}, N_{\mathrm{RB}}, m) = \sum_{\ell=m}^{N_{\mathrm{RB}}-1} \binom{N_{\mathrm{RB}}-1}{\ell}\binom{\ell}{m} \times (-1)^{\ell-m}$. When we take the derivative m times with respective to x of the binomial expansion of $(1-x)^{N_{\mathrm{RB}}-1} = \sum_{\ell=0}^{N_{\mathrm{RB}}-1} \binom{N_{\mathrm{RB}}-1}{m}(-1)^{\ell}x^{\ell}$ and divide both sides by $m!$, we have

$$(-1)^m \tbinom{N_{\mathrm{RB}}-1}{m}(1-x)^{N_{\mathrm{RB}}-m-1} = \sum_{\ell=m}^{N_{\mathrm{RB}}-1} \tbinom{N_{\mathrm{RB}}-1}{\ell}\tbinom{\ell}{m}(-1)^{\ell}x^{\ell-m}. \tag{A.5}$$

When we plug $x = 1$ in both sides and divide both sides by $(-1)^m$, we can find that $e_1(N_{\mathrm{RB}}, N_{\mathrm{RB}}, m) = \sum_{\ell=m}^{N_{\mathrm{RB}}-1} \binom{N_{\mathrm{RB}}-1}{\ell}\binom{\ell}{m}(-1)^{\ell-m} = 1$ for $m = N_{\mathrm{RB}} - 1$, and 0 otherwise.

A.3 Derivation of the conditional CDF of X_r

Following the notations in Section 2.3.1, since a selected user is k and the number of users who provided CQI to the transmitter is n, we have the conditional CDF of X_r as

$$F_{X|\ k_r^*=k,|S_r|=n}(x) \overset{(a)}{=} \Pr\{X_r \le x \mid k_r^* = k, |S_r| = n\} \tag{A.6}$$

$$\overset{(b)}{=} \Pr\{Y_{k,r} \le x \mid k_r^* = k, |S_r| = n\}$$
$$\overset{(c)}{=} \Pr\left\{U_{k,r} \le \frac{x}{\rho c_k} \mid k_r^* = k, |S_r| = n\right\}$$
$$\overset{(d)}{=} \Pr\left\{U_{i,r} \le \frac{x}{\rho c_k},\ \forall i \in S_r \mid |S_r| = n\right\}$$
$$\overset{(e)}{=} \prod_{i \in S_r, |S_r|=n} \Pr\left\{U_{i,r} \le \frac{x}{\rho c_k}\right\} \overset{(f)}{=} \prod_{i \in S_r, |S_r|=n} \Pr\{\rho c_k U_{k,r} \le x\}$$
$$\overset{(g)}{=} \prod_{i \in S_r, |S_r|=n} F_{Y_k}(x) = \left\{F_{Y_k}(x)\right\}^n,$$

where (a) follows from the definition of CDF; (b) from $X_r = Y_{k,r}$ because user-k is selected; (c) from the definition of $U_{k,r}$; (d) from that $U_{k,r}$ is the maximum among users in S_r; (e) from *i.i.d.* property of $U_{i,r}$ in i; (f) from the identical distribution of $U_{i,r}$ in i; (g) from the definition of $Y_{k,r}$ and its CDF.

A.4 Proof of Lemma 2

From (2.5) and (2.8), we have

$$F_{X|\ k_r^*=k,|S_r|=n}(x) = \{F_{Y_k}(x)\}^n = \{F_{Z_k}(\tfrac{x}{\rho})\}^{nN_{\mathrm{RB}}} \left\{\sum_{m=0}^{N_{\mathrm{FB}}-1} \frac{e_1(N_{\mathrm{RB}}, N_{\mathrm{FB}}, m)}{\{F_{Z_k}(\frac{x}{\rho})\}^m}\right\}^n. \tag{A.7}$$

Applying the same technique as in [47, 0.314] and [85, (16)] to a finite-order polynomial, we can express the above equation in a polynomial form and compute the coefficients for each term. More specifically, regarding (A.7) as a polynomial in $\frac{1}{F_{Z_k}(\frac{x}{\rho})}$, we can calculate coefficients for $\frac{1}{F_{Z_k}(\frac{x}{\rho})}$ in a recursive form as given by (2.11), and $F_{X|\ k_r^*=k,|S_r|=n}(x)$ has the form given by (2.10).

A.5 Derivation of $I_1(x, y, z)$

Following the approach in [7], we can compute $I_1(x, y, z)$ in (2.15). We note that the final form we have in (2.15) is much better than that in [7, (15), (42)] in evaluating large values for the arguments.

The PDF of Z which follows the Gamma distribution with $\mathcal{G}(\alpha, \beta)$ is given by $f_Z(z) = \frac{\beta^\alpha}{\Gamma(\alpha)} z^{\alpha-1} e^{-\beta z}$ from the derivative of CDF in (2.2). When α is a positive integer,

the CDF in (2.2) is represented by direct integration as $F_Z(z) = 1 - e^{-\beta z}\sum_{i=0}^{\alpha-1}\frac{(\beta z)^i}{i!}$. Since $d\{F_Z(z)\}^n = n\{F_Z(z)\}^{n-1}f_Z(z)dz$, we have from [86, (18)] and [7, (40)]

$$d\{F_Z(z)\}^n = \tfrac{n}{(\alpha-1)!}\sum_{k=0}^{n-1}(-1)^k\tbinom{n-1}{k}\sum_{i=0}^{k(\alpha-1)} b_{k,i}\beta^{\alpha+i}e^{-(k+1)\beta z}z^{\alpha+i-1}dz \tag{A.8}$$

for $b_{k,i}$ in (2.16). Then, using the integration identity $\int_0^\infty z^{n-1}e^{-xz}\ln(1+z)dz = (n-1)!e^x\sum_{\ell=1}^{n}\frac{\Gamma(\ell-n,x)}{x^\ell}$ [87, (78)], we have for $I_1(\alpha,\beta,n) = \int_0^\infty \log(1+z)d\{F_Z(z)\}^n$ as [7, (42)]

$$\begin{aligned}&\tfrac{n}{(\alpha-1)!\ln 2}\sum_{k=0}^{n-1}(-1)^k\tbinom{n-1}{k}\sum_{i=0}^{k(\alpha-1)} b_{k,i}\beta^{\alpha+i}e^{(k+1)\beta}(\alpha+i-1)!\\ &\qquad\times\sum_{\ell=1}^{\alpha+i}\left[\tfrac{1}{(k+1)\beta}\right]^\ell\Gamma(\ell-\alpha-i,(k+1)\beta).\end{aligned} \tag{A.9}$$

By adjusting summation index for ℓ and replacing α, β, and n with x, y, and z respectively, we can have (2.15). When $\alpha = 1$, we follow the same procedure and use the integration identity $\int_0^\infty e^{-xt}\ln(1+yt)dt \overset{(a)}{=} \frac{1}{x}e^{\frac{x}{y}}\int_{\frac{x}{y}}^\infty\frac{e^t}{t}dt \overset{(b)}{=} \Gamma(0,\frac{x}{y})$ to obtain (2.17), where (a) follows from [47, 4.337.2, 8.211.1] and (b) follows from [47, 8.350.2].

A.6 Proof of *i.i.d.* property for $U^{\mathrm{Q}}_{k,r}$

Since $U^{\mathrm{Q}}_{k,r}$ is equivalent to a quantized value of $U_{k,r}$ by the policy in (2.19), we have

$$\begin{aligned}\Pr\{U^{\mathrm{Q}}_{k,r} = J_\ell\} &\overset{(a)}{=} \Pr\{\xi_\ell \le U_{k,r} < \xi_{\ell+1}\}\\ &\overset{(b)}{=} \Pr\{\xi_\ell \le U_{m,n} < \xi_{\ell+1}\} \overset{(c)}{=} \Pr\{U^{\mathrm{Q}}_{m,n} = J_\ell\}\end{aligned} \tag{A.10}$$

where (a) and (c) follows from the quantization policy in (2.19) and (b) follows that $U_{k,r}$ is identically distributed. Therefore, $U^{\mathrm{Q}}_{k,r}$ is identically distributed. Further, we have

$$\begin{aligned}&\Pr\left\{\bigcap_{k=1}^{N_{\mathrm{US}}}\bigcap_{r=1}^{N_{\mathrm{RB}}} U^{\mathrm{Q}}_{k,r} = J_{\ell_{k,r}}\right\}\\ &\overset{(a)}{=}\Pr\left\{\bigcap_{k=1}^{N_{\mathrm{US}}}\bigcap_{r=1}^{N_{\mathrm{RB}}}\xi_{\ell_{k,r}} \le U_{k,r} < \xi_{\ell_{k,r}+1}\right\}\\ &\overset{(b)}{=}\prod_{k=1}^{N_{\mathrm{US}}}\prod_{r=1}^{N_{\mathrm{RB}}}\Pr\{\xi_{\ell_{k,r}} \le U_{k,r} < \xi_{\ell_{k,r}+1}\}\end{aligned}$$

$$\overset{(c)}{=} \prod_{k=1}^{N_{\mathrm{US}}} \prod_{r=1}^{N_{\mathrm{RB}}} \Pr\{U_{k,r}^{\mathrm{Q}} = J_{\ell_{k,r}}\} \tag{A.11}$$

where (a) and (c) follows from the quantization policy in (2.19) and (b) follows that $U_{k,r}$ is independent. Therefore, $U_{k,r}^{\mathrm{Q}}$ is independent. From (A.10) and (A.11), we find that $U_{k,r}^{\mathrm{Q}}$ is *i.i.d.*.

A.7 Derivation of the conditional PMF

Following the notations in Section 2.3.2, let us suppose that n users provided the quantization index at block-r. The probability that the quantization index of a selected user is J_ℓ is the same as the probability that the maximum of $U_{k,r}^{\mathrm{Q}}$ for all users is J_ℓ. Thus it is given by

$$\Pr\{J_\ell \text{ is selected} \mid |S_r| = n\} = \Pr\left\{ \max_{k' \in S_r} U_{k',r}^{\mathrm{Q}} \leq J_\ell \right\} - \Pr\left\{ \max_{k' \in S_r} U_{k',r}^{\mathrm{Q}} \leq J_{\ell-1} \right\} \tag{A.12}$$

$$\overset{(a)}{=} \Pr\left\{ \max_{k' \in S_r} U_{k',r} \leq \xi_{\ell+1} \right\} - \Pr\left\{ \max_{k' \in S_r} U_{k',r} \leq \xi_\ell \right\} \overset{(b)}{=} \{F_U(\xi_{\ell+1})\}^n - \{F_U(\xi_\ell)\}^n$$

where (a) follows from the quantization policy in (2.19) and (b) follows from the order statistics [48, 2.1.1]. Since user selection is based on *i.i.d.* normalized CQI values, the probability that each user is selected for a transmission is $\frac{1}{N_{\mathrm{US}}}$. Considering that the modulation level is determined as $\rho c_k \xi_\ell$ for user-k when it is selected, the conditional PMF that $X_r^{\mathrm{Q}} = \rho c_k \xi_\ell$ is given by (2.22). We note that the sum of this probability over n and ℓ is 1, which verifies the validity as the PMF.

A.8 Derivation of (2.23)

From the conditional PMF in (2.22), the sum rate for the system with partial feedback of quantized CQI is given by

$$R_{\mathrm{SUM}} = \frac{1}{N_{\mathrm{RB}}} \sum_{r=1}^{N_{\mathrm{RB}}} \mathbb{E}[\log(1 + X_r^{\mathrm{Q}})] \overset{(a)}{=} \mathbb{E}[\log(1 + X_r^{\mathrm{Q}})]$$

$$= \mathbb{E}_{|S_r|} \mathbb{E}_{X_r^{\mathrm{Q}}} [\log(1 + X_r^{\mathrm{Q}}) \mid |S_r| = n \neq 0]$$

$$\overset{(b)}{=} \sum_{k=1}^{N_{\mathrm{US}}} \sum_{\ell=0}^{L} \frac{\log_2(1+\rho c_k \xi_\ell)}{N_{\mathrm{US}}} \sum_{n=1}^{N_{\mathrm{US}}} \binom{N_{\mathrm{US}}}{n} \left(\frac{N_{\mathrm{FB}}}{N_{\mathrm{RB}}} \right)^n$$

$$\times \left(1 - \tfrac{N_{\mathrm{FB}}}{N_{\mathrm{RB}}}\right)^{N_{\mathrm{US}}-n} \left[\{F_U(\xi_{\ell+1})\}^n - \{F_U(\xi_\ell)\}^n\right], \tag{A.13}$$

where (a) follows from that X_r^{Q} is identically distributed in r and (b) follows from the conditional PMF of X_r^{Q} in (2.22) and the PMF of $|S_r|$ in (2.7). From the binomial theorem [49], we have

$$\begin{aligned}
&\sum_{n=1}^{N_{\mathrm{US}}} \tbinom{N_{\mathrm{US}}}{n} \left(\tfrac{N_{\mathrm{FB}}}{N_{\mathrm{RB}}}\right)^n \left(1 - \tfrac{N_{\mathrm{FB}}}{N_{\mathrm{RB}}}\right)^{N_{\mathrm{US}}-n} \{F_U(\xi_{\ell+1})\}^n \\
&\quad = \left\{1 - \tfrac{N_{\mathrm{FB}}}{N_{\mathrm{RB}}}(1 - F_U(\xi_{\ell+1}))\right\}^{N_{\mathrm{US}}} - \left(1 - \tfrac{N_{\mathrm{FB}}}{N_{\mathrm{RB}}}\right)^{N_{\mathrm{US}}}.
\end{aligned} \tag{A.14}$$

Thus, (A.13) reduces to (2.23) for $I_2(x, y, z, r)$ in (2.23).

Appendix B

Optimal Frequency Selectivity to Multiuser Diversity in an OFDMA Scheduling System

B.1 Derivation of $\rho_{\mathbf{SC}}(|\Delta_n|)$

Let $\mathbf{x} = [H_{n_1}, H_{n_2}]^T$ for H_n in (3.2). Since we assume that H_n's follow jointly Gaussian distribution, $\mathbf{x}$ follows $\mathcal{CN}(\mathbf{0}, R_{\mathbf{x}})$ where $R_{\mathbf{x}}$ denotes a covariance matrix and its elements are in (3.9). Considering $\gamma_n = P|H_n|^2/\sigma_w^2$ in Section 3.2 and using $R_{\mathbf{x}}$, we have the general order correlation as [88, 2.14 in p.86]

$$\mathbb{E}[\gamma_{n_1}^{\alpha}\gamma_{n_2}^{\beta}] = \overline{\gamma}^{\alpha+\beta}\alpha!\beta!\sum_{m=0}^{\min\{\alpha,\beta\}}\binom{\alpha}{m}\binom{\beta}{m}|\mathrm{cov}(H_{n_1}, H_{n_2})|^{2m} \tag{B.1}$$

where $\overline{\gamma} = \mathbb{E}[\gamma_n]$. Then, covariance is given by

$$\mathrm{cov}(\gamma_{n_1}, \gamma_{n_2}) = \mathbb{E}[\gamma_{n_1}\gamma_{n_2}] - \overline{\gamma}^2 = \overline{\gamma}^2|\mathrm{cov}(H_{n_1}, H_{n_2})|^2. \tag{B.2}$$

Noting that $\mathrm{cov}(H_n, H_n) = 1$ in (3.9), we have $\mathrm{var}[\gamma_n] = \overline{\gamma}^2$ in (B.2). Using these results and following the definition of the correlation coefficient in (3.7), we lead to (3.8).

B.2 Statistics of C_b

Noting that γ_n follows Gamma distribution and is identically distributed over n, we have without loss of generality

$$\mathbb{E}[C_b] = \mathbb{E}[\log_2(1+\gamma_1)] = \frac{e^{\frac{\sigma_w^2}{P}}\ \mathrm{Ei}(1, \frac{\sigma_w^2}{P})}{\ln 2} \tag{B.3}$$

where $\mathrm{Ei}(a,x) = \int_1^\infty e^{-xt}t^{-a}dt$ [89] and the integral equality in [47, 4.337.2 in p.603] is used as following.

$$\int_0^\infty e^{-xt}\ln(1+yt)dt = \frac{1}{x}e^{\frac{x}{y}}\mathrm{Ei}\left(1, \frac{x}{y}\right). \tag{B.4}$$

Instead of using a slowly converging infinite series in computing $\mathrm{cov}(\log_2(1+\gamma_{n_1}), \log_2(1+\gamma_{n_2}))$ [90], we use the delta method which is known as the Taylor series method [56]. When we take the Taylor series expansion of $\log_2(1+\gamma_n)$ about $\mathbb{E}[\gamma_n]$, we have [56]

$$\log_2(1+\gamma_n) = \log_2(1+\mathbb{E}[\gamma_n]) + \sum_{m=1}^{\infty} \frac{(-1)^{m-1}(\gamma_n - \mathbb{E}[\gamma_n])^m}{m(1+\mathbb{E}[\gamma_n])^m \ln 2}. \tag{B.5}$$

For the first order expansion of $\log_2(1+\gamma_n)$ in (B.5) (*i.e.,* $m=1$), we have from (3.3)

$$C_b \simeq \log_2(1+\mathbb{E}[\gamma_n]) + \frac{1}{S_{\mathrm{RB}}} \sum_{n=(b-1)S_{\mathrm{RB}}}^{bS_{\mathrm{RB}}} \frac{\gamma_n - \mathbb{E}[\gamma_n]}{(1+\mathbb{E}[\gamma_n])\ln 2}. \tag{B.6}$$

Using the bilinear property of covariance [69] and considering that covariance does not change by the addition of a constant and that $\mathrm{cov}(\gamma_{n_1}, \gamma_{n_2}) = \mathrm{var}[\gamma_1]\rho_{\mathrm{SC}}(|\Delta_n|)$ in (3.7), covariance between C_{b_1} and C_{b_2} is given by

$$\mathrm{cov}(C_{b_1}, C_{b_2}) = \frac{\mathrm{var}[\gamma_1]}{((1+\mathbb{E}[\gamma_1])\ln 2)^2}\ \Psi_{\mathrm{SC}}(1, |\Delta_b|, S_{\mathrm{RB}}). \tag{B.7}$$

From (3.15) and the fact that $\mathrm{var}[C_b] = \mathrm{cov}(C_b, C_b)$, we have

$$\mathrm{var}[C_b] = \frac{\mathrm{var}[\gamma_1]}{\{(1+\mathbb{E}[\gamma_1])\ln 2\}^2}\Psi_{\mathrm{SC}}(1, 0, S_{\mathrm{RB}}). \tag{B.8}$$

Thus, the correlation coefficient between C_{b_1} and C_{b_2} is given by (3.16).

For the second order expansion of $\log_2(1+\gamma_n)$ in (B.5) (*i.e.,* $m=2$), we have

$$\log_2(1+\gamma_n) = A_1 + A_2\gamma_n + A_3\gamma_n^2 \tag{B.9}$$

where $A_1 = \log_2(1+\mathbb{E}[\gamma_n]) - \frac{\mathbb{E}[\gamma_n]}{(1+\mathbb{E}[\gamma_n])\ln 2} - \frac{\mathbb{E}^2[\gamma_n]}{2(1+\mathbb{E}[\gamma_n])^2\ln 2}$, $A_2 = \frac{1}{(1+\mathbb{E}[\gamma_n])\ln 2} + \frac{\mathbb{E}[\gamma_n]}{(1+\mathbb{E}[\gamma_n])^2\ln 2}$, and $A_3 = \frac{-1}{2(1+\mathbb{E}[\gamma_n])^2\ln 2}$. From (3.3), we have

$$C_b \simeq A_1 + A_2 \sum_{\substack{n=1+\\(b-1)S_{\mathrm{RB}}}}^{bS_{\mathrm{RB}}} \frac{\gamma_n}{S_{\mathrm{RB}}} + A_3 \sum_{\substack{n=1+\\(b-1)S_{\mathrm{RB}}}}^{bS_{\mathrm{RB}}} \frac{\gamma_n^2}{S_{\mathrm{RB}}}. \tag{B.10}$$

From (B.1) and (3.8), we have in the same way as (B.2)

$$\mathrm{cov}(\gamma_{n_1}, \gamma_{n_2}^2) = 4\mathbb{E}^3[\gamma_n]\rho_{\mathrm{SC}}(|\Delta_n|), \tag{B.11}$$

$$\mathrm{cov}(\gamma_{n_1}^2, \gamma_{n_2}^2) = 4\mathbb{E}^4[\gamma_n]\ \{4\rho_{\mathrm{SC}}(|\Delta_n|) + \rho_{\mathrm{SC}}^2(|\Delta_n|)\}. \tag{B.12}$$

From (B.10), (B.11), (B.12) and the bilinear property of covariance [69], we have for the covariance between C_{b_1} and C_{b_2} as

$$\mathrm{cov}(C_{b_1}, C_{b_2}) = B_1\Psi_{\mathrm{SC}}(1, |\Delta_b|, S_{\mathrm{RB}}) + B_2\Psi_{\mathrm{SC}}(2, |\Delta_b|, S_{\mathrm{RB}}) \tag{B.13}$$

where $B_1 = \mathbb{E}^2[\gamma_n](A_2^2 + 8A_2A_3\mathbb{E}[\gamma_n] + 16A_3^2\mathbb{E}^2[\gamma_n])$, $B_2 = 4A_3^2\mathbb{E}^4[\gamma_n]$, and $\Psi_{\mathrm{SC}}(r, |\Delta_b|, S_{\mathrm{RB}})$ is defined in (3.10). Thus, we have

$$\mathrm{var}[C_b] = B_1\Psi_{\mathrm{SC}}(1, 0, S_{\mathrm{RB}}) + B_2\Psi_{\mathrm{SC}}(2, 0, S_{\mathrm{RB}}). \tag{B.14}$$

Appendix C

Interference Management in an Uplink Interference-limited Multi-cell Environment

C.1 Derivation of $R_{\mathbf{SUM}}$ for SDMA in (4.5)

Let $A \triangleq \sum_{j\in\Pi_i} \sqrt{\rho_{ij}} H_{ij}^{(i)} \mathbf{w}_{ij} x_{ij}$ and $B \triangleq \sum_{k=1,k\neq i}^{N_{\mathrm{BS}}} \sum_{j\in\Pi_k} \sqrt{\eta_{kj}^{(i)}} H_{kj}^{(i)} \mathbf{w}_{kj} x_{kj}$ in (4.1). Then, $\mathbf{y}_i = A + B + \mathbf{z}_i$. The covariance of the signal is given by

$$Q_{\mathrm{SIG},i} = \mathrm{cov}\,(A, A) = \mathbb{E}\left[\sum_{j\in\Pi_i} \sqrt{\rho_{ij}} H_{ij}^{(i)} \mathbf{w}_{ij} x_{ij} \left(\sum_{\ell\in\Pi_i} \sqrt{\rho_{i\ell}} H_{i\ell}^{(i)} \mathbf{w}_{i\ell} x_{i\ell}\right)^{\mathrm{H}}\right], \tag{C.1}$$

which reduces to (4.6) because $\mathbb{E}[x_{kj} x_{\ell m}^*] = \delta_{k\ell}\delta_{jm}$ where $\delta_{k\ell}$ denotes the Kronecker delta. In the same way, $Q_{\mathrm{INT},i} = \mathrm{cov}(B, B)$, which reduces to (4.7). We also note that $\mathrm{cov}(A, B)$ is a matrix with all zero entries. Then, covariance of the received signal $\mathrm{cov}\,(\mathbf{y}_i, \mathbf{y}_i)$ is given by

$$\mathrm{cov}\,(A + B + \mathbf{z}_i, A + B + \mathbf{z}_i) = Q_{\mathrm{SIG},i} + Q_{\mathrm{INT},i} + \mathbf{I}_{N_{\mathrm{R}}}, \tag{C.2}$$

since $\mathbf{z}_i$ follows $\mathcal{CN}(\mathbf{0}, \mathbf{I}_{N_{\mathrm{R}}})$. Thus, the achievable rate at BS-i is given by [83]

$$C_i = \log_2 \frac{\det(A + B + \mathbf{I}_{N_{\mathrm{R}}})}{\det(B + \mathbf{I}_{N_{\mathrm{R}}})}, \tag{C.3}$$

which reduces to the summand in (4.5) since $B + \mathbf{I}_{N_{\mathrm{R}}}$ is non-singular. By summing C_i over all the BSs and taking an average over all the realization of the channel coefficients, we have (4.5) for the sum rate.

C.2 Derivation of SINR

Let $A \triangleq \sum_{k=1,k\neq i}^{N_{\mathrm{BS}}} \sum_{j=1}^{N_{\mathrm{ST}}} \mathbf{h}_{kj}^{(i)} x_{kj}$ in (4.38). Then, covariance of A is given by

$$\mathrm{cov}\,(A,A) = \mathbb{E}\left[\sum_{k=1,k\neq i}^{N_{\mathrm{BS}}}\sum_{j=1}^{N_{\mathrm{ST}}} \mathbf{h}_{kj}^{(i)} x_{kj} \left(\sum_{\ell=1,\ell\neq i}^{N_{\mathrm{BS}}}\sum_{m=1}^{N_{\mathrm{ST}}} \mathbf{h}_{\ell m}^{(i)} x_{\ell m}\right)^{\mathrm{H}}\right] = P\sum_{k=1,k\neq i}^{N_{\mathrm{BS}}}\sum_{j=1}^{N_{\mathrm{ST}}} \mathbf{h}_{kj}^{(i)}\mathbf{h}_{kj}^{(i)^{\mathrm{H}}} \tag{C.4}$$

because $\mathbb{E}[x_{kj}x_{\ell m}^{*}] = \delta_{k\ell}\delta_{jm}P$ where $\delta_{k\ell}$ denotes the Kronecker delta. Since $\mathbf{z}_i$ is a white Gaussian noise vector, covariance of $\mathbf{z}_i$ is given by

$$\mathrm{cov}\,(\mathbf{z}_i,\mathbf{z}_i) = \sigma_w^2 \mathbf{I}_{N_{\mathrm{R}}\times N_{\mathrm{R}}}. \tag{C.5}$$

Then, covariance of $\mathbf{H}_i^{\dagger}(A+\mathbf{z}_i)$ is given from (C.4) and (C.5) by

$$\begin{aligned}\mathrm{cov}\left(\mathbf{H}_i^{\dagger}(A+\mathbf{z}_i), \mathbf{H}_i^{\dagger}(A+\mathbf{z}_i)\right) &= \mathbf{H}_i^{\dagger}\mathrm{cov}\,(A,A)\,\mathbf{H}_i^{\dagger^{\mathrm{H}}} + \mathbf{H}_i^{\dagger}\mathrm{cov}\,(\mathbf{z}_i,\mathbf{z}_i)\,\mathbf{H}_i^{\dagger^{\mathrm{H}}} \\ &= P\,\mathbf{H}_i^{\dagger}\sum_{k=1,k\neq i}^{N_{\mathrm{BS}}}\sum_{j=1}^{N_{\mathrm{ST}}} \mathbf{h}_{kj}^{(i)}\mathbf{h}_{kj}^{(i)^{\mathrm{H}}}\mathbf{H}_i^{\dagger^{\mathrm{H}}} + \sigma_w^2(\mathbf{H}_i^{\mathrm{H}}\mathbf{H}_i)^{-1}\end{aligned} \tag{C.6}$$

The SINR of the selected user $\pi_i(\ell)$ in (4.38) is given by

$$\mathrm{SINR}_{i\ell} = \frac{P}{\left\langle \mathrm{cov}\left(\mathbf{H}_i^{\dagger}(A+\mathbf{z}_i), \mathbf{H}_i^{\dagger}(A+\mathbf{z}_i)\right)\right\rangle_{\ell\ell}} \tag{C.7}$$

where cov denotes covariance. Then, we can see that (C.7) reduces to (4.39) from (C.5) for $\mathrm{SNR} = \frac{P}{\sigma_w^2}$.

Bibliography

[1] B. Sklar, "Rayleigh fading channels in mobile digital communication systems Part II: Mitigation," *IEEE Commun. Mag.*, vol. 35, no. 7, pp. 102–109, Jul. 1997.

[2] D. G. Brennan, "Linear diversity combining techniques," *Proceedings of IEEE*, vol. 91, no. 2, pp. 331–356, Feb. 2003.

[3] J. Mietzner, R. Schober, L. Lampe, W.H. Gerstacker, and P.A. Hoeher, "Multiple-antenna techniques for wireless communications - A comprehensive literature survey," *Communications Surveys Tutorials, IEEE*, vol. 11, no. 2, pp. 87–105, 2009.

[4] R. Knopp and P. Humblet, "Information capacity and power control in single-cell multiuser communications," in *Proc. 1995 IEEE Intl. Conf. Commun.*, Seattle, WA, Jun. 1995, pp. 331–335.

[5] P. Viswanath, D. N. C. Tse, and R. Laroia, "Opportunistic beamforming using dumb antennas," *IEEE Trans. Inf. Theory*, vol. 48, no. 6, pp. 1277–1294, Jun. 2002.

[6] S. H. (Paul) Hur, M. J. Rim, B. D. Rao, and J. R. Zeidler, "On the optimal frequency selectivity to multiuser diversity in OFDMA scheduling systems," in preparation.

[7] C.-J. Chen and Li-Chun Wang, "A unified capacity analysis for wireless systems with joint multiuser scheduling and antenna diversity in Nakagami fading channels," *IEEE Trans. Commun.*, vol. 54, no. 3, pp. 469–478, Mar. 2006.

[8] M. Pugh and B.D. Rao, "Reduced feedback schemes using random beamforming in MIMO broadcast channels," *IEEE Trans. Sig. Processing*, vol. 58, no. 3, pp. 1821–1832, Mar. 2010.

[9] Qinghua Li, Guangjie Li, Wookbong Lee, Moon il Lee, D. Mazzarese, B. Clerckx, and Zexian Li, "MIMO techniques in wimax and lte: a feature overview," *Communications Magazine, IEEE*, vol. 48, no. 5, pp. 86–92, May. 2010.

[10] 3GPP WG1, *TS 36.201 V9.1.0 - LTE Physical Layer - General Description (Release 9)*, Mar. 2010.

[11] M. Sharif and B. Hassibi, "On the capacity of MIMO broadcast channel with partial side information," *IEEE Trans. Inf. Theory*, vol. 51, no. 2, pp. 506–522, Feb. 2005.

[12] I. Koffman and V. Roman, "Broadband wireless access solutions based on ofdm access in ieee 802.16," *Communications Magazine, IEEE*, vol. 40, no. 4, pp. 96 –103, apr 2002.

[13] H. Ekstrom, A. Furuskar, J. Karlsson, M. Meyer, S. Parkvall, J. Torsner, and M. Wahlqvist, "Technical solutions for the 3g long-term evolution," *Communications Magazine, IEEE*, vol. 44, no. 3, pp. 38 – 45, march 2006.

[14] X. Liu, E. K. Chong, and N. B. Shroff, "A framework for opportunistic scheduling in wireless networks," *Computer Networks*, vol. 41, no. 4, pp. 451–474, Mar. 2003.

[15] Y.S. Al-Harthi, A.H. Tewfik, and M.-S. Alouini, "Multiuser diversity with quantized feedback," *IEEE Trans. Wireless Commun.*, vol. 6, no. 1, pp. 330–337, Jan. 2007.

[16] Jin-Ghoo Choi and Saewoong Bahk, "Cell-throughput analysis of the proportional fair scheduler in the single-cell environment," *IEEE Trans. Veh. Technol.*, vol. 56, no. 2, pp. 766–778, Mar. 2007.

[17] E.A. Jorswieck, A. Sezgin, and Xi Zhang, "Throughput versus fairness channel-aware scheduling in multiple antenna downlink," *EURASIP Journal on Wireless Communications and Networking*, vol. 2009, pp. 1–13, 2009.

[18] D. J. Love, R. W. Heath Jr., V. K. N. Lau, D. Gesbert, B. D. Rao, and M. Andrews, "An overview of limited feedback in wireless communciation systems," *IEEE J. Selected Areas Commun.*, vol. 26, no. 8, pp. 1341–1365, Oct. 2008.

[19] T. Eriksson and T. Ottosson, "Compression of feedback for adaptive transmission and scheduling," *Proceedings of IEEE*, vol. 95, no. 12, pp. 2314–2321, Dec. 2007.

[20] V. Hassel, D. Gesbert, M. Alouini, and G. E. Oien, "A threshold-based channel state feedback algorithm for modern cellular systems," *IEEE Trans. Wireless Commun.*, vol. 6, no. 7, pp. 2422–2426, Jul. 2007.

[21] P. Svedman, S. K. Wilson, L. J. Cimini, and B. Ottersten, "Opportunistic beamforming and scheduling for ofdma systems," *Communications, IEEE Transactions on*, vol. 55, no. 5, pp. 941 –952, may 2007.

[22] Zhong-Hai Han and Yong-Hwan Lee, "Opportunistic scheduling with partial channel information in ofdma/fdd systems," in *Vehicular Technology Conference, 2004. VTC2004-Fall. 2004 IEEE 60th*, sept. 2004, vol. 1, pp. 511 – 514 Vol. 1.

[23] Jieying Chen, R. Berry, and M. Honig, "Limited feedback schemes for downlink OFDMA based on sub-channel groups," *Selected Areas in Communications, IEEE Journal on*, vol. 26, no. 8, pp. 1451 –1461, october 2008.

[24] J. Leinonen, J. Hämäläinen, and M. Juntti, "Performance analysis of downlink OFDMA resource allocation with limited feedback," *IEEE Trans. Wireless Commun.*, vol. 8, no. 6, pp. 2927–2937, Jun. 2009.

[25] J. Leinonen, J. Hamalainen, and M. Juntti, "Capacity analysis of downlink MIMO-OFDMA frequency allocation with imperfect feedback information," in *Signal Processing Advances in Wireless Communications, 2009. SPAWC '09. IEEE 10th Workshop on*, Jun. 2009, pp. 141–145.

[26] J. Leinonen, J. Hamalainen, and M. Juntti, "Outage capacity analysis of resource allocation in downlink MIMO-OFDMA systems with the best-m feedback method," in *Signal Processing Advances in Wireless Communications, 2009. SPAWC '09. IEEE 10th Workshop on*, june 2009, pp. 146 –150.

[27] Young-June Choi and Saewoong Bahk, "Partial channel feedback schemes maximizing overall efficiency in wireless networks," *Wireless Communications, IEEE Transactions on*, vol. 7, no. 4, pp. 1306 –1314, april 2008.

[28] Y. Choi and S. Rangarajan, "Analysis of best channel feedback and its adaptive algorithms for multi-carrier wireless data systems," *IEEE Trans. Mobile Computing*, pre-print 2011.

[29] B. C. Jung, T. W. Ban, W. Choi, and D. K. Sung, "Capacity analysis of simple and opportunistic feedback schemes in OFDMA systems," in *Proc. 2007 IEEE Intl. Symp. on Comm. and Info. Techn.*, Oct. 2007, pp. 203–208.

[30] K. Pedersen, T. Kolding, I. Kovacs, G. Monghal, F. Frederiksen, and P. Mogensen, "Performance analysis of simple channel feedback schemes for a practical OFDMA system," *Vehicular Technology, IEEE Transactions on*, vol. 58, no. 9, pp. 5309 –5314, nov. 2009.

[31] W. C. Y. Lee, *Mobile communications design fundamentals*, Wiley, New York, 1993.

[32] F. Floren, M.Z. Win, O. Edfors, and B.-A. Molin, "Dependence of the mean snr on the interaction between multiuser diversity, multipath diversity, and feedback delay," in *Proc. 2005 IEEE 61th Veh. Technol. Conf.*, May-1 Jun. 2005, vol. 3, pp. 1898–1902 Vol. 3.

[33] S. Shamai and A.D. Wyner, "Information-theoretic considerations for symmetric, cellular, multiple-access fading channels. I," *Information Theory, IEEE Transactions on*, vol. 43, no. 6, pp. 1877 –1894, Nov. 1997.

[34] J.G. Andrews, Wan Choi, and R.W. Heath, "Overcoming interference in spatial multiplexing mimo cellular networks," *Wireless Communications, IEEE*, vol. 14, no. 6, pp. 95 –104, 2007.

[35] F. Rashid-Farrokhi, K.J.R. Liu, and L. Tassiulas, "Transmit beamforming and power control for cellular wireless systems," *Selected Areas in Communications, IEEE Journal on*, vol. 16, no. 8, pp. 1437 –1450, oct 1998.

[36] B. Song, R.L. Cruz, and B.D. Rao, "Network duality for multiuser mimo beamforming networks and applications," *Communications, IEEE Transactions on*, vol. 55, no. 3, pp. 618 –630, march 2007.

[37] Byong Lee, Hui Je, Oh-Soon Shin, and Kwang Lee, "A novel uplink mimo transmission scheme in a multicell environment," *Wireless Communications, IEEE Transactions on*, vol. 8, no. 10, pp. 4981 –4987, 2009.

[38] M. Sadek, A. Tarighat, and A.H. Sayed, "A leakage-based precoding scheme for downlink multi-user mimo channels," *Wireless Communications, IEEE Transactions on*, vol. 6, no. 5, pp. 1711 –1721, May 2007.

[39] M. Sadek, A. Tarighat, and A.H. Sayed, "Active antenna selection in multiuser mimo communications," *Signal Processing, IEEE Transactions on*, vol. 55, no. 4, pp. 1498 –1510, 2007.

[40] Bang Chul Jung and Won-Yong Shin, "Opportunistic interference alignment for interference-limited cellular tdd uplink," *Communications Letters, IEEE*, vol. 15, no. 2, pp. 148 –150, Feb. 2011.

[41] D. Gesbert and M.-S. Alouini, "How much feedback is multi-user diversity really worth?," in *Proc. 2004 IEEE Intl. Conf. Commun.*, Jun. 2004, vol. 1, pp. 234–238.

[42] Z. Chen, J. Yuan, and B. Vucetic, "Analysis of transmit antenna selection/maximal-ratio combining in Rayleigh fading channels," *IEEE Trans. Veh. Technol.*, vol. 54, no. 4, pp. 1312–1321, Jul. 2005.

[43] A. Dammann and S. Kaiser, "Standard conformable antenna diversity techniques for OFDM systems and its application to the DVB-T system," in *Proc. 2001 IEEE Global Telecomm. Conf.*, 2001, pp. 3100–3105.

[44] S. M. Alamouti, "A simple transmit diversity technique for wireless communications," *IEEE J. Selected Areas Commun.*, vol. 16, pp. 1451–1458, Oct. 1998.

[45] Guocong Song and Ye Li, "Asymptotic throughput analysis for channel-aware scheduling," *IEEE Trans. Commun.*, vol. 54, no. 10, pp. 1827–1834, Oct. 2006.

[46] N. L. Johnson, S. Kotz, and N. Balakrishnan, *Continuous Univariate Distributions*, John Wiley, MA, 2nd edition, 1994.

[47] I. S. Gradshteyn and I. M. Ryzhik, *Table of Integrals, Series, and Products*, Academic Press, 2000.

[48] H. A. David and H. N. Nagaraja, *Order Statistics*, John Wiley & Sons Inc., 3rd edition, 2004.

[49] A. Leon-Garcia, *Probability and Random Processes for Electrical Engineering*, Addison-Wesley, MA, 2nd edition, 1994.

[50] M. Abramowitz and I. A. Stegun, *Handbook of mathematical functions with formulas, graphs, and mathematical tables*, US Dept. of Commerce, New York: Dover, 9th edition, 1970.

[51] J. G. Proakis, *Digital Communications*, McGraw Hill, New York, 3rd edition, 1995.

[52] H. Jafarkhani, *Space-Time Coding*, Academic Press, 2005.

[53] D. N. C. Tse, "Optimal power allocation over parallel Gaussian channels," in *Proc. 1997 IEEE Intl. Symp. on Info. Theory*, Ulm, Germany, Jun. 1997.

[54] Jr. Jakes, W.C., "A comparison of specific space diversity techniques for reduction of fast fading in uhf mobile radio systems," *IEEE Trans. Veh. Technol.*, vol. 20, no. 4, pp. 81–92, nov 1971.

[55] Yao Ma, R. Schober, and Dongbo Zhang, "Exact ber for m-qam with mrc and imperfect channel estimation in rician fading channels," *Wireless Communications, IEEE Transactions on*, vol. 6, no. 3, pp. 926–936, Mar. 2007.

[56] A. Assalini, "Maximizing outage capacity of OFDM transmit diversity systems," *IEEE Trans. Veh. Technol.*, vol. 58, no. 9, pp. 4786–4794, Nov. 2009.

[57] G. Bauch, "Capacity optimization of cyclic delay diversity," in *Proc. 2004 IEEE 60th Veh. Technol. Conf.*, Sep. 2004, pp. 1820–1824.

[58] N. Seshadri and J. H. Winters, "Two signaling schemes for improving the error performance of frequency-division-duplex(fdd) transmission systems using transmitter antenna diversity," in *Proc. 1993 IEEE 43rd Veh. Technol. Conf.*, May 1993, pp. 508–511.

[59] D. S. Yoo and W. E. Stark, "Characterization of WSSUS channels: Normalized mean square covariance," *IEEE Trans. Wireless Commun.*, vol. 4, no. 4, pp. 1575–1584, Jul. 2005.

[60] D. S. Yoo and W. E. Stark, "Characterization of WSSUS channels: Normalized mean square covariance and diversity combining," *IEEE Trans. Wireless Commun.*, vol. 4, no. 4, pp. 1307–1310, Jul. 2005.

[61] Quan Zhou and Huaiyu Dai, "Asymptotic analysis on the interaction between spatial diversity and multiuser diversity in wireless networks," *IEEE Trans. Sig. Processing*, vol. 55, no. 8, pp. 4271–4283, Aug. 2007.

[62] G. Barriac and U. Madhow, "Characterizing outage rates for space-time communication over wideband channels," *IEEE Trans. Commun.*, vol. 52, no. 12, pp. 2198–2208, Dec. 2004.

[63] Yong-June Kim, Ho-Yun Kim, Minjoong Rim, and Dae-Woon Lim, "On the optimal cyclic delay value in cyclic delay diversity," *IEEE Trans. Broadcasting*, vol. 55, no. 4, pp. 790–795, Dec. 2009.

[64] D. Tse and P. Viswanath, *Fundamentals of Wireless Communication*, Cambridge University Press, 2005.

[65] B.M. Hochwald, T.L. Marzetta, and V. Tarokh, "Multiple-antenna channel hardening and its implications for rate feedback and scheduling," *IEEE Trans. Inf. Theory*, vol. 50, no. 9, pp. 1893–1909, Sept. 2004.

[66] F. Khan and C. V. Rensburg, "An adaptive cyclic delay diversity technique for beyond 3G/4G wireless systems," in *Proc. 2006 IEEE 64th Veh. Technol. Conf.*, Sep. 2006, pp. 1–6.

[67] N. Himayat, S. Talwar, W. Choi, J. Y. Kim, J. Koo, J. Choi, Y. Noh, and J. Kim, "System performance of transmit diversity schemes for interference-limited cellular systems," in *Proc. 2007 IEEE Global Telecomm. Conf.*, Nov. 2007, pp. 4215–4220.

[68] G. Bauch and J. S. Malik, "Cyclic delay diversity with bit-interleaved coded modulation in orthogonal frequency division multiple access," *IEEE Trans. Wireless Commun.*, vol. 5, no. 8, pp. 2092–2100, Aug. 2006.

[69] E. Weisstein, *Covariance*, MathWorld - A Wolfram Web Resource, http://mathworld.wolfram.com/Covariance.html.

[70] Q. T. Zhang and S. H. Song, "Exact expression for the coherence bandwidth of Rayleigh fading channels," *IEEE Trans. Commun.*, vol. 55, no. 7, pp. 1296–1299, Jul. 2007.

[71] Y. C. Liang, W. S. Leon, Y. Zeng, and C. Xu, "Design of cyclic delay diversity for single carrier cyclic prefix (SCCP) transmissions with block-iterative GDFE (BI-GDFE) receiver," *IEEE Trans. Wireless Commun.*, vol. 7, no. 2, pp. 677–684, Feb. 2008.

[72] T. S. Rappaport, *Wireless Communications Principles and Practice*, Prentice-Hall Inc., 2002.

[73] W. C. Y. Lee, *Mobile Cellular Telecommunications Systems*, McGraw Hill, NY, 1989.

[74] R.H. Etkin, D.N.C. Tse, and Hua Wang, "Gaussian interference channel capacity to within one bit," *Information Theory, IEEE Transactions on*, vol. 54, no. 12, pp. 5534 –5562, 2008.

[75] V.R. Cadambe and S.A. Jafar, "Interference alignment and degrees of freedom of the K-user interference channel," *Information Theory, IEEE Transactions on*, vol. 54, no. 8, pp. 3425 –3441, 2008.

[76] Anh H. Nguyen and Bhaskar D. Rao, "The effect of channel estimation error on the throughput of broadcast channels," in *Acoustics, Speech and Signal Processing, 2011. ICASSP 2011 Proceedings. 2011 IEEE International Conference on*, May 2011, vol. 9.

[77] Taesang Yoo, N. Jindal, and A. Goldsmith, "Multi-antenna downlink channels with limited feedback and user selection," *IEEE J. Selected Areas Commun.*, vol. 25, no. 7, pp. 1478–1491, Sep. 2007.

[78] F.R. Farrokhi, G.J. Foschini, A. Lozano, and R.A. Valenzuela, "Link-optimal space-time processing with multiple transmit and receive antennas," *Communications Letters, IEEE*, vol. 5, no. 3, pp. 85 –87, Mar. 2001.

[79] Q.H. Spencer, A.L. Swindlehurst, and M. Haardt, "Zero-forcing methods for downlink spatial multiplexing in multiuser mimo channels," *Signal Processing, IEEE Transactions on*, vol. 52, no. 2, pp. 461 – 471, 2004.

[80] Jung-Lang Yu and Chien-Chung Yeh, "Generalized eigenspace-based beamformers," *Signal Processing, IEEE Transactions on*, vol. 43, no. 11, pp. 2453 –2461, Nov. 1995.

[81] Seijoon Shim, Jin Kwak, R. Heath, and J. Andrews, "Block diagonalization for multi-user mimo with other-cell interference," *Wireless Communications, IEEE Transactions on*, vol. 7, no. 7, pp. 2671 –2681, 2008.

[82] D. Gesbert, S. Hanly, H. Huang, S. Shamai Shitz, O. Simeone, and Wei Yu, "Multi-cell mimo cooperative networks: A new look at interference," *Selected Areas in Communications, IEEE Journal on*, vol. 28, no. 9, pp. 1380 –1408, 2010.

[83] R. S. Blum, "MIMO capacity with interference," *IEEE J. Selected Areas Commun.*, vol. 21, no. 5, pp. 793–801, Jun. 2003.

[84] G. Golub and C. V. Loan, *Matrix Computations*, The Johns Hopkins Univ. Press, Baltimore, MD, 3rd edition, 1996.

[85] C. Chen and L. Wang, "A unified capacity analysis for wireless systems with joint multiuser scheduling and antenna diversity in Nakagami fading channels," *IEEE Trans. Commun.*, vol. 54, Mar. 2006.

[86] G. Fedele, "N-branch diversity reception of M-ary DPSK signals in slow and nonselective Nakagami fading," *Eur. Trans. Commun.*, vol. 7, pp. 119–123, Mar. 1996.

[87] M.-S. Alouini and A.J. Goldsmith, "Capacity of Rayleigh fading channels under different adaptive transmission and diversity-combining techniques," *IEEE Trans. Veh. Technol.*, vol. 48, no. 4, pp. 1165–1181, Jul. 1999.

[88] K. S. Miller, *Complex Stochastic Processes: An Introduction to Theory and Application*, Addison-Wesley, Reading, MA, 1974.

[89] M. Abramowitz and I. A. Stegun, *Handbook of mathematical functions with formulas, graphs, and mathematical tables*, US Dept. of Commerce, New York: Dover, 9th edition, 1970.

[90] M.R. McKay, P.J. Smith, H.A. Suraweera, and I.B. Collings, "On the mutual information distribution of OFDM-based spatial multiplexing: Exact variance and outage approximation," *IEEE Trans. Inf. Theory*, vol. 54, no. 7, pp. 3260–3278, Jul. 2008.